OULUN YLIOPISTO

UNIVERSITY of OULU

FACULTY OF TECHNOLOGY

Basic testwork with the Outotec pilot HIGmill$^{\text{TM}}$

Juho Junnola

Master´s Thesis

Process Engineering

December 2013

ABSTRACT
FOR THESIS
University of Oulu Faculty of Technology

Degree Programme (Bachelor's Thesis, Master's Thesis)	Major Subject (Licentiate Thesis)
Master's Thesis	

Author	Thesis Supervisor
Juho Junnola	Hannu Kuopanportti

Title of Thesis

Basic testwork with the Outotec pilot HIGmill^{TM}

Major Subject	Type of Thesis	Submission Date	Number of Pages
Process Engineering		11.12.2013	75

Abstract

Mineralogical complexity and declining ore grades poses new challenges to the mining industry. From the grinding point of view, this means that in order to liberate minerals, particles would have to be ground to a finer particle size. Already, comminution is the biggest energy consumer in the concentrating mill. When particles are ground to even smaller particles sizes, costs and energy consumption increase significantly. This coupled with the fact that conventional tumbling mills are ineffective in a size range under 50 μm, has increased interest towards in the use of stirred media mills.

This thesis provides basic knowledge about grinding phenomenona in general, the basics of stirred media mills and a a basic testwork conducted with the Outotec stirred media mill (HIGmill^{TM}). The target of the testwork was to investigate the effect of parameters on grinding efficiency. The parameters under investigation were tip speed, milling density, retention time, size and type of the grinding media, and feed scalping. The secondary target of the testwork was to create a standardized test environment and achieve test repeatability. In addition, two different test methods were tested and compared.

In the test, the repeatability of the pilot HIGmill^{TM} tests was achieved successfully. The HIGmill^{TM} proved to be very flexible regarding a change in parameters. If the specific grinding energy was kept constant, the grinding efficiency stayed the same regardless of the change in tip speed, retention time, or milling density. Even the wear of the mill internals proved to have no notable effect on the grinding result. This fact gives the HIGmill^{TM} a clear advantage when used in industrial applications. In the testwork semi-continuous and continuous test methods were compared and verified to give the same result. In addition dumping between grinding stages in the semi-continuous test method turned out to be overly cautious.

Additional Information

TIIVISTELMÄ
OPINNÄYTETYÖSTÄ Oulun yliopisto Teknillinen tiedekunta

Koulutusohjelma (kandidaatintyö, diplomityö)	Pääaineopintojen ala (lisensiaatintyö)
Diplomityö	

Tekijä	Työn ohjaaja yliopistolla
Juho Junnola	Hannu Kuopanportti

Työn nimi			
Basic testwork with the Outotec pilot HIGmill™			

Opintosuunta	Työn laji	Aika	Sivumäärä
Prosessitekniikka		11.12.2013	75

Tiivistelmä

Maailmanlaajuisesti malmioiden mineraalipitoisuudet ovat heikentyneet ja mineraalirakeiden rakenteet ovat tulleet monimuotoisemmiksi. Jauhatuksen näkökulmasta katsottuna tämä tarkoittaa, että mineraalin hienonnus täytyy suorittaa pienempään partikkelikokoon. Jauhaminen on yksikköprosessina rikastamoiden suurin energian kuluttaja ja siirryttäessä jauhamisessa pienenpään hienouteen, energian kulutus moninkertaistuu. Lisäksi perinteiset rumpumyllyt ovat osoittautuneet tehottomiksi mentäessä pienempään hienouteen kuin 50 µm.

Tämän diplomityön tarkoituksena on esitellä vaihtoehto perinteiselle jauhatukselle. Työssä käydään läpi hienonnuksen perusperiaatteita, esitellään pystymyllyjen toimintaperiaate ja suoritetaan perustutkimuksia Outotecin pystymyllyllä (HIGmill™). Testiohjelmassa tutkitaan eri parametrien vaikutusta HIG myllyn hienonnustehokkuuteen. Parametreja joita tutkitaan, ovat myllyn sekoittimen nopeus, lietteen tiheys, syöttönopeus, syötteen luokitus, jauhinkappaleiden koko sekä eri valmistajien jauhinkappaleet. Testiohjelmassa tarkastellaan myös kahden testimenetelmän eroavaisuutta. Lisäksi yksi testiohjelman keskeisemmistä tavoitteista on kehittää toistettava testimetodi pilottiajoille.

Testeissä onnistuttiin rakentamaan toimiva ympäristö testien tekemiselle, myös testien toistettavuus saavutettiin. Parametrien testauksessa HIGmill™ osoittautui hyvin joustavaksi. Jos syötetty energia tonnia kohden pidettiin vakiona, jauhatustehokkuus pysyi samana huolimatta muutoksista myllyn sekoittimen nopeudessa, lietteen syöttönopeudessa tai tiheydessä. Myöskään myllyn sekoittimen kiekkojen kuluminen ei vaikuttanut jauhatustehokkuuteen. Testeissä todistettiin myös jatkuvan ja puolijatkuvan ajon vastaavuus. Lisäksi puolijatkuvassa ajossa mahdollinen näytteen heittäminen pois jauhatusvaiheiden välissä osoitettiin tarpeettomaksi.

Muita tietoja

TABLE OF CONTENTS

TERMS AND ABBREVIATIONS

b constant acquired from test data [-]

B equivalent energy per revolution [kWh/t]

c_i is transfer factor between stress energy and bead stress energy [-]

C is constant which depends on material properties and grinding method [kWh/t]

C_s is fraction of critical velocity [-]

d_{GM} is diameter of the grinding media [m]

D is mill internal diameter inside liners [m]

E is energy input during grinding time t [J]

E is specific energy [kWh/t]

E_m is specific energy [J kg^{-1}]

E_m is specific energy [kWh/t]

$E_{m,grind}$ is effective specific energy [J kg^{-1}]

$E_{m,M}$ is specific energy consumed by the mill [J kg^{-1}]

$E_{m,P}$ is specific energy transferred to the product [J kg^{-1}]

F is 80% passing size for the feed [μm]

F80 is 80% passing size for the feed [μm]

G is mass of undersize material produced per revolution [g]

G_{bp} is a measure of grindability [-]

k is energy dissipated into heat at the grinding chamber wall [m]

K is constant chosen to balance the units of the equation

kWb is kW per ton of balls at the trunnion [kW]

n is minerals in pure form [-]

n is order of the process [-]

n is number of revolutions [s^{-1}]

N is power input [W]

N is total amount of minerals [-]

N is mill revolutions [-]

m is mass of the product [t]

m_p is mass of the solid ground product [kg]

m_p is mass flow rate [kg/h]

$m_{P,tot}$ is total mass of the product [kg]

M$_i$ is index related to the breakage property of the ore [kWh/t]

M_d is torque measured during comminution [Nm]

$M_{d,0}$ is no load torque [Nm]

$M\text{-}W_i$ is work index of the Mergan method [kWh/t]

Milling density is amount of solids in mill feed [% w/w]

P is Power [W]

P is product particle size that 80 % passes trough [μm]

P_1 is size of the cutting sieve [μm]

P80 is 80% passing size for the product [μm]

P50 is 50% passing size for the product [μm]

S_{GC} is surface of the grinding chamber [m^2]

SE is stress energy [J]

$\overline{SE}$ is mean stress energy [J]

SE_{GM} is stress energy of the grinding media [J]

SN_{tot} is total number of stress events [-]

SGE is specific grinding energy

t is comminution time [s]

t_{grind} is grinding time [s]

tip speed is circumferential speed of stirrer [m/s]

U is percentage of product in the feed [-]

v' is flow rate [l/h]

v_t is stirrer tip speed [m s^{-1}]

v_E is energy transfer factor [-]

$v_{E,S}$ is energy transfer factor [-]

V_{GC} is volume of the grinding chamber [m^3]

V_p is volumetric fraction of the mill occupied by balls [-]

$V_{tot,i}$ is corresponding volume [m^3]

W is specific energy [kWh/t]

W_i is material specific work index value [kWh/t]

x is feed solids [% w/w]

x is particle size [μm]

x_1 is 80% passing size for the feed [μm]

x_2 is 80% passing size for the product [μm]

x_f is feed particle size [μm]

x_{f80} is 80% passing size for the feed [μm]

x_p is product particle size [μm]

x_{p80} is 80% passing size for the product [μm]

Y_{GM} is modulus of elasticity of the grinding media [Pa]

Y_P is modulus of elasticity of the feed material [Pa]

ρ is density   [t/m^3]

ρ_{GM} is density of the grinding media [kg m^{-3}]

ω_d is angular velocity of the stirrer [s^{-1}]

1 INTRODUCTION

Mineralogical complexity and declining ore grades poses new challenges to the mining industry. From a grinding point of view, this means that in order to liberate minerals, particles have to be ground to a finer particle size. Already, comminution is the biggest energy consumer in the mills and operating costs account for 60 – 70 % of the overall operating costs for a concentrating mill (Lofthouse & Johns 1999). When an ore is ground to even smaller particle size, costs and energy consumption increases significantly. This, coupled with the fact that conventionally tumbling mills are ineffective in a size range under 50 µm, has increased the interest in the use of stirred media mills. (Lichter and Davey 2006)

Tuunila (1997:7) describes stirred media mills as an immovable vertical or horizontal cylinder which is loaded with grinding beads and feed material. In addition to an immovable grinding chamber, stirred mills also comprise liners, stirrers attached to the driving shaft, and a motor which circulates the shaft. A rotating shaft imparts motion through stirrers to the charge, which causes interaction between beads and particles. This interaction causes a size reduction. (Lichter & Davey 2006).

This study gives basic knowledge about the grinding phenomenon in general, the basics of stirred media mills and basic testwork conducted with the Outotec stirred media mill (HIGmill^{TM}). The target of the testwork was to investigate the effects of the parameters on grinding efficiency. The parameters under investigation were tip speed, milling density, flow rate, size and type of the grinding media, and feed scalping. The secondary target was to create a standardized test environment and achieve test repeatability. In addition, two different test methods were tested and compared.

2 COMMINUTION FUNDAMENTALS

2.1 Basics

In mineral processing, comminution can be considered to consist of blasting, crushing, and grinding processes (Wills 2006: 108). The unifying factor of these processes is that the product material size is smaller than that of the incoming feed material. Thus it can be stated that the most fundamental function of comminution is a size reduction. In this work blasting and crushing are excluded and the focus will be on grinding.

Size reduction in grinding is done in order to liberate a valuable mineral from gangue and to reduce the particle size for the forthcoming concentrate processes. (Wills 2006: 108-109). Figure 1 shows the structure of two different minerals. The picture clarifies the difference between mineral sizes and show how valuable minerals can be attached to the ore body. The size of the mineral determines how much grinding the ore requires to achieve satisfactory mineral liberation. If the particle is ground to a smaller size than needed, energy is wasted and valuable minerals may not be captured in subsequent concentration processes. If the ground size exceeds the optimum and the particles are not liberated fully, the recovery in forthcoming processes declines. On the other hand, over-grinding can be beneficial if the processes after grinding profit from an increased surface area. The term degree of liberation (1) describes the purity of the particle. This indicates how large portion of the mineral is in liberated form compared to the total amount of the mineral (Lukkarinen 1984). (Wills 2006)

$$r = \frac{n}{N} * 100 \ \% \qquad\qquad (1)$$
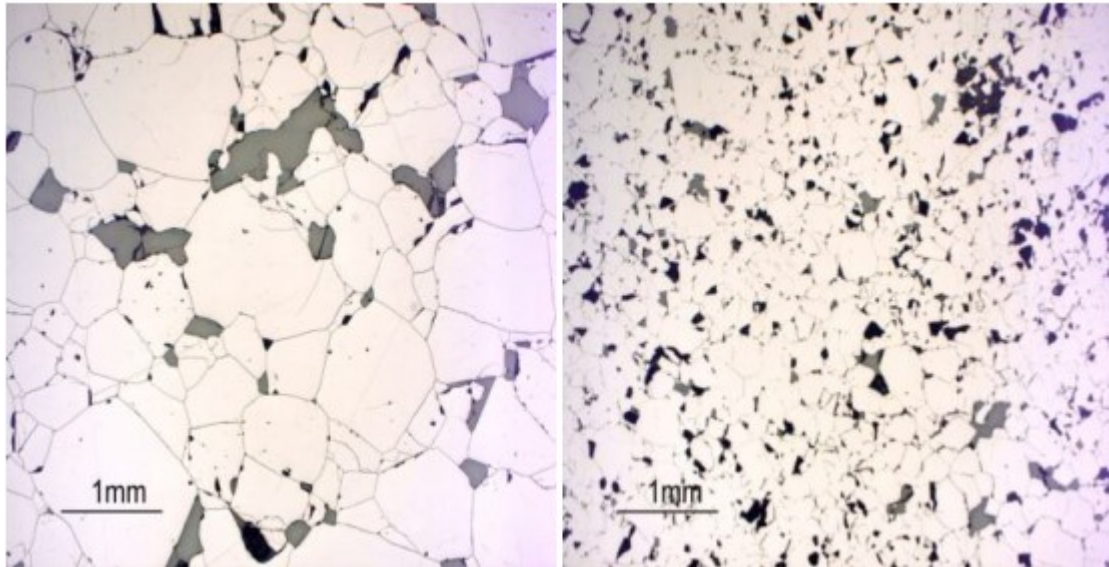
Figure 1. Mineral structures (Lehto et. al. 2013)

The way a material behaves in the comminution process depends on its properties. Properties are ultimately determined by the material structure. On the basic level, the material structure can be considered to consist of one or more phases. The configurations of the phases are determined by the size and types of physical and chemical bonds in which atoms or molecules are attached to each other. The main types of physicals and chemicals bonds are covalent-, ionic-, metallic-, and secondary bonds. Phases can be seen as a defined part of the material, which have a uniform composition and structure. Phases are formed from components, whereas components are the biggest single units that can form all the materials phases of the material in balanced conditions. A component can be a single atom or a molecule. To understand the multitude effects of grinding it is essential to know the concept of material structure. (Wills 2006: 109)

Based on the material structure, the material can behave either plastically or elastically. Elastic behavior means that the material stores energy and changes shape but the shape recovers when the stress stops. This kind of behavior can be characterized by Young's modulus and Poisson's ratio. In plastic behavior, the shape shifting is permanent and typically all materials shows plastic behavior if enough stress is imparted. Visco-elastic material exhibits elastic as well as plastic behavior and is strongly affected by temperature.

Figure 2 demonstrates the mechanical behaviors of solids. Usually in particle breakage, a material shows more than one of the characteristic behaviors mentioned based on the amount of stress applied. (Bernotat & Schönert 2000), (Peukert 2004)
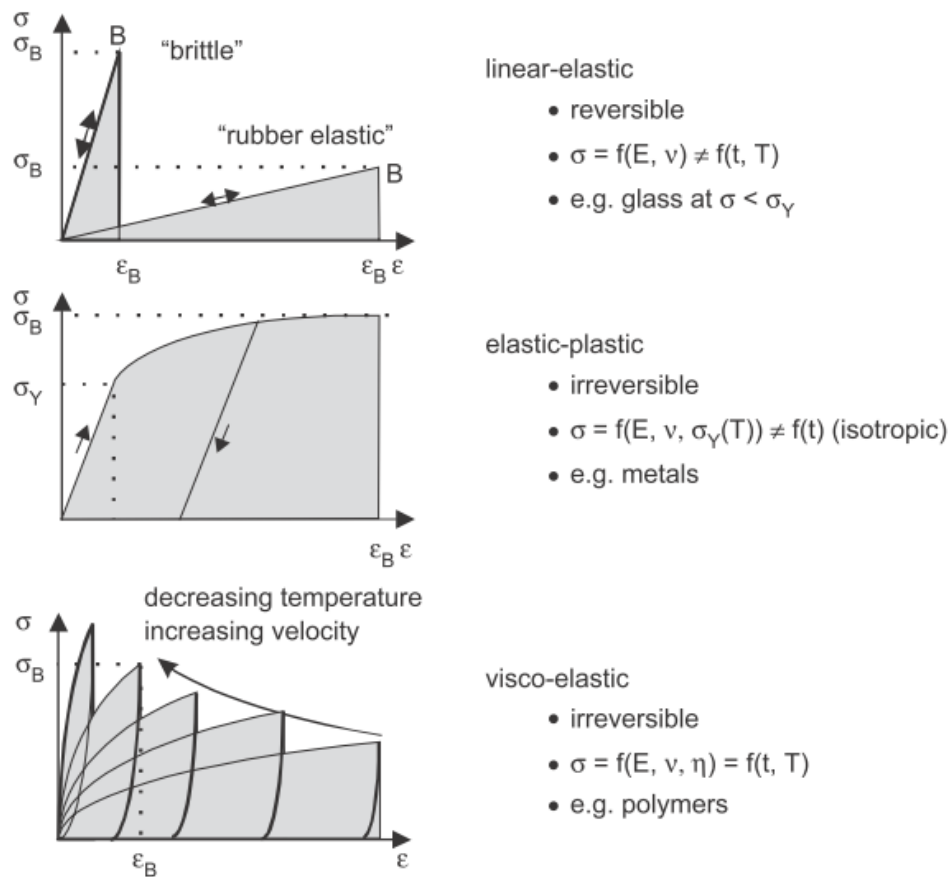
Figure 2. Mechanical behavior of solids (Peukert 2004)

2.2 Particle breakage

A breakage event takes place when enough stress is directed on the ore. The necessary amount of stress is proportional to the material properties, such as shape, size, elasticity, crystal defects, and the type of stress applied. In practice, materials are not as strong as the theoretical strength of bonds binding them. All minerals contain structural defects which make them weaker. Other points of high stress concentration, like pre-existing cracks and sharp corners also exists (NDT 2013). Such stress sites act as starting points for fracturing. (Roufail &Klein 2010), (Bernotat & Schönert 2000)

Peukert (2004) explains a breakage event by functions affecting the grinding result. The property function describes the size, shape, morphology and surface properties of a material. These factors directly affect the product properties. The property function can be altered by changing the parameters or the process. The effects of the process are defined as the process function and this includes the type of machine used and the conditions in which the machine is operated. In addition to these two functions, the author also introduces a material function regarding to the grinding process. The material function describes the behavior of the particles under grinding conditions. It also gives the rate of breakage and accounts for the effects of previous stressing events. In practice, the material function for the grinding process is very hard to determine. Every particle, stress event and stress frequency differs, so values that represent the whole system are very hard to resolve. (Peukert 2004)

The material can be subjected to the necessary stress for breakage by direct or tangential stresses (Figure 3.). Direct stress means tensile- or compressive stress and tangential stress refers to shearing stress. Further, direct and tangential stresses can be classified into categories based on the energy densities they create (Table 1). The problem with this sort of classification is the definition of low or high energy density (Kariranta 2012). Another way to categorize particle stresses is to describe what part of the ore is contacted. Pitchumani et al. (2004) classify ore stresses in surface, body and other mechanisms (Figure 4).
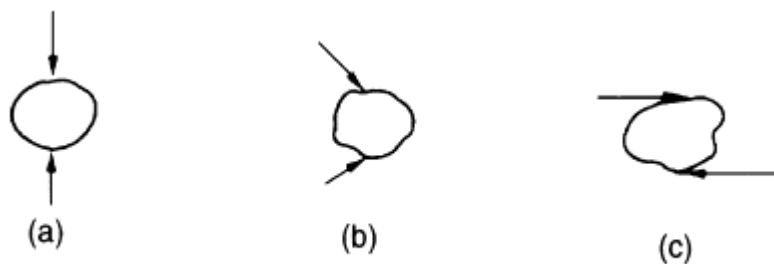
Figure 3. Mechanisms of breakage a) direct stress b) direct and tangential stress c) tangential stress (Wills 2006)

Table 1. Classification of stress mechanisms (Kariranta 2012)

• Attrition is direct stress with low energy density
• Compression is direct stress with medium energy density
• Impact is direct stress with high energy density
• Abrasion is tangential stress with low energy density
• Shearing is tangential stress with medium or high energy density
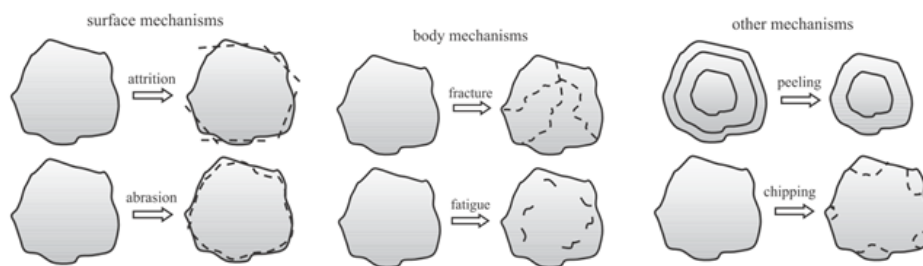
Figure 4. Breakage mechanisms (Pitchumani et al. 2004)

The type of stress the material is exposed to depends on the mill type used and operational conditions (Peukert 2004). Grinding mill types can be classified into tumbling mills or stirred mills according to the way they impart motion to the ore. Tumbling mills are the industry standard for grinding particles between 5 – 250 mm to a size between 40 – 300 µm. Rajamani et al. (2000) define a tumbling mill as a cylindrical drum fitted with conical end plates on both sides. As the grinding medium, steel rods, balls, or the rock itself are used. Tumbling mills impart motion to a mill charge via a rotating drum shell. In stirred mills, the milling shell is stationary and the motion is provided by the movement of the internal stirrer. Stirred mills are described in more detail in section three and the differences between the above-mentioned mill types in section 3.6. (Wills 2006)

2.3 Energy consumption

Energy consumption is widely used as a measurement for grinding efficiency, although precise energy consumption in the actual grinding is very hard to measure. The problem is that only a small amount of the inputted energy is expended on breaking the ore. For example, it is suggested that, in a ball mill, only 1 % of the inputted energy is used for actual grinding. Correct calculations cannot be made unless the energy consumed in creating a new surface can be measured. In spite of the above-mentioned problem, theories regarding energy consumption have been introduced over the years. The most well known are the Bond, Von Rittenger, and Kick theories. These theories assume that there is a relationship between the energy required to break the material and the new surface produced. These theories also presume that all materials are brittle. So no plastic behavior occurs, which would adsorb energy without creating notable amounts of new surface. For example, deformations by elongation or contraction are disregarded in the calculations. (Wills 2006)

Despite the weaknesses mentioned, these theories can predict energy consumption in grinding with some limitations. Bond's theory (2) in particular is widely used in the industry. Bond suggests that the energy used in grinding is inversely proportional to the square root of the particle size. (Wills 2006)

$$E = W_i \left(\frac{10}{\sqrt{x_{P80}}} - \frac{10}{\sqrt{x_{F80}}} \right) \qquad\qquad (2)$$

According to Von Rittinger, the energy consumed in grinding is directly proportional to the new surface produced. Equation (3) shows Von Rittenger's grinding theory. (Hukki 1964)

$$E = C \left(\frac{1}{x_P} - \frac{1}{x_F} \right) \qquad\qquad (3)$$

According to Kick energy needed for particle deformation is directly proportional to the mass or volume of the material (4). (Hukki 1964)

$$E = C \, ln\left(\frac{x_F}{x_P}\right) \tag{4}$$

All three theories can be derived from the Gilliland's equation (5).

$$dE = -C \, \frac{dx}{x^n} \tag{5}$$

From these equations Hukki made an evaluation in which he showed that all of the theories have a particle size range that they apply. Figure 5 demonstrates this evaluation. According to the figure, Von Rittinger's theory can predict energy consumption in the fine grinding range, Bond's in the conventional grinding range and Kick's in the crushing range. Based on Hukki's research, Morrel (2004) made modifications to Bond's equation. Morrel applied a function that takes changes in material properties regarding particle size into account. In addition, changes in behavior between different rock types are recognized. Application of Morrel's model (6) has shown good correlation with industrial grinding circuit solutions. (Morrel 2004), (Wills 2006)

$$W = M_i K \left(x_2^{f(x_2)} - x_1^{f(x_1)}\right) \tag{6}$$
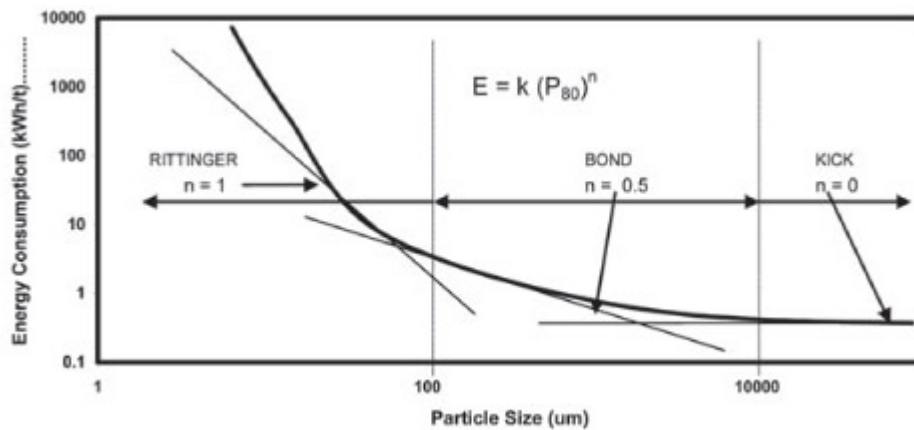
Figure 5. Correlation of grinding theories in different particle sizes (Van Schoor & Sandenbergh 2012)

3 FINE GRINDING

The definition of fine grinding depends strongly on the subject area in which it is used. In mineral processing, there is no standardized method for the classification. For the purpose of this study, fine grinding in considered to be P80 < 40 µm and ultrafine grinding P80 < 20 µm. P80 represents the value where 80% of the particles by mass are smaller than that particle size.

The need for fine grinding is increasing due to declining ore grades and more complex ore bodies. Figure 6 shows the trend of energy consumption as the particle size decreases. As the particle becomes smaller, the amount of structural defects diminishes making it stronger (Pöllänen & Kuopanportti 1994). Thus more energy is needed for particle breakage. Lichter and Davey (2006) categorize the mill types typically used in fine grinding into four categories: ball mills, stirred media mills, centrifugal mills, and jet mills. Of these designs, ball mills and stirred mills are mainly used for industrial purposes. Traditional ball mills have been found to be ineffective in the size range under 50 µm, thus causing increased interest in stirred media mills. (Lichter and Davey 2006), (Lofthouse & Johns 1999), (Peukert 2004),
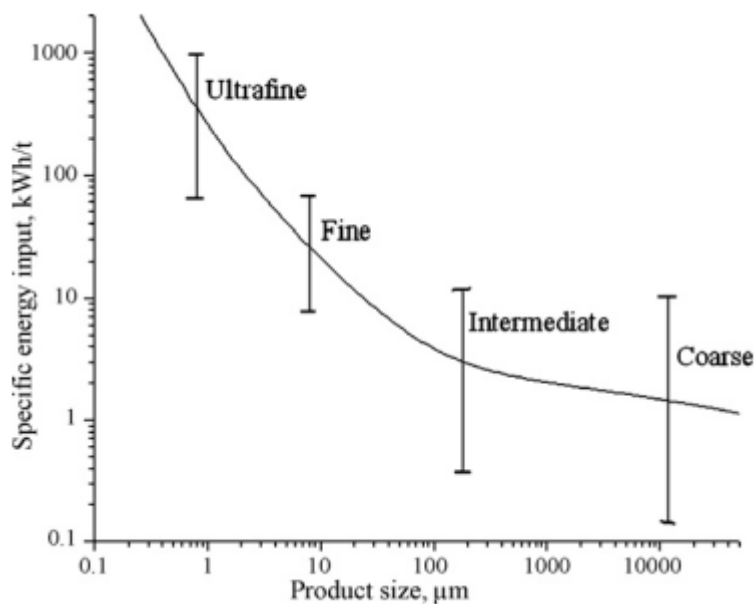
Figure 6. Required energy for size reduction in comminution (Wang & Forsberg 2007)

3.1 Basics of stirred media mills

The first vertical stationary mill which included a stirrer was proposed in 1928. This can be regarded as the first stirred media mill. From the outset, it was designed to improve energy efficiency in the fine grinding size range (Kwade 1999). In these mills, the circumferential speed of the stirrer was about 6 m/s. Similar designs are still made for fine grinding applications. In addition, present mills with a stirrer speed of over 20 m/s have been developed.

Tuunila (1997) describes stirred media mills as an immovable vertical or horizontal cylinder loaded with grinding beads and feed material. The feed material is either dry or wet. Beads can be screened sand, ceramic materials, steel, or glass. The structures of these mills are relatively simple. Besides an immovable grinding chamber, stirred mills consist of stirrers attached to the driving shaft, a motor which circulates the shaft, and liners. A rotating shaft imparts motion through stirrers, which causes interaction between beads and particles. This interaction causes a size reduction. (Tuunila 1997), (Kwade 1999a)

Kwade's and Schwedes' (2007) notion is that there are three ways in which particles are stressed by the media in stirred media mills. According to Kwade (1999b), the first mentioned is the most important type.

- Beads moving fast in the tangential direction collide into beads with lower velocities, crushing the particle caught in between
- The stirrer accelerates beads toward the grinding chamber, creating kinetic energy for the beads, which is used for grinding
- Centrifugal acceleration presses beads towards the wall and pressure creates the grinding force

Yue and Klein (2006) divide stirred mills into two categories according to how fast the stirrer rotates. The first class includes mills that operate with lower stirrer speeds (verti/tower mills). They also use larger media sizes. The second category includes mill designs which have stirrer speeds of up to 23 m/s (ISAmill) and smaller media sizes. This classification is unambiguous and some of the present mills (HIG, Deswik) fall

between these two categories with a small bead size and tip speed range from 10 – 15 m/s. In vertical stirring mills, tip speeds are limited by pressure. At high speeds, pressure is generated at the bottom of the cylinder. Too high a pressure can damage the drive shaft and produce uneven media wear. In horizontal stirred media mills, pressure is distributed more evenly, so a higher stirrer speed can be used. (Yue & Klein 2006), (Gao & Weller 1994)

Stirrer speed strongly affect the power intensity of the mill. Power intensity is determined by the power draw per unit of mill volume. However, high power intensity is not a guarantee for good grinding performance, because the term does not describe how effectively the energy is used to cause size reduction. When measuring power intensity it must be noted that it is not equal in every part of the mill. It has been pointed that two high intensity zones exist. One zone is near the outer tip of the stirrer and the other is at the grinding chamber wall. Near the outer tip of the stirrer the grinding beads are accelerated by centrifugal forces, thus increasing the kinetic energy of the beads. At the grinding chamber wall, the intensity increases due to the pressure exerted between the beads. About 90 % of the energy is dissipated in the high intensity zones. In relation to the mill net volume, the volume taken by high intensity zones is small, only about 10 % of the mill net volume. (Kwade 1999), (Nesset et al. 2006), (Shi et al. 2009)

Besides the stirrer tip speed, the stirrer type also varies between mill designs. For example, discs, pins, screws, and impellers are used. In addition, some mill designs include static counterparts to prevent slurry flow. Mill designs also differ in the way they prevent bead transportation from the mill to the product stream. Rotating separation gap, sieve and centrifugal separation are used. Some mills are also equipped with cooling jackets, to avoid an excessive rise in temperature. (Kwade & Swedes 2007)

3.2 Stress model

A stress model was introduced by the Institute for Particle Technology at the Technical University of Braunschweig. The model was developed from two different viewing angles, firstly, the perspective of the particle and secondly, mill performance. The mill related stress model considers how strongly and how frequently the stress is applied. The mill model itself cannot describe the whole grinding process without the product-

related model. The product-related stress model considers the size of the stressed particle and how many particles are stressed in one stress event. The model describes the connection between the product fineness, energy consumption, and the most important parameters affecting the grinding result. The stress model is based on specific energy calculations and the concept of the stress number and stress energy of the grinding media. (Breitung-Faes & Kwade 2013), (Kwade & Schwedes 2007)

3.2.1 Specific energy

Specific energy is defined as energy transferred to the grinding chamber related to the mass of the product and can be calculated by using equation (7). In equation (8) no load power has been separated from specific energy consumption. In the studies made by Schwedes, Stehr and Weit specific energy is shown to depict grinding efficiency quite accurately, if the grinding media size is kept constant (Kwade et al. 1996). The authors also derived an equation (9) to depict the results gained from the testwork. The equation can also be derived from the Gilliland equation (5). Although a regression coefficient of 0,985 has been obtained in the testwork conducted, a variation of more than ± 25 % from the fitted curve occurs when different grinding media sizes are used. (Kwade et al. 1996), (Kwade & Schwedes 2007)

$$E_m(t) = \frac{E(t)}{m_p} = \frac{\int_0^t N(t)dt}{m_p} \tag{7}$$

$$E_m(t) = \frac{\int_0^t (M_d(t) - M_{d,0})\omega_d dt}{m_p} \tag{8}$$

$$x_p = C * E_m^b \quad \text{if } x_f \gg x_p \tag{9}$$

The energy consumed by a mill is not equal to the energy transferred to particle breakage. For example, friction forces consume inputted energy without decreasing the particle size. The energy transferred to the actual particle breakage can be described by the stress number and stress energy, in relation to the total mass of the particles combined with the term v_E (10). The term v_E includes all the energy which does not participate in the grinding of the particle. (Kwade & Schwedes 2007)

$$\frac{SN_{tot} * \overline{SE}}{m_{P,tot}} = E_{m,P} = v_E E_{m,M} \tag{10}$$

3.2.2 Stress energy of the grinding media

The stress energy of the grinding media SE$_{GM}$ (11) is a characteristic number which describes the effects of the stirrer tip speed, bead size and bead density. The term stress intensity of the grinding media is also used in the literature. The stress energy of the beads can be used as a measure for the stress energy in the mill. The stress energy of the grinding media is not a constant in all cases, but varies between stress events. Variations exist because of the different velocity gradients and the resulting differences in media velocities. For an accurate description, the distribution of stress intensity must be used. But according to Kwade and Schwedes (2007), in practice averages of the distribution are often sufficient to describe the stress energy. (Kwade & Schwedes 2007)

$$SE_{GM} = d_{GM}^3 \rho_{GM} v_t^2 \tag{11}$$

The equation is built using the following assumptions (Kwade 2006):

- Tangential velocity of the beads is caused by the tip speed of the discs
- Mill geometry does not change
- Viscosity of the feed is not too high
- Elasticity of the beads is considerably higher than the elasticity of the product material
- Only one particle is stressed at a time

The assumptions made in creating the stress energy equation do not apply in all cases. For example, if the elasticity of the feed material is equal to or higher than that of one of the grinding beads, it has to be taken into account. Therefore equation (11) is expanded to consider the energy lost in the deformation of the beads. Similarly, high viscosity can also be attached to the equation. The effects of elasticity are attached in the stress energy of the grinding beads equation as shown below (12). (Kwade & Schwedes 2007)

$$SI_{GM} = d_{GM}^3 \rho_{GM} v_t^2 \left(1 + \frac{Y_P}{Y_{GM}}\right)^{-1} \tag{12}$$

For a certain process and process parameters, the optimum stress energy can be found. The stress energy is optimal when the energy is sufficient to break a particle with a single contact. When the energy is less than the optimum, multiple stress events have to be carried out and if the energy is too high, energy efficiency decreases. Stress energy is a powerful tool when studying the effect of different parameters on the grinding result. This fact was also recognized by Rahal et al. (2011a) in the paper that introduces the Knelson-Deswik mill. In addition Jankovic (2003) noted in his studies that variables have a strong interaction between each other and showed that optimal parameters can be found for the SAM and Tower mills. On the other hand, optimal stress energy must be determined separately for the geometry of each mill. Although the stress energy of the grinding beads remains constant, the stress energy that the beads translate to the mill varies between geometries. (Kwade & Schwedes 2007).

3.2.3 Stress number

The stress number (SN_{tot}) is the average number of stress events which affects each particle in the mill. It depends on how frequently the grinding action happens (SF_F) and the mean grinding time (t_{grind}). The more stress events, the higher the stress number and the particle is ground to a finer size. The stress number is strongly affected by the speed of the stirrer, solids concentration, filling ratio of the beads and the size of the grinding media. If the size and the filling ratio of the grinding beads are kept constant, the stress number can be expressed as reduced stress number SN_r (13). (Kwade & Schwedes 2007)

$$SN_r = n * t_{grind} * \left(\frac{x}{d_{GM}}\right)^2 \qquad (13)$$

3.2.4 Stress model in scale-up

This section focuses on the scale-up using the stress model. In most cases, grindability tests cannot be done directly with production scale mills, so testwork is conducted on laboratory or pilot scale. The basic idea of the scale-up is to transfer knowledge gained from laboratory or pilot scale tests to the production size mill. Usually, the main focus of the scale-up testwork is to obtain the specific energy consumption when grinding to the desired particle size. (Kwade & Schwedes 2007)

Stirred media mills are not directly scalable to production scale by the stress model. A change in grinding chamber size modifies the motion patterns of the grinding media, thus changing the distributions of stress energy and stress number. Also, the energy transfer factor changes along with the grinding chamber size. Therefore, unless these factors are included, a correct scale-up cannot be done with the stress model. (Kwade & Schwedes 2007)

In order to take into account changes in mill chamber size, Stender et al. (2004) derived an equation in which the mean stress energy is determined from equation (14). With this equation, a change in the stress energy in different mill chamber sizes is taken into account. To correct the inaccuracy in energy lost in different mill sizes, an additional equation has been derived. Equation (15) assumes that mill chamber size affects only the amount of energy dissipated at the grinding chamber wall. In the equation, the term k is a constant which depends on the surface conditions and product properties, so it is determined separately for each material. Also, at least two mills with different chamber sizes are advisable to verify coefficient k. If two mills give the same particle size with the same effective specific energy, the coefficient k is adjusted correctly. By taking these two correction factors into consideration, the stress model can be used for scale-up as shown by Kwade and Schwedes (2007). (Kwade & Schwedes 2007)

$$\overline{SE} = SE_{GM} \frac{\sum(c_i * V_{tot,i})}{V_{GC}} \tag{14}$$

$$E_{m,grind} = v_{E,S} E_m = \left(1 - k \frac{S_{GC}}{V_{GC}}\right) E_m \tag{15}$$

3.3 Effect of parameters

More than 40 variables affecting the grinding result have been identified (Molls and Hornle 1972). Most of these are of minor importantance. Kwade and Schwedes (2007) divide the more important parameters into four groups: operating parameters, operating mode, composition of the suspension, and to mill geometry. In the following sub-sections these groups are viewed more closely. Only the composition of the suspension is given less attention. Solvents and additives are used more in submicron sizes and at present the mineral industry cannot cope with such low particle size ranges. The content of each group can be seen in Table 2. (Kwade et al. 1996), (Jankovic 2003)

Table 2. Important parameters of stirred media mills (Kwade & Schwedes 2007)

Group	Parameters
Operating parameters	Grinding or dispersing time
	Throughput
	Stirrer tip speed
	Grinding media size
	Grinding media material (density, elasticity and hardness)
	Filling ratio of the grinding media
Operation mode	One or multiple passage mode
	Pendulum or circuit operation
Composition of the suspension	Solids concentration
	Type of solvent
	Additives or dispersing agents
Mill geometry	Type of mill
	Size and dimensions of mill

3.3.1 Operating parameters

Both the stress model approach and specific energy can be used to describe the effect of the operating parameters. Specific energy is calculated by dividing the power draw by the mass. In practice, this means that every parameter that has an effect on either of the above-mentioned parameters is counted. For example, flow rate, tip speed, bead density, bead size, bead filling rate and slurry density all affect the specific energy.

According to Kwade & Schwedes (2007), the stress model and especially stress energy of the grinding beads and stress number can be used to describe the effects of the parameters on grinding result. The most important parameters and parameters, which are taken into account in the stress energy equation, are the size and density of the grinding media and the tip speed of the stirrer. According to equation (11), the diameter of the media affects the stress energy by the power of three, so media size is crucial parameter for the stirred media mills.

Kwade and Stender (1998) suggest that there is an optimal media size for specific conditions where no energy is wasted and the desired product fineness is achieved. Too small a media will not produce enough stress energy to break a feed particle. Increasing the media size will increase the stress intensity and with multiple collisions the feed particle size will decreases. Further increases in media size will make stress intensity high enough to deliver enough energy to break the particle with a single contact. If the media size is still increased, more energy is consumed than needed and energy efficiency decreases. In addition, bead size affects the number of stress events, and bigger the bead size, the lower the stress number. Figure 7 presents a graph which depicts the effects of the grinding media sizes. Studies presented by Kwade et al. (1996) shows that the size has a significant influence on grinding efficiency and that specific energy cannot solely describe energy efficiency when different media sizes are used. (Kwade & Stender 1998)
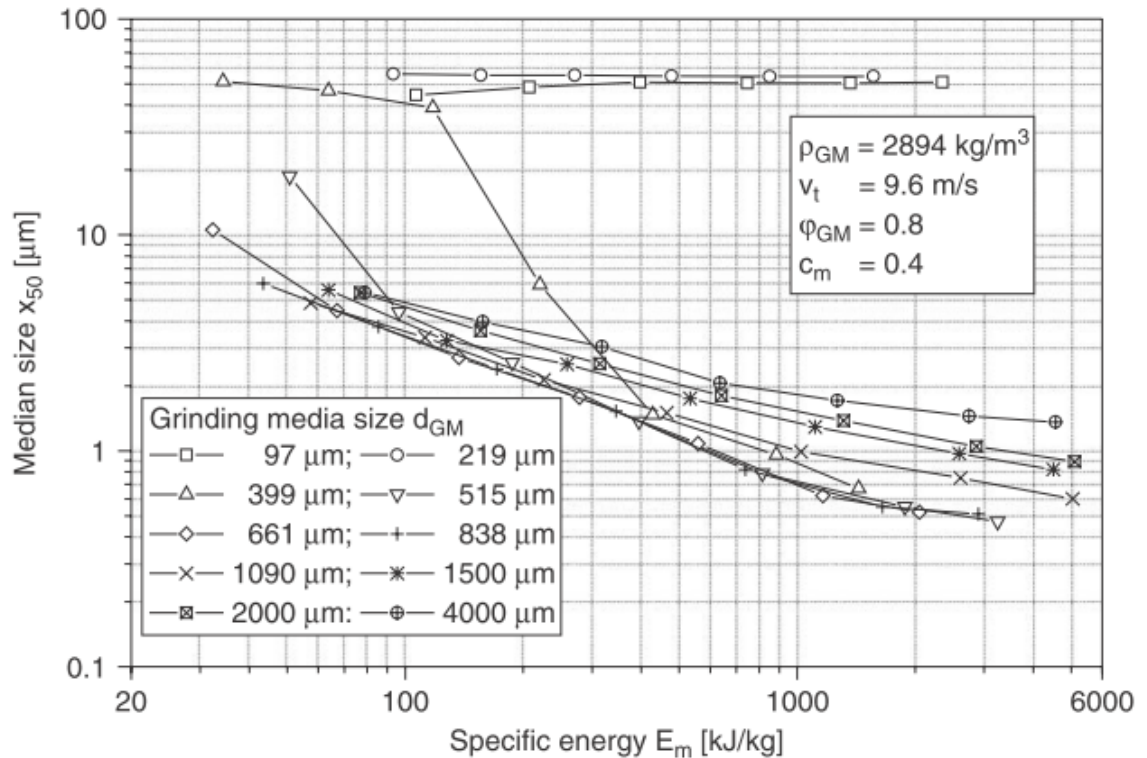
Figure 7. Influence of grinding media size (Kwade and Schwedes 2007)

Bead size also affects to the product size distribution and Yue and Klein suggest (2006) that larger beads produce a narrower product distribution. They state that greater potential causes massive fractures due to higher kinetic energy, thus producing a narrower distribution. They also suggest that the wide size distribution caused by smaller particles may be a result of lower SE (stress energy) promoting attrition over fracture. As mentioned earlier higher SE consumes more energy and the decision between a narrow size distribution and higher energy consumption has to be made on a case-by-case basis. In addition, a graded media charge can be used and is recommended if the particle size distribution of the feed is wide. The proportion between small and large beads that is chosen should reflect the feed particle size distribution. (Gao & Weller 1994)

In addition to media size, the media filling ratio is also a parameter which has an effect. Increasing the milling load means better usage of the net volume of the mill. More grinding events take place and the distance between beads decreases, thus increasing the probability of a breaking event. the power draw increases with the bead load and this

increases process capacity. However, if the filling ratio is too high, beads will not have enough space to grind efficiently. (Wang & Forsberg 2007), (Kwade & Schwedes 2007)

According to the stress energy equation the tip speed of the mill stirrer is the second most effective parameter next to the size of the grinding beads. In equation (11), the value of the tip speed is squared. Tip speed also has a big effect on the frequency of grinding events. As the tip speed increases, so does the number of collisions. In addition power input can be changed by altering the tip speed of the stirrer, thus changing the specific energy value. The higher the tip speed, the higher the power input.

Bead density has the lowest effect of the three parameters that form the equation of grinding bead stress energy. Bead density affects how the stirrer speed is connected to the speed of the beads. If the filling rate is constant, the denser the beads, the more power needed to put the beads in motion. Thus, more power is needed and the specific energy consumption rises. The choice between different media types is strongly affected by the cost and availability of the bead type. Often the bead which gives the best grinding result is not selected due to its high cost or low availability. (Nesset et al. 2006)

In some cases, slurry density is also included in to the grinding media stress energy equation. Slurry density indicates the amount of particles in a certain volume. When looking at the definition of the stressing energy of grinding beads, it was determined that only one particle is stressed at a time. When slurry density increases, the probability that more than one particle is caught between two beads and stressed at the same time increases. The amount of solids also affects the stress number. When slurry density is low, less contact between beads and particles occurs. Kwade & Schwedes (2007) suggest that a higher amount of particles also reduces the wear of the media if the feed material is weaker than the media. According to studies made by Jankovic (2003), a higher slurry density gives better grinding results with the same energy consumption to the limit when high density starts to affecting the ability of the slurry to flow due to increasing viscosity. Based on his study, Jankovic states that grinding efficiency appears to reach its maximum with respect to the slurry solids after the point of 64 % of solids. Slurry density also has an effect on the power draw. When the tip speed is kept constant, a thicker slurry draws more power, thus increasing the specific energy (Gao et al. 1996). (Kwade & Schwedes 2007)

3.3.2 Operating mode

The operating mode implies how the mill is operated and how the resulting product is handled. Kwade and Schwedes (2007) identify four different operating modes: batch, continuous, pendulum, and circuit mode. The only mode used in the mineral industry on production scale is continuous mode. However, on pilot or laboratory scale other methods are also used. In continuous mode, the feed is fed to the mill and the product is ready once the slurry has passed through the mill. Specific grinding energy is calculated in a continuous test according to equation (14). In a pendulum test, the product particle is routed to a mixer from which it acts as the feed for the next grinding step. A pendulum test can be considered a semi-continuous test and this name is used from here on. A semi-continuous test is described more accurately in the testwork section. In a semi-continuous test specific grinding energy is calculated as a sum of the specific energies of each individual passage.

$$E = \frac{P}{m_p} = \frac{P}{m*v} \qquad (16)$$

Besides the operating modes, there are a few other points worth mentioning when operating a full-scale mill circuit. A mill can be operated as a closed cycle in which the product is sized after grinding and can be returned to the mill if the size range is not acceptable. The feed can also be scalped before milling, so that particles already in the size range of the product are not recycled to the mill. Although this does not change the way mill specific energy is calculated, it affects the specific energy used and the throughput of the mill. Scalping is usually done with a hydrocyclone. A hydrocyclone is a classifier that uses centrifugal force to accelerate the settling rate of particles and divide the feed stream into an underflow and overflow (Wills 2006). Centrifugal forces lift lighter/smaller particles to the top of the cyclone, where particles are discharged via the overflow. Coarser particles drop to the bottom of the cyclone and are discharged via the underflow.

3.3.3 Mill geometry

Stender et al. (2004) present studies regarding different behavior of mill parameters at different mill chamber sizes. The studies show that the optimal grinding parameters change if the mill geometry is changed. In Figure 8 the effect of mill geometry on the relation between product fineness and grinding media size is illustrated. The graph shows that the optimum grinding media size changes in different mill volumes. The differences are explained by the change in mean stress energies when the mill size is changed. The changes in mean stress energies are caused by the change in motion of the grinding media. Breitung-Faes and Kwade (2013) presented a term to describe different mill geometries. The term is called the mill factor (f_m). The mill factor expresses the median stress energy and is added to the stress energy equation as follows (17).
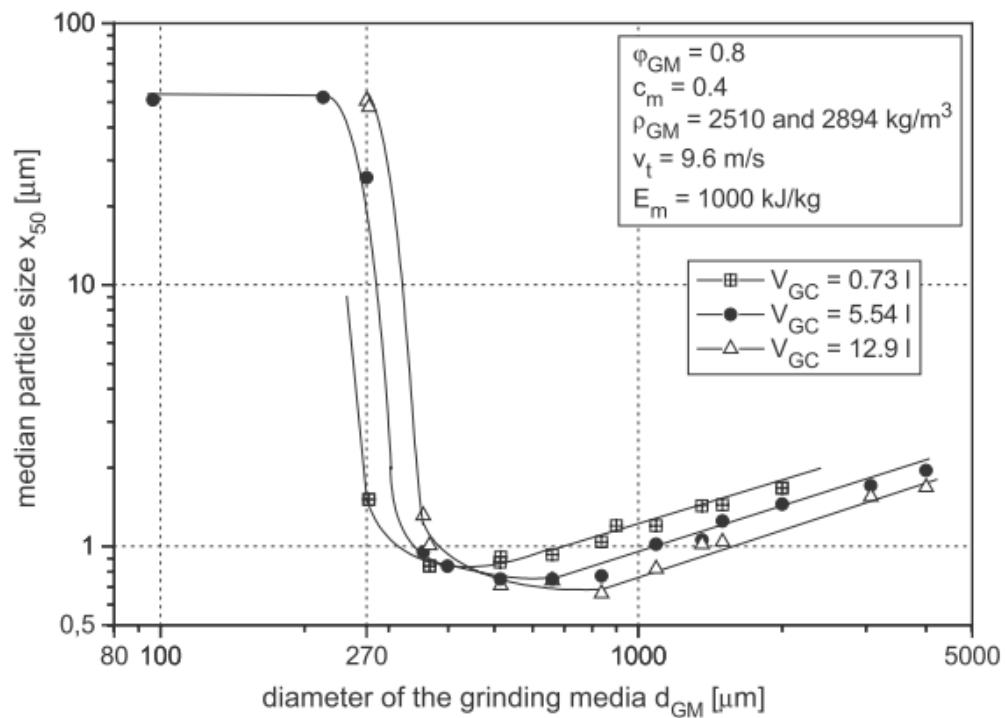
Figure 8. Effect of grinding chamber size (Stender et al. 2004)

$$SI_{GM} = f_m d_{GM}^3 \rho_{GM} v_t^2 \tag{17}$$

Radziszewski (2012) introduced a model that can compare different mill designs. The model assumes that shear/attrition is the only mechanism in the mill that causes size reduction and the author derived an equation based on that assumption. The equation is based on the fluid mechanics definition of shear stress. In Radsziszewski's model, grinding efficiency is expressed by the term "shear volume." The author compared different mill designs and disc stirrers with static counter discs were found to be the best alternative among the commercially available mills in industrial scale.

3.4 Wear of the mill and grinding media

In stirred media mills, the shear forces are significant. Wear occurs in the grinding media, stirrer, grinding chamber and in the separation device. The wear can be a major expenditure in the overall grinding cost. Also, downstream processes may be affected by the particles sheared from the media, specially when ground to below 1 μm. The amount of wear is strongly dependent on the material that is ground and the material of the wear parts. The wear can be decreased considerably by applying wear resistant mill parts, choosing a stronger media type than the feed material and by optimizing the grinding parameters. Optimum grinding parameters are crucial, so that too much energy is not inputted to the mill, which would ultimately increase the wear. The wear resistant materials used in stirred media mills include alloy steels, natural rubber, polyurethane, and ceramics. Some of these materials have a low heat transfer coefficient which has to be taken into account if high temperatures occur during the grinding. Heat transfer problems can be overcome using a cooling system. (Kwade & Schwedes 2007)

Kwade and Schwedes (2007) proposal for investigating media wear was to measure the weight of the beads before and after grinding. The problem with this arrangement is that this demands a large amount of feed material and long comminution times before wear is observable. Usually the amount of feed material needed for the wear test is not available. In some cases, it may also be hard to collect all the beads after grinding and lost beads may account for a substantial amount of the weight loss observed. The authors also suggested that media wear decreases with an increasing grinding chamber volume. Thus a correlation factor has to be applied when using wear results gained from pilot or a laboratory test for scaling up to an industrial size unit.

3.5 Different types of stirred media mills

A variety of different types of stirred media mills have been introduced over the years. Mill designs differ in stirrer types, mill geometry, the separator used for separating the beads from the product and in the way they are positioned, horizontally or vertically (Kwade 1999). The following section presents Outotec's HIGmill and briefly introduces other available stirred media mill technologies.

3.5.1 HIGmill[TM]

The HIGmill[TM] is Outotec's response to the increasing demand for fine grinding mills. The abbreviation HIG stands for High Intensity Grinding. The mill is vertically oriented and as a stirrer it uses specially designed discs. It also uses stationary counters discs. Typical applications for the mill are regrinding of concentrates, iron ore tertiary grinding, fine grinding of precious metals and fine grinding for hydrometallurgical processes. The technology behind the HIGmill[TM] has been utilized for more than 30 years and over 260 mill units have been installed for the processing of paper fillers and carbonate coatings.

The main components and operation principles of the HIGmill[TM] are shown in Figure 9. Slurry is pumped to the mill from the bottom and the ground product is discharged from the top of the mill. Discharge occurs as an overflow, so no high pressures are involved. The mill is filled with grinding beads, which are put into motion using internal stirrer. As the slurry travels upwards, particles are exposed to the movement of the beads. This movement causes size reduction of particles by attrition. Multiple grinding media options and sizes can be used and the choice is made to reflect the feed size, availability, and cost of the beads.

The mill is operated in continuous mode with a single pass and no external classification required. The mill structure works as a classifier and the larger particles spend more time in the grinding zone. In addition, a hydroclassifier installed in the top of the chamber prevents the grinding media from being mixed up with the product. In a circuit, the HIGmill[TM] is typically placed after the scalping hydrocyclone. The hydrocyclone classifies the feed so that particles already in the target product size are not circulated through the mill. In addition, target density is adjusted before the slurry is pumped in.

Online particle size measurement provides up-to-date information and specific energy can be adjusted accordingly. The main method for regulating the power draw and through that the specific energy is by changing the speed of the stirrer. The mill is installed with a variable speed drive to widen the control range.
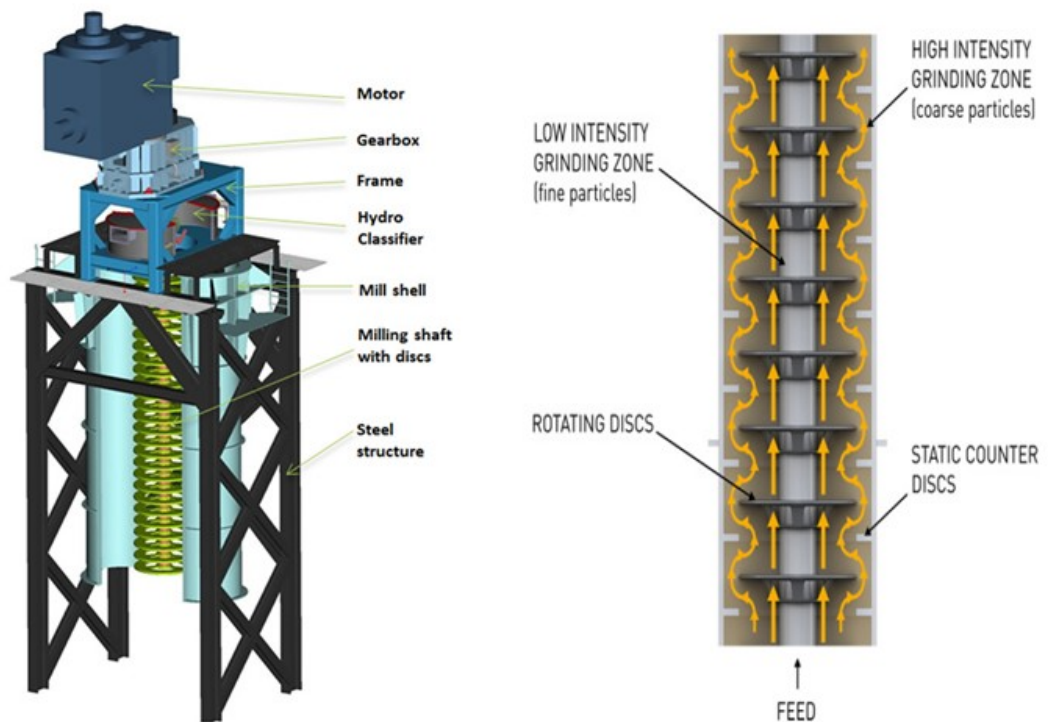
Figure 9. Main components and operating principle. (Outotec 2013) (STM 2013)

Outotec offers a wide range of industrial units. Volumes from 400 l to 27500 l and corresponding motor power from 132 kW to 5000 kW are available. The amount of discs depends on the application chosen and can be up to 30 discs. In addition, disc and counter disc sizes can be adjusted to reflect the particle size of the feed. The feed size F80 for the mill is < 200 μm in fine grinding and in ultra-fine grinding < 70 μm. Outotec offers HIG5 and HIG25 pilot mill units for defining specific grinding energy and operating parameters. A HIG25 container unit is also available for continuous on-site tests.

3.5.2 VXPmill

The VXPmill was originally developed in the mid 1990s for the fine pigment industry. The design was made by Des Erasmus and his son Wikus, who founded the company Deswik Ltd. The mill also carried the company's name. In 2010 Deswik and Knelson signed a corporate partnership and the name was changed to the Knelson-Deswik mill. In 2012 Knelson became a part of the FLSmidth group and the mill received its present name: the FLSmidth VXPmill.

For the most part, the mill has the same design as the HIGmill^{TM}. The stationary cylinder is vertically oriented, it uses perforated discs as a stirrer, and is normally operated in an open circuit. The reported feed size F80 for the mill is 300 – 400 μm, optimum milling density is between 1,2 and 1,5 kg/l and the tip speed between 10 – 12 m/s. The biggest difference between the VXPmill and HIGmill^{TM} is that VXPmill does not have counter discs and the product is discharged through a wire mesh screen. The VXPmill also utilizes a water jacket for cooling purposes and the top of the mill is open. Figure 10 presents the VXPmill (Rahal et al. 2011a), (Rahal et al. 2011b)

Figure 10.   VXPmill (FLSmidth 2013)

3.5.3 Vertimill

The Vertimill, previously known as the tower mill, was introduced in 1953 by Nichitsu Mining Industry CO., Ltd. In 1991 tower mill technology was obtained by Svedela Industries, which is now acting under Metso Minerals Ltd. The technology in these mills is relatively simple. The chamber of the mill is oriented vertically. The suspension is charged to the mill at the top and is ground as it falls to the bottom. The ground product is carried upwards by the overflow and by the pumped recycle flow. At the top of the mill, the product stream goes through the classifier and oversized particles are led back to the mill from the bottom up. A screw stirrer rotates steel balls or pebbles at a speed of around 20 – 60 rpm. As the stirrer rotates, it lifts the grinding media. Thus, in addition to size reduction caused by attrition, the Vertimill also causes size reduction by impact when the grinding media falls. According to Wills (2006), Vertimills are used at the coarse end of the fine grinding spectrum due to their relatively coarse media (6 mm). A diagram of the mill can be seen in Figure 11 (Jankovic 2008), (Wills 2006), (Gao & Weller 1994)
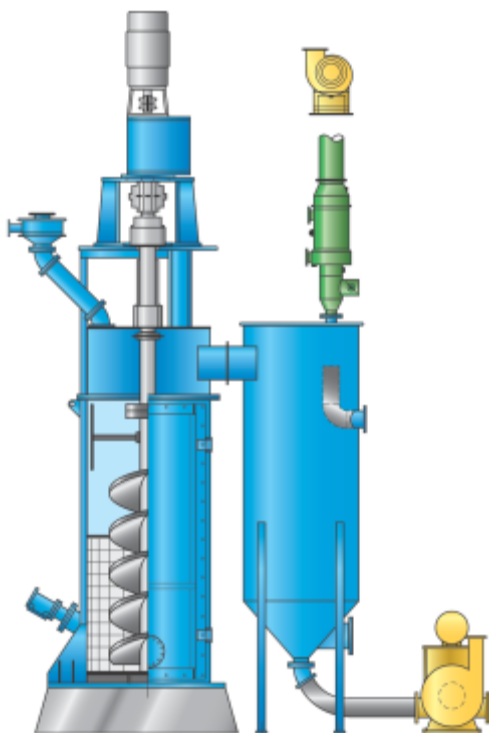
Figure 11.   Vertimill (Metso 2013)

3.5.4 Stirred Media Detritor

Stirred Media detritors (SMD) were developed in the 60s by a company called English China Clays. SMDs were also used first for grinding calcium carbonate and kaolin. In 1997, this technology was obtained by Svedala Industries, which is now part of Metso Minerals Ltd. SMDs utilize low speed impellers as an agitator. The feed is routed into the mill from the top. For grinding media, it usually utilizes natural silica sand or ceramic media. Ground product is floated out from the screens situated in the top half of the unit. Screens also prevent the discharge of the grinding media to the product feed. The SMD operates normally in an open circuit and handles a feed size in the range of 100-30 µm. According to Davey (2002), SMD mills can be scaled-up directly from laboratory test results. A diagram of the SMD mill is presented in Figure 12. (Jankovic 2008), (Wills 2006)

Figure 12.   Stirred Media Detritor (Metso 2013)

3.5.5 IsaMill

The IsaMill was developed from the Netszch stirred mill in cooperation between Netszch Feinmahltechnik GmbH and Mt Isa Mines Limited in the 1990s. The mill is horizontally oriented and uses discs as stirrers. Due to its horizontal orientation, the stirrer can be operated at a relatively high speed, up to 23 m/s. For that reason a small media charge can also be used. Instead of screens the IsaMill uses a separator based on g-forces to keep the grinding media away from the product stream. Figure 13 shows the main components of the IsaMill.
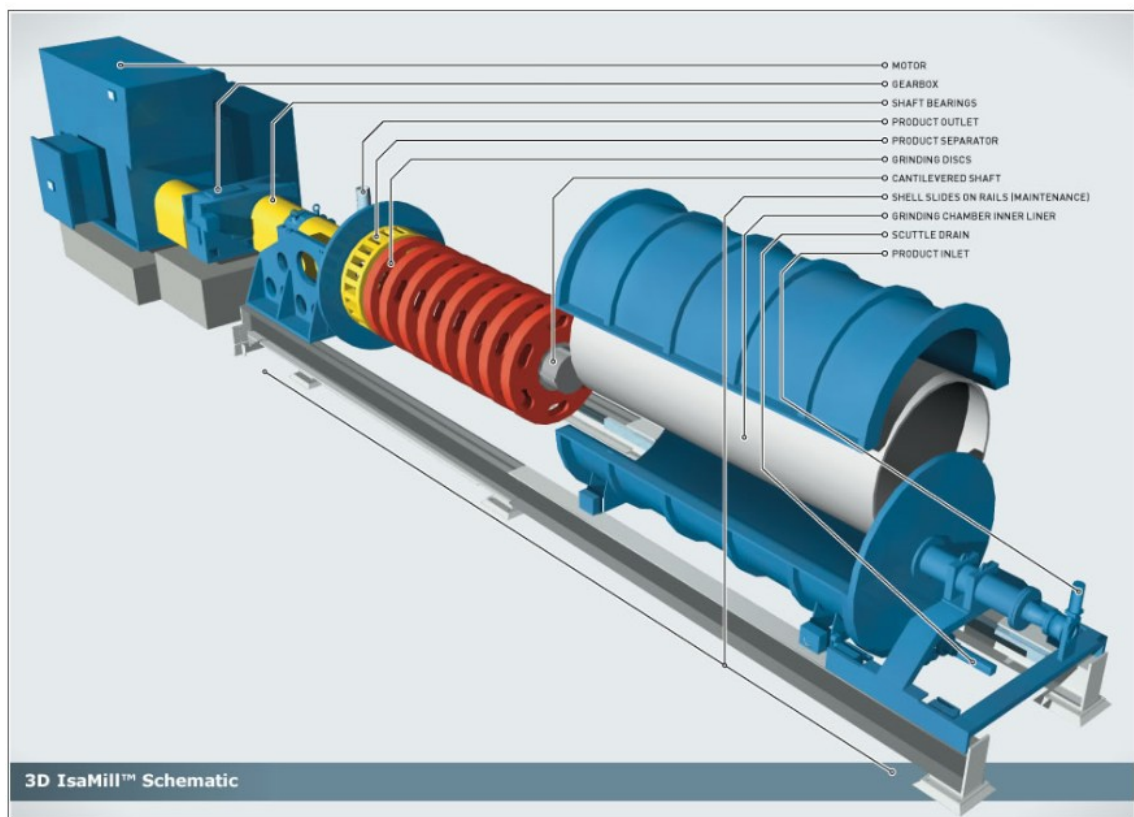
Figure 13.   IsaMill (IsaMill 2013)

The working principles of IsaMill are characteristic of all stirred media mills. The feed is routed continuously to the grinding chamber. Stirrers agitate the grinding media and feed particles, thus leading to the grinding phenomenon. The stirrers are mounted on a shaft which is coupled to a motor and gearbox. Rubber and polyurethane are used for coating the mill compounds to reduce the wear of the mill. (Gao et al. 2002)

3.6 Comparison between stirred media mills and tumbling mills

The main difference between the two milling technologies is the way they impart motion to the ore charge. Stirred media mills impart motion via an internal stirrer and tumbling mills via a rotating drum shell. The operating speed of tumbling mills is limited by the mill's critical speed at which the grinding charge starts to rotate along the periphery of the cylinder, stopping the grinding action. This makes the power intensity relatively small and for that reason fine grinding would need long comminution times. In addition, energy density is determined by the energy discharged when the grinding media falls so that it cannot be controlled flexibly because of the speed limit. Moreover in tumbling mills, the volume of the mill is not effectively used as grinding occurs in a small area. It is suggested that less than 50 % of the mill volume is involved directly in the actual grinding process. In addition, the filling ratio of tumbling mills has to be kept low so that the mill charge has space to tumble around. (Gao & Weller 1994), (Wills 2006) (Kwade 1999).

The tumbling mill functions fairly well at the traditional grinding size. When the particle size decreases, so does the energy efficiency of the tumbling mill. Usually tumbling mills are used in a size range 600 – 75 µm but when required particle size is below 50 µm, the effectiveness is reduced significantly. The graph presented in Figure 14 depicts typical stirred media mill performance against that of a conventional ball mill. At small particle sizes, stirred media mills consume 50 % less energy than tumbling mills. (Lofthouse & Johns 1999)
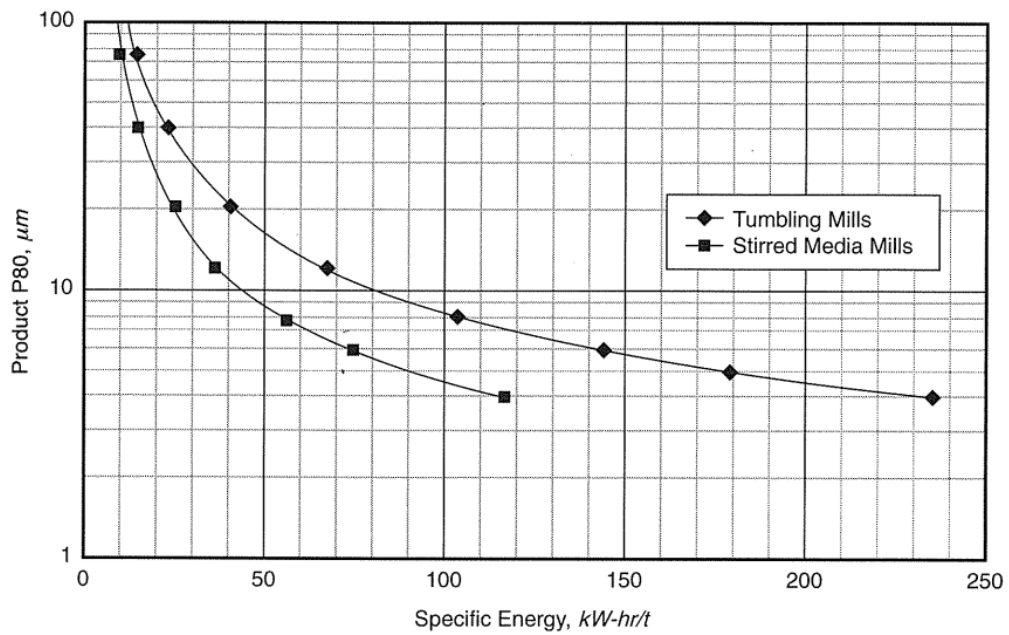
Figure 14.   Energy consumption comparison between tumbling and stirred media mill
(Lichter & Davey 2006)

In stirred mills, the grinding charge is not rotated in the periphery and a much higher
stirrer speed can be used, thus producing a much higher power charge to the mill
chamber. A smaller bead size can be used which is essential for producing fine particle
sizes with acceptable energy consumption. Furthermore stirred mills are operated at a
much higher grinding media filling ratio, meaning more contact between media and
particles. According to Kwade (1999), the filling ratio can be up to 85 % of the
chamber's net volume. Due to the high filling ratio and high stirrer speeds, the
comminution time is reduced significantly compared to tumbling mills. In addition
Lofthouse and Johns (1999) list the following factors proposed by Holmes (1995) and
Gao & Weller (1994) that are beneficial for stirred media mills: Lower capital,
maintenance and installation costs, smaller footprint, less noise, and high level of
controllability (Altun et. al. 2013), (Gao & Holmes 2007).

4 TEST METHODS

This section introduces the test methods used for determining the energy needed when grinding to the desired product size. These methods are used for different mill types and by different mill manufacturers. Traditionally, mill designers use Bond's test or tests derived from Bond's test for mill sizing. In the fine and especially ultra-fine grinding size range, the Bond test is not practicable. Besides the Bond test, a few other test methods, which suit fine grinding better, are briefly introduced.

4.1 Bond test

The Bond test was developed to obtain material specific energy consumption. It is based on the Bond's third law (2). Bond's third law gives the energy consumption when grinding from an infinite particle size to a size which is 80 % smaller than 100 μm. For actual testwork, the infinite particle size is not practicable so instead energy consumption is measured from feed size F80 to product size P80. In order to calculate energy consumption using the Bond test, a value called the work index must be determined. The work index describes ore grindability and it is assumed that it remains the same regardless of the particle size. For ball mills, the work index is calculated according to equation (18). (Kurki 2006), (Wills 2006)

$$W_i = \frac{49,1}{P_1^{0,23} * G_{bp}^{0,82} * \frac{10}{\sqrt{P_{80}}} - \frac{10}{\sqrt{F_{80}}}} \qquad (18)$$

A laboratory test is mandatory for the work index calculation. For conducting the test, Bond developed a specially designed mill and usd a specific media charge. The diameter and length of the Bond mill is 305 mm and it rotates 70 revolutions per minute. The weight of the media charge is 20,125 kg and it contains 285 balls. The size of the media varies from 12,7 mm to 31,8 mm. The feed amount for the test is the mass of 700 ml of material which is smaller than 6 mesh (3,35 mm). (Kurki 2006) (Levin 1989)

The Bond test is widely used in the grinding sector for grindability testing and the sizing procedure. Originally it was designed to calculate the energy consumed by a wet grinding mill of 2,44 m in diameter operating with a 250 % circulation load in a circuit closed with a classifier. Efficiency factors can be used to adapt the Bond test result for a desired mill circuit design. It has been experienced that the test works fairly well in the conventional grinding range. However, when particles are ground to a fine grinding size range, the test becomes inaccurate. A few methods have also been developed based on the Bond test to cover fine grinding. (Kurki 2006), (Wills 2006)

4.2 Levin test

The Levin test method was developed to describe energy consumption in the fine grinding range more accurately. For calculations it uses equivalent energy per revolution term "B" obtained from the Bond tests. The term can be calculated using equation (19) and is expected to be constant. The value calculated by Levin (1989) from the available data, gave B the following value: 198 x 10^{-7} kWh/rev. However, this value is not constant for all materials and the value is closest to the correct value when the material particle size distribution is traditional. (Levin 1989)

$$B = \frac{4,9*10^{-3}*G^{0,18}}{P_1^{0,23}*(100-U)} \qquad (19)$$

The operating conditions specified in the Bond test are also used in Levin's method. In laboratory tests, a determined amount of material is ground for several different numbers of revolutions. The number of revolutions which gives the desired particle size is estimated from the results. The required amount of energy can then be calculated from equation (20). This energy applies to open-circuit wet grinding in a mill with a diameter of 2,44 m. The same efficiency factors as those used in Bond tests can be used to predict energy consumptions in mills whose design differs from that mentioned above. When simulating a closed circuit, a limiting screen can be used and the energy consumption can be determined accordingly. (Levin 1989)

$$E = \frac{19,8kWh*N}{m} \qquad (20)$$

4.3 Mergan

Niitti (1970) developed the Mergan test method to study ore grindability. The test is performed in batch mode with a specially designed ball mill. The measurements of the mill are 268 x 268 mm. The grinding parameters for the laboratory tests were determined by a test series conducted by Niitti. These tests included the following parameters: the amount of grinding media, the amount of feed material, the circulation speed of the mill, and slurry density. To summarize these tests, the ball charge weight was determined to be 22kg, the size of the ball charge between 15-40 mm, the amount of feed material 1500 ml, the circulation speed of the mill 60 rpm, and the feed density to between 50 – 60 % w/w.

The ball charge mentioned is for a coarse feed and is very similar to the ball charge used in the Bond test. For a finer feed, a different ball charge can be used. A finer ball charge reflects the decreased feed size and gives a better grinding result. From the result obtained in the grinding test, the work index can be calculated by using equation (21) (Kurki 2006)

$$M - W_i = E_0 \left(\frac{\sqrt{F}}{\sqrt{F} - \sqrt{P}} \right) \sqrt{\frac{P}{100}} \qquad (21)$$

4.4 Donda

Donda's model was developed in response to the need to predict the specific energy consumption of regrinding operations. The objective was to perform testwork in a small-scale pilot mill and obtain a reliable specific energy consumption result for full-scale applications. According to Peres et al. (2004), the developed method is simple, standardized, reproducible, and needs only a small amount of test material. Equation (22) used for the energy consumption calculation is shown below. (Peres et al. 2004)

$$kWb = 6,3D^{0,3} \sin \frac{51 - 22(2,44 - D)}{2,44} * \left(3,2 - V_p \right) * C_s \left(1 - \frac{0,1}{2^{9 - 10C_s}} \right) \qquad (22)$$

The parameters and the size of laboratory mill used for testwork are as follows: the mill length and diameter are 254 mm, the density of the slurry is 75 % w/w, the rotating

speed of the mill is 65 % of the critical value, the feed charge weight is 3,5 kg, the ball charge weight is 18 kg, and the diameter of the grinding media varies from 15 mm to 30 mm. Peres et al. (2004) compared the results gained from laboratory tests to the results gained from an industrial size unit. For this particular case Donda's method gave comparable results. The method is not widely used in the industry and there are only a few publications on this subject. (Peres et al. 2004)

4.5 Isa M4

Isa M4 test is a laboratory grinding test. It is used to study grindability, scale-up and effects of parameters on the IsaMill^{TM}. The volume of the mill used in the tests is four liters. The M4 test is operated in pendulum mode. The term signature plot test is also used. The principles of the pendulum mode are described in section 3.3.2. Variables that can be changed in testwork are tip speed, slurry density, grinding media, amount of media, and flow rate. For each stage a sample is taken for particle size analysis. In addition power consumption is recorded by an integrated digital power meter. The laboratory mill uses the same configurations as the full-scale mill. This means continuous feed, internal classifier, the same grinding action, and the same grinding media. Gao et al. (2002) suggested that, according to the studies of Weller et al. (1999b), scale-up can be done directly from the laboratory mill results with no correction factors needed. This has also been proven by results from full size industrial applications. (Shi et al. 2009)

4.6 Jar mill

The Jar mill bench test is a grindability test offered by Metso for the purpose of Vertimill selection. The test is performed with a tumbling mill and in batch mode. It provides specific energy consumption when grinding from F80 to P80. Also various operating parameters can be studied with the test including grinding media size, slurry density and energy inputs. Very little information is available about this test and no articles regarding this subject have been published.

5 TESTWORK

5.1 Test targets

The target of the testwork was to investigate the effect of parameters on grinding efficiency. The parameters under investigation are the tip speed, milling density, flow rate, size and type of grinding media and feed scalping. Table 3 shows the test matrix generated from the aforementioned parameters. The full testwork plan is presented in Appendix 1. A secondary target of the testwork was to create a standardized test environment and achieve test repeatability. Also, two different test methods, continuous and semi-continuous, were tested and compared. In addition, different ways to conduct semi-continuous tests were examined.

Table 3. Test matrix

Filling ratio [v-%]	Milling density % [w/w]	Tip speed [m/s]	Retention time [min]	Bead size [mm]	Bead type	Scalping [µm]
60	43	2	1	1,0-1,2	minerax	20
	53	4	2	2,0-2,2	milmax	35
	63	6	4	2,4-2,6	keramos	50
				3,5	steel	

The effect of the parameters on grinding efficiency was investigated by describing the energy consumption in relation to particle size, so particle size analysis was a major part of the study conducted. When examining the results from the particle size analysis, the characteristics of the test method must be considered. Different analysis methods give different results and for example results from sieving and laser can differ significantly. Non-spherical particles appear larger when spinning in water but a sieve allows larger particles than the screen size to get through (Nesset et al. 2006). Differences between different laser analyzers also exist (Etzler & Deanne 1997) and even between the same devices used by different operators. When measuring particle size in a fine grinding range even a small error or difference in measurement may have a significant effect on the energy consumption. Davey (2002) states that 1 micron difference in sub 5 micron grinds can affect the predicted power draw by more than 50 %.

5.2 Test material

Quartz was chosen as the test material because of its high availability and uniform quality. It can be found in sedimentary, metamorphic and igneous rocks and these rock types occur worldwide. The color of quartz can be brown, violet, gray, yellow or colorless. The density of quartz varies between 2.60 - 2,65 g/cm^3. The molecular formula is SiO_2 and its molecular weight is 60,08 g/mol. On the Mohs scale quartz hardness is seven. The Mohs scale range is from one to ten, ten being diamond. This means that quartz is a very hard mineral and when ground, it demands more energy and causes more wear than most other minerals. (Mineralogy Database 2013)

The quartz for the tests was supplied by Sibelco Nordic. The chemical composition of the quartz according to the supplier is 99,1 % SiO_2, 0,35 % Al_2O_3 and 0,030 % Fe_2O_3 and the particle size is 70- 80 % under 63µm. The particle size given by the supplier was analyzed by sieving. Particle size analysis made by laser gave a P80 value of ~ 90 µm. Laser analyses of the feed samples are presented in Appendix 3.

5.2.1 Scalped feed

The scalped feed was prepared by the Geological Survey of Finland. Scalping was done with a hydrocyclone. In scalping a certain proportion of the feed is classified into two streams that have different particle size distributions. In the hydrocyclone the streams are called the overflow and underflow, the overflow containing the smaller particle size fraction and the underflow the bigger size fraction. After scalping the underflow is pumped to the mill and the overflow is fed to the mill product stream without milling. In the study, the parameters for the hydrocyclone were chosen so that three different feed samples with different particle size distributions were obtained. Table 4 shows the specifications of this classification and Figure 15 the particle size distribution of the hydrocyclone underflow.

Table 4. Scalped feed

	Sample 1		Sample 2		Sample 3	
	overflow	underflow	overflow	underflow	overflow	underflow
Portion of feed [%]	20	80	56	44	44	56
P80 [μm]	10	97	40	129	25	121
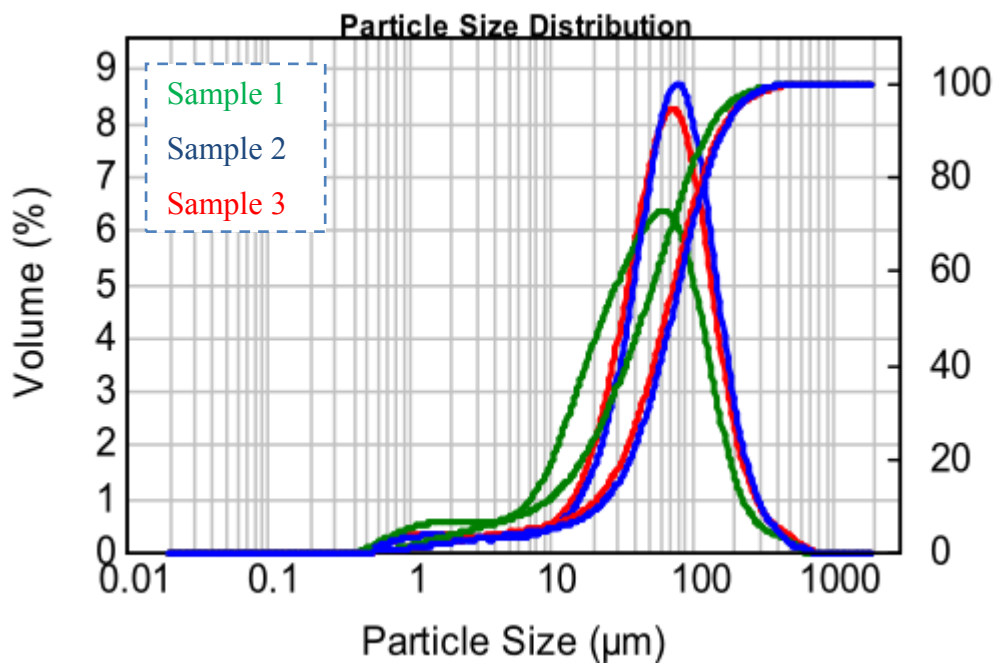
Figure 15. Particle size distribution of the hydrocyclone underflow

5.3 Test methods

Two different test methods, continuous and semi-continuous, were used to test grindability in the HIGmill^{TM}. Most of the tests were made in continuous form. In the continuous test slurry is pumped continuously through the mill and samples are taken after grinding conditions are stabilized. In semi-continuous tests the same material is ground multiple times so considerably less material is needed. The suggested amount for a continuous test is over 100 kg and for a semi-continuous test, 50 kg. Specific energy consumption is calculated in a continuous test according to equation (7) and in a semi-continuous test energy consumption is calculated as a sum of the energy consumption of each pass. In the results section, the power draw calculated from the torque dial is used.

5.3.1 Continuous tests

The test procedure begins with the mill start-up. The tip speed of the mill stirrer is adjusted according to the test plan. Before mill start-up, a water line is connected to the mill. Water is pumped to the mill to impart motion to the beads. The Next step is to set up the circulation to the mixing tank. This is done by installing a pump, which circulates slurry from the bottom of the mixing tank to the top of the tank. This prevents clogging from occurring. When circulation of the feed tank is ready, the making of the slurry batch can be started. In continuous tests, one slurry batch contains enough material to conduct three to four grinding tests. First, water is added to the mixing tank and the mixing is turned on. After that, the right amount of feed material is measured and mixed into the tank. The proportion of the water and feed material is adjusted according to the test plan. A density sample is taken from the end of the circulation hose. Also, mill feed samples for particle size analysis are taken from the same point. The slurry feed rate is adjusted by changing the pump speed to reflect the desired flow rate. If the density and the feed rate are in the right range, the water line going to the mill can be changed to the slurry feed hose.

During start-up, the mill is full with water so before actual grinding starts, the water must be displaced by the slurry. This can be monitored by taking density measurements from the product flow. After the density is stabilized, both the test and the recording from the DriveWindow can be commenced. A sample for particle size analysis can be taken after the slurry has exceeded the mill volume by four times. Usually two to three samples for particle size analysis are taken from one test point. From each sample point power measurements calculated from the torque and given by the frequency converter are stored on Excel. In addition, the torque, pump speed, and mill stirrer speed are saved on the Excel. DriveWindow also saves the data in history files and allows back-checking. In addition, the flow rate and density of the slurry are monitored at each sample point.

The process parameters are changed according to the test plan after the first sample has been taken. Usually the parameter that is changed is the tip speed of the mill stirrer. After the change of parameter, the time that it takes for the slurry to fill four times the mill volume is waited and samples and parameter values are collected from the new test point.

This continues until the planned test is completed. After the testwork, the mill test unit is cleaned thoroughly. The final step of the test procedure is to save the DriveWindow and Excel data and collect the particle size samples for the particle size analysis.

5.3.2 Semi-continuous tests

The basic idea of the semi-continuous test is the same as in the continuous tests. Slurry is prepared and the parameters are adjusted in the same way. The same parameters are monitored and sampling is also done in the same way. The difference between the test methods is that the product from the first grinding stage is used as the feed for the next stage. Thus, semi-continuous testwork requires two mixing tank. In the first grinding stage, mixing tank one is filled with the feed material and mixing tank two is empty. The milled product is fed to the empty mixing tank number two. The first stage continues until tank one is empty. In the second stage, tank two becomes the feed tank. This change is made immediately after tank one is empty. At the beginning of the second stage, the mill is still full of the product ground in the first stage, so the particle size distribution of the product is the same as that of feed. Thus the first mill volume of product can be fed to the feed tank. In the meantime, tank one, acting as a product tank in stage two, is cleaned carefully so that the bigger particles from the previous stage will not become mixed up with the new product. After the first mill volume of slurry has passed through, the product from the previous stage and the new product are mixed up. One choice is to dump the product until steady state is achieved. This would require a bigger test sample. Another way is to feed the slurry directly to the product tank, regardless of possible mixing. The effects of dumping and different dumping times are shown in the results section.

5.4 Equipment used

The testwork was conducted with the pilot scale HIGmill^{TM}, also referred to as the HIG5 mill. A photo of the test set-up is presented in Figure 16. The net volume of this mill is 6,2 l. The internals of the mill can be changed depending on the particle size of the feed. Standard internals consist of twelve discs and responding counter discs. The diameter of the standard disc is 115 mm. When the feed is coarser and bigger beads are used, the internals are changed to coarse internals. The coarse internals contains nine

discs with a diameter of 105 mm. All the testwork presented here was done with standard internals. To rotate the pilot mill stirrer and the discs, a 5,5 kW motor was installed. Slurry was pumped to the mill with a hose pump and feed rates of up to 300 l/h could be used. Table 5 presents other operational and monitoring parameters.

Figure 16.   HIG5 pilot mill set-up with standard internals

Table 5. Operational and monitoring parameters

Operational parameters:	**Monitoring parameters:**
• Tip speed [m/s]	• Power draw [W]
• Feed flow rate [l/h]	• Feed flow rate [l/h]
• Milling density [% w/w]	• Milling density [% w/w]
• Size and type of the bead [-]	• Particle size [μm]
• Filling rate of the beads [%]	• Slurry temperature [ºC]

Tip speed is adjusted using a frequency converter. Power is also calculated from the torque dial installed in the stirrer shaft. Feed pumps and mixer stirrers are adjusted from the frequency converter panel. Data and measurements are recorded in the DriveWindow-program. DriveWindow has the option of saving history data and drawing an online graph from the measurements. Parameters recorded by DriveWindow are: mill tip speed, power gained from the frequency converter, power calculated from torque and pump speed. Besides these parameters, the slurry feed rate, milling density and slurry temperature are also monitored.

In the testwork campaign, four different types of grinding beads were used. The beads were provided by Saint-Gobain, Keramos and Mekeltek. Mekeltek provided steel beads that were originally manufactured for bearings. Saint-Gobain and Keramos provided ceramic beads specially designed for fine grinding. Table 6 presents more detailed information about the beads.

Table 6. Grinding media

Supplier	Brand	Bead size used [mm]	Bead density [g/cm^3]	Bead hardness [HV]	Chemical composition
Saint-Gobain	Minerax	1,0-1,2 2,0-2,2, 3,5	3,9	1250	ZrO_2 15%, SiO_2 7%, Al_2O_3 75 %
Saint-Gobain	Milmax	2,4-2,6	4,1	1050	ZrO_2 46 %, SiO_2 28 %, Al_2O_3 22 %
Keramos	92 series	approx. 2	3,6-3,63	1550	Al_2O_3 92 %, $SiO_2 < 6$ %
Mekeltek	Ball-bearings	approx. 2	7,83	790-890	Fe 96 – 97 %, C 0,9-1,1 & Cr 1,3-1,6 %

Particle size was analyzed using a Malvern Mastersizer 2000 laser analyzer. A photo of the Mastersizer is shown in Figure 17. The Mastersizer uses an optical unit to capture the scattering pattern reflected by a particle. From the scatter, the Mastersizer calculates the particle size. The model used to calculate the particle size was Fraunhofer's model. The main target of the analysis was to compare the results within the test program. Thus it was highly important to analyze all the data with the same procedure. (Malvern Guide 1999)

Figure 17.   Malvern Mastersizer 2000

6 RESULTS

6.1 Power draw

The power draw of the HIGmill^{TM} is affected by the tip speed of the stirrer, retention time, bead size, bead density and bead filling ratio. By changing one of these parameters, the power draw will either decrease or increase. Figures 18 - 21 show how the power draw reacts to these changes. The data behind the figures are presented in Appendix 4.

Figure 18 shows the effect of tip speed. In the test, the bead type, filling ratio and water flow rate were kept constant. The figure shows that the power draw increases exponentially when the tip speed is increased. In Figure 19, the effect of tip speed and flow rate on the power draw is presented when quartz is used as a feed material. Bead size and filling ratio were kept constant. The figure shows two different flow rate values with increasing tip speed. The results indicate that flow rate does not have a big effect on the power draw in the range tested. The tip speed effect on the power draw when the feed material is quartz differs slightly from the results gained from water runs. At a tip speed of 6m/s, the power draw increases exponentially, but after that point, the increase in the power draw reduced.

Effect of tip speed on the power draw

Bead filling ratio: 60 %
Minerax 2,0 - 2,2 mm
Flow rate: 175 l/h

$y = 89.686x^{1.6054}$
$R^2 = 0.9982$
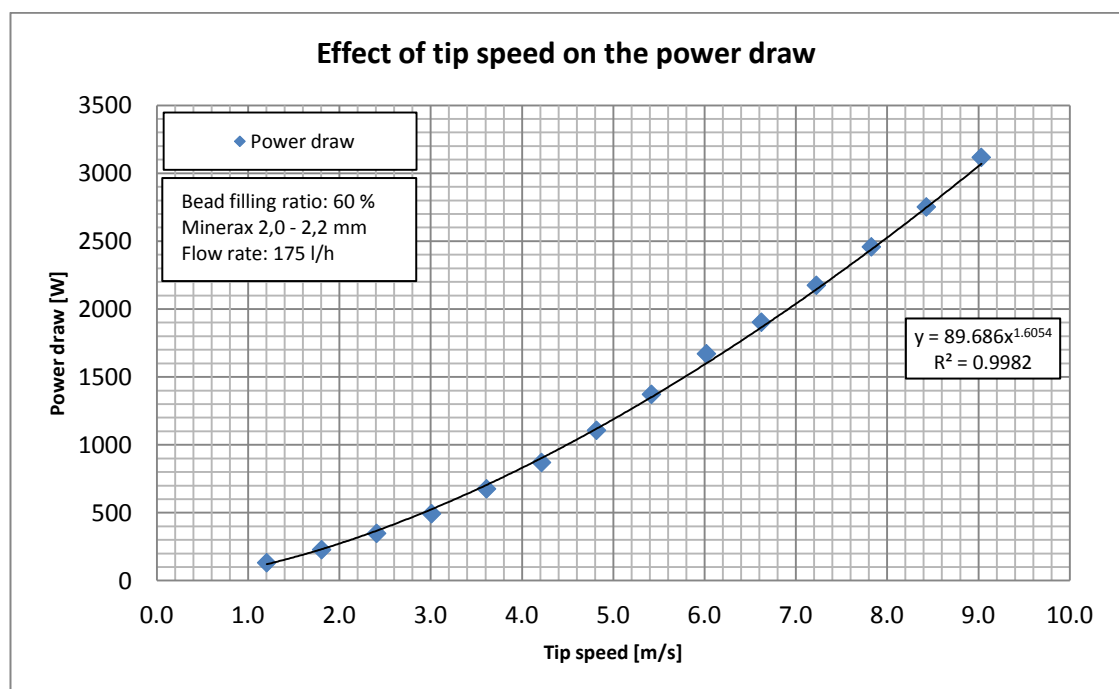
Figure 18.   Effect of tip speed on power draw
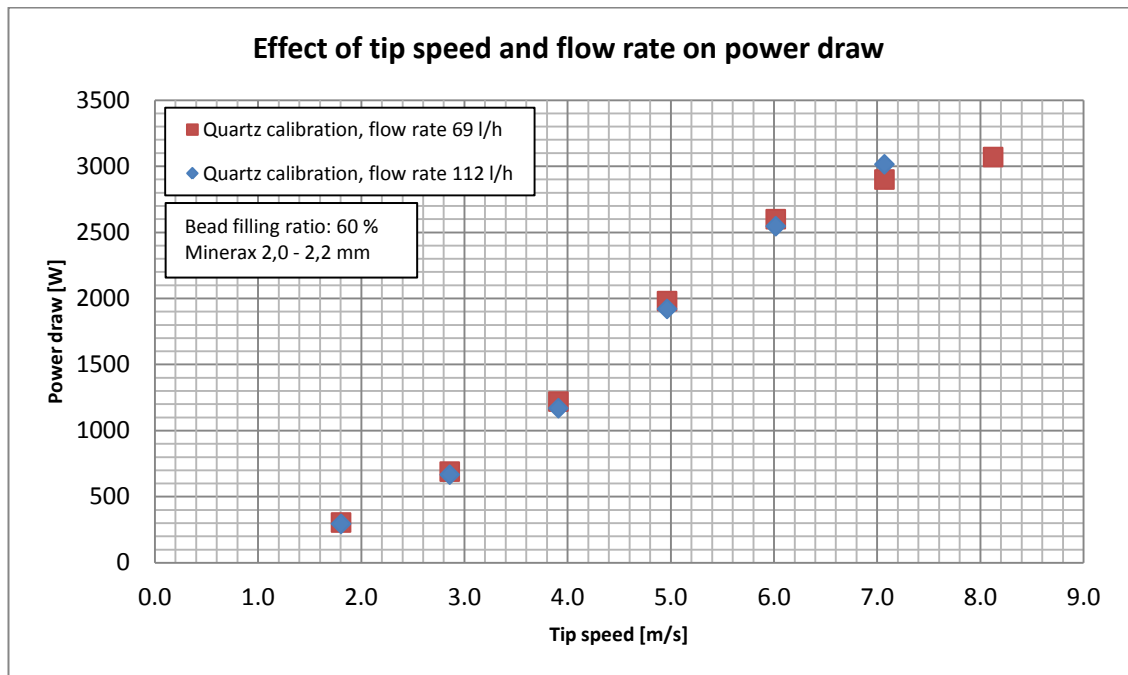
Figure 19.   Effect of tip speed and flow rate on power draw

Besides tip speed, the bead size and density also have a major effect on the power draw. Figure 20 shows trends of different bead sizes at increasing tip speeds. In the testing, three different sizes of Minerax beads were used. During the tests water were continuously pumped to the mill at a constant flow rate. The bead filling ratio was also kept constant. The figure shows that the larger the bead diameter, the higher the power draw. The upper limit of the tip speed was determined to be ~ 7 m/s. After that point, the power draw starts to behave unpredictably and the result are not repeatable.

The effects of bead types are presented in Figure 21. In the testwork four different bead types were compared. The specifications of the beads are shown in Table 6. All the beads have a nearly identical diameter of ~ 2mm. Also, the water flow rate and bead filling ratio were kept constant. Although the filling ratio was constant, variations in bead densities caused variations in the bead load. For example, the load of steel beads was significantly higher than the load of ceramic beads. This of course increases the power draw. However, the two ceramic beads result in almost identical power draws.
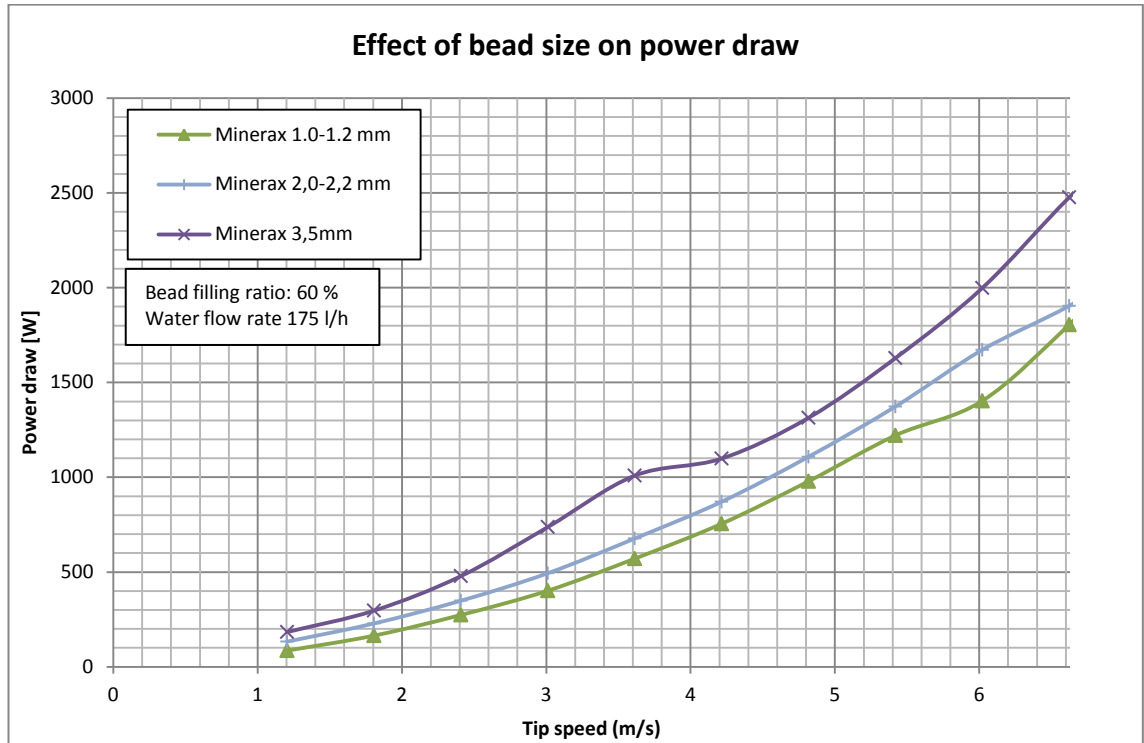
Figure 20. Effect of bead size on power draw
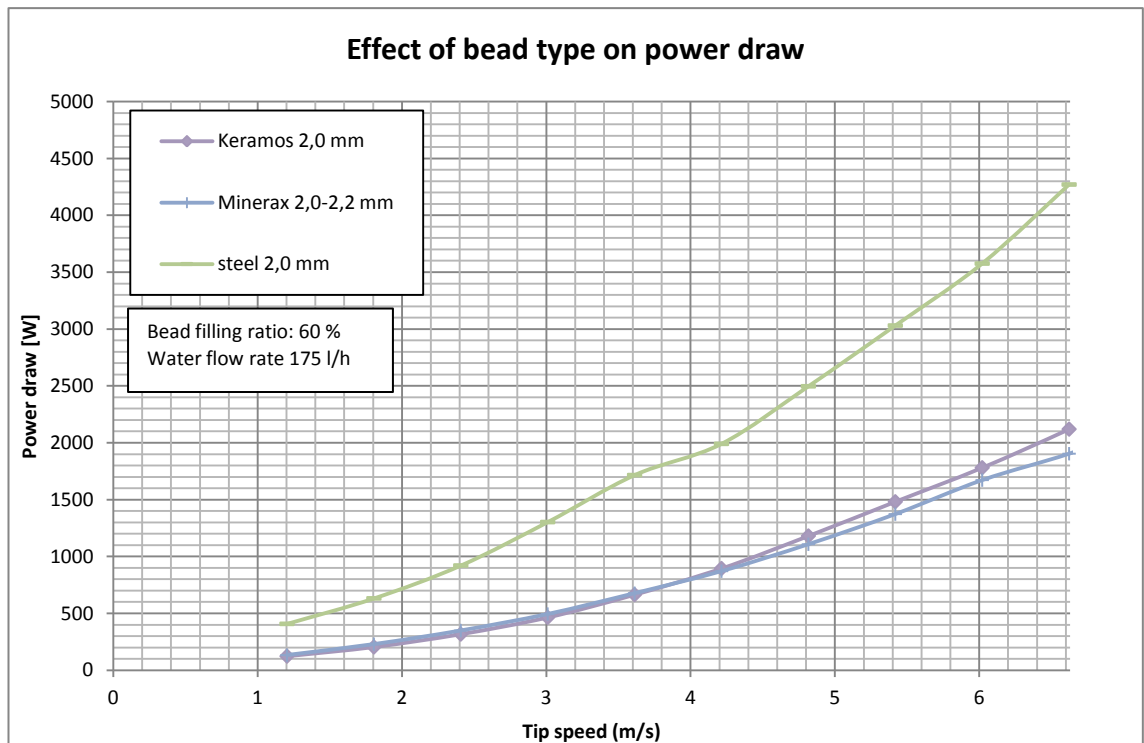
Figure 21. Effect of bead type on power draw

6.2 Grinding efficiency

Grinding efficiency is determined by specific grinding energy (SGE) consumed to obtain a certain particle size (P80). Energy consumption is calculated according to equation (23). All particle size distributions and the data required for SGE calculations can be found in Appendix 5.

$$E_m = \frac{N}{m_p} = \frac{N}{x * \rho * v'} \tag{23}$$

In some studies no load power draw is reduced from the total energy consumption. Equation (24) can be used if the aim is not to exclude any load power draw. In the pilot model HIG5 mill, no load power draw can be calculated using equation (25). The equation (25) is acquired from the testwork presented in Appendix 2. In this study no load power draw is included in the specific grinding energy calculations.

$$E_m = \frac{N - N_o}{m_p} = \frac{N - N_o}{x * \rho * v'} \tag{24}$$

$$N_0 = 8{,}541 * v - 4{,}2857 \tag{25}$$

6.2.1 Effect of tip speed and retention time on grinding efficiency

Figure 22 shows SGE versus particle size with different tip speeds and retention time combinations. Particle size distributions are presented as P80 and P50 values. Tests were made in continuous mode and both variables were tested with three different values. The tip speeds used were 2, 4, and 6 m/s and retention times 1, 2 and 4 min. Retention time describes the time that the slurry takes to fill up one mill volume, i.e. the grinding time. The corresponding flow rates for the above-mentioned retention times in HIG5 mill are 80, 120 and 240 l/h. The other parameters of the test (filling ratio, bead size, bead type, milling density) were kept constant. The tip speed values for test points are presented on the right side of P50 values. The figure shows that the specific energy increases when tip speed increases. Bigger retention time i.e. lower flow rate also increases the SGE value. Moreover, the test point forms a trend that all the data can be described by one curve. This means that, if the specific energy is kept constant, the grinding efficiency stays the same regardless of the tip speed and retention time.
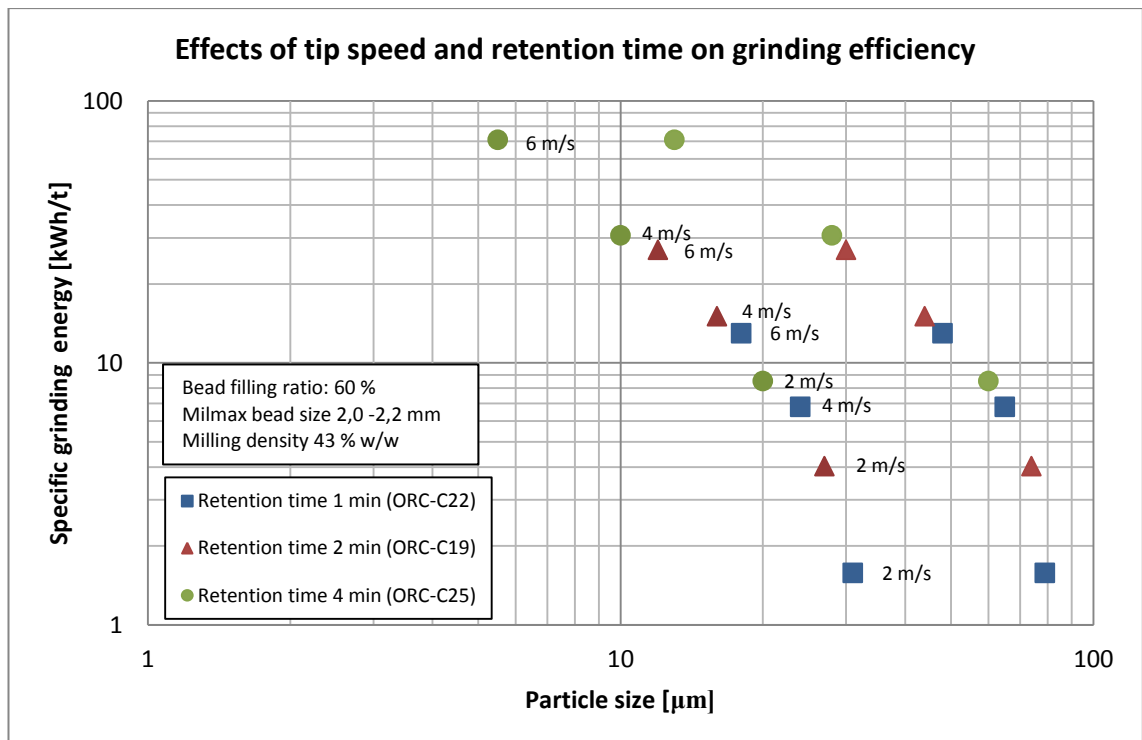
Figure 22.   Effects of tip speed and retention time on grinding efficiency

6.2.2 Effect of milling density on grinding efficiency

Figure 23 demonstrates the effect of milling density on grinding efficiency. The density varied between 43, 53 and 63 % w/w and is presented as a function of SGE and particle size distribution. Particle size distributions are presented as P80 and P50 values. Energy levels are changed by adjusting the tip speed and retention time. The bead filling ratio, bead size and type are kept constant. Basically the test is the same as the one presented in section 6.2.1 but with three different milling densities. Also the same tests (ORC-C19 & ORC-C22 & ORC-C25) are used to present the results when the milling density is 43 % w/w. From the results presented in Figure 23, it can be stated that grinding efficiency stays the same regardless of the milling density in the density range tested.
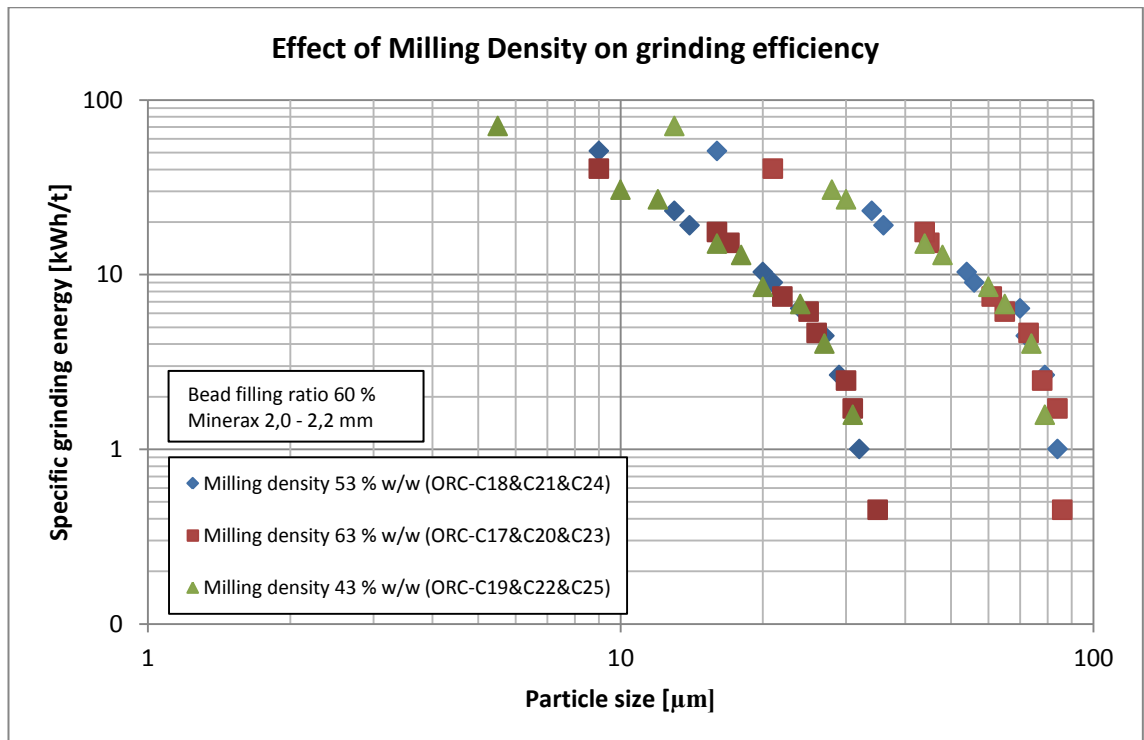
Figure 23. Effect of milling density on grinding efficiency

6.2.3 Effect of bead type on grinding efficiency

The effect of bead type on grinding efficiency was tested with four different bead types. Energy levels were adjusted using the tip speed and retention time. More information about the bead properties can be found in section 5.4. The sizes of the beads used in the test were fairly similar. The filling ratio was 60 % of the mill net volume. Nine points were tested with Milmax, six points with Keramos and three points with Minerax and steel beads. Bead densities varied from 3,6 g/cm^3 to 7,8 g/cm^3 thus the mass of the media charge also varied significantly. For example with beads with the lowest density 8,6 kg was enough to achieve a 60 % filling ratio, but when steel media was used the mass required to acquire the same filling ratio was 18,6 kg. This means that the power draw was substantially higher when steel media was used. Furthermore the difference in power draw affects the SGE, meaning that the same SGE can be achieved with significantly different operational parameters.

For example at the point circled in Figure 24 the same SGE was achieved with steel beads when the tip speed was 1,5 m/s and retention time 2 min and with Milmax beads when the tip speed was 4,0 m/s and retention time 1 min. However, when comparing the grinding efficiency, all the bead types ended up on the same curve, meaning that if the same SGE was used, the grinding efficiency is not affected by bead type or bead density. Figure 24 below compares the effects of the bead type.
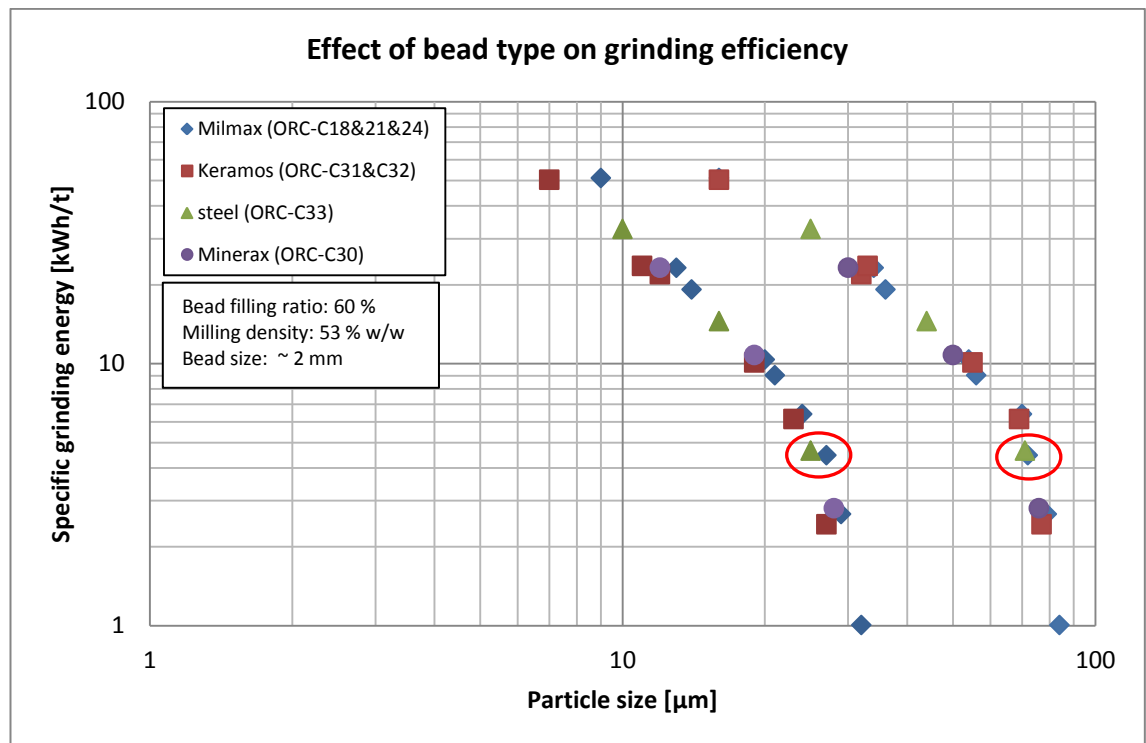
Figure 24. Effect of bead type on grinding efficiency

6.2.4 Effect of bead size on grinding efficiency

The effect of bead size on the grinding efficiency is presented in Figure 25. Particle size distributions are presented as P80 and P50 values. Four different bead sizes were used in this testwork: Milmax 1,0 - 1,2, 2,0 - 2,2, 3,5 mm and Minerax 2,4 - 2,6 mm. The filling ratio was 60 % of the mill net volume and milling density 53 % w/w. Energy levels were adjusted using the tip speed and retention time. The figure shows that the three largest bead sizes produce a nearly identical grinding result if the SGE is kept constant. However, the smallest bead size gives a worse grinding result than the larger beads. This is especially evident when comparing the SGE with the P80 value.
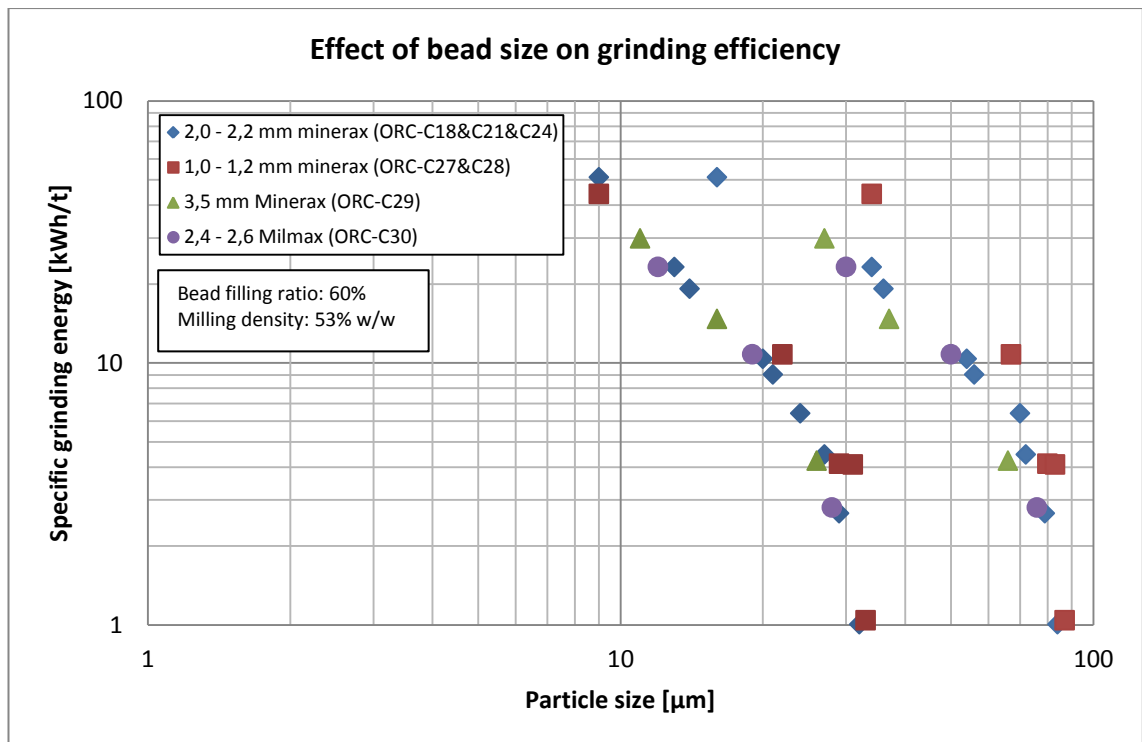
Figure 25.   Effect of bead size on grinding efficiency

6.3 Semi-continuous dumping tests

Semi-continuous dumping tests were made to compare the effects of dumping between grinding stages. At the beginning of each grinding step the mill is filled with the slurry from the previous step. When the grinding stage is changed the first mill volume can be considered to contain the same particle size fraction as the feed. Thus it can be routed back to the feed tank. As the grinding continues, the product particle size becomes smaller than the feed particle size. At this point one option is to dispose of the product, i.e. dump the product until the grinding conditions are stabilized. Stabilized conditions can be considered to be after the slurry has passed four times the mill volume. Another option is to route the product straight to the product tank and ignore any possible mixing. In this test, a comparison was made between dumping three mill volumes and with no dumping. Minerax 2,0 -2,2 mm was used as grinding media and the filling ratio was 60 % of the mill net volume. The tip speed chosen was 4 m/s, the retention time 2 min and the milling density 53 % w/w. The parameters were kept constant during the whole test. Figure 26 shows the result of the dumping test. The figure indicates that dumping has no observable effect on grinding efficiency
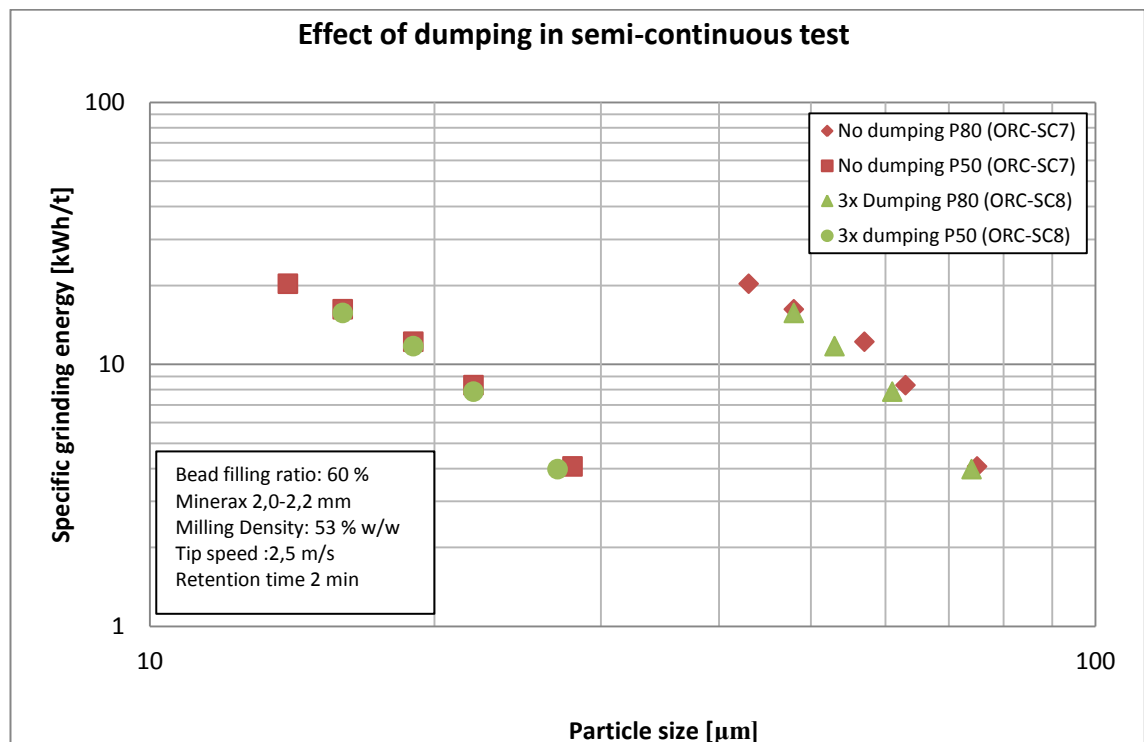
Figure 26.   Effect of dumping in semi-continuous test

6.4 Continuous vs. semi-continuous

In Figure 27, results from the semi-continuous test were compared to the results obtained from the continuous test. In the continuous test energy levels were varied by changing the tip speed, retention time and milling density. In both tests, the bead filling ratio were kept at 60 % and Minerax 2,0 – 2,2 mm was used as grinding media. The plotted semi-continuous tests results are the same dumping test results that were used in the previous section. The result of this comparison is depicted in Figure 27. Both, the dumping and no dumping results from the semi-continuous tests are shown in the graph. The presented particle size distributions are P80 and P50 values. Based on the test data shown in the figure, the semi-continuous and continuous tests give equivalent result.
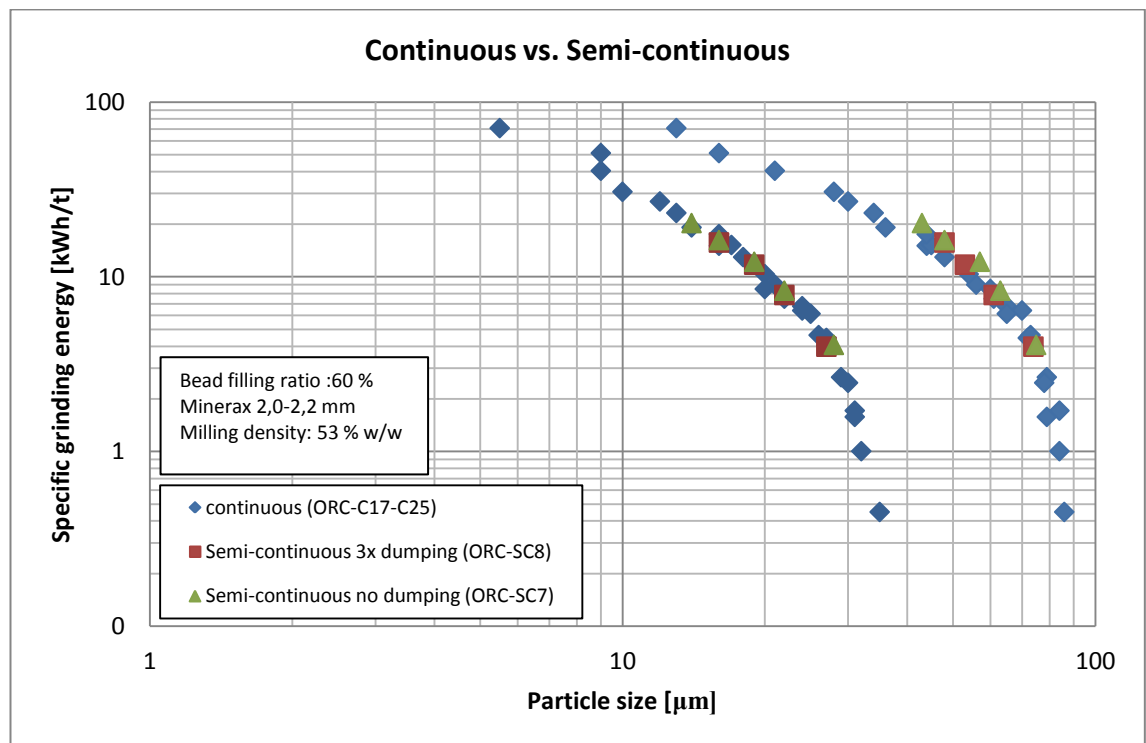
Figure 27.   Comparison between continuous and semi-continuous test methods

6.5 Test repeatability

Basic data for the repeatability test were acquired from the tests where the effect of tip speed, retention time and slurry density was studied. As seen in the previous sections, the above-mentioned parameters did not have an effect on the grinding efficiency if the SGE were kept constant. Thus in Figure 29 all of the results from these tests are plotted under the term "continuous". Furthermore these "continuous" data were compared to the re-test results. The re-test was made solely to study whether the results in the continuous data could be repeated. In the re-test, six points were plotted and the energy levels were adjusted by means of the tip speed and retention time. In both tests, Milmax 2,0 - 2,2 mm were used as a grinding media and the filling ratio was 60 % of the mill net volume. The equivalence of the tests can be seen in Figure 28.
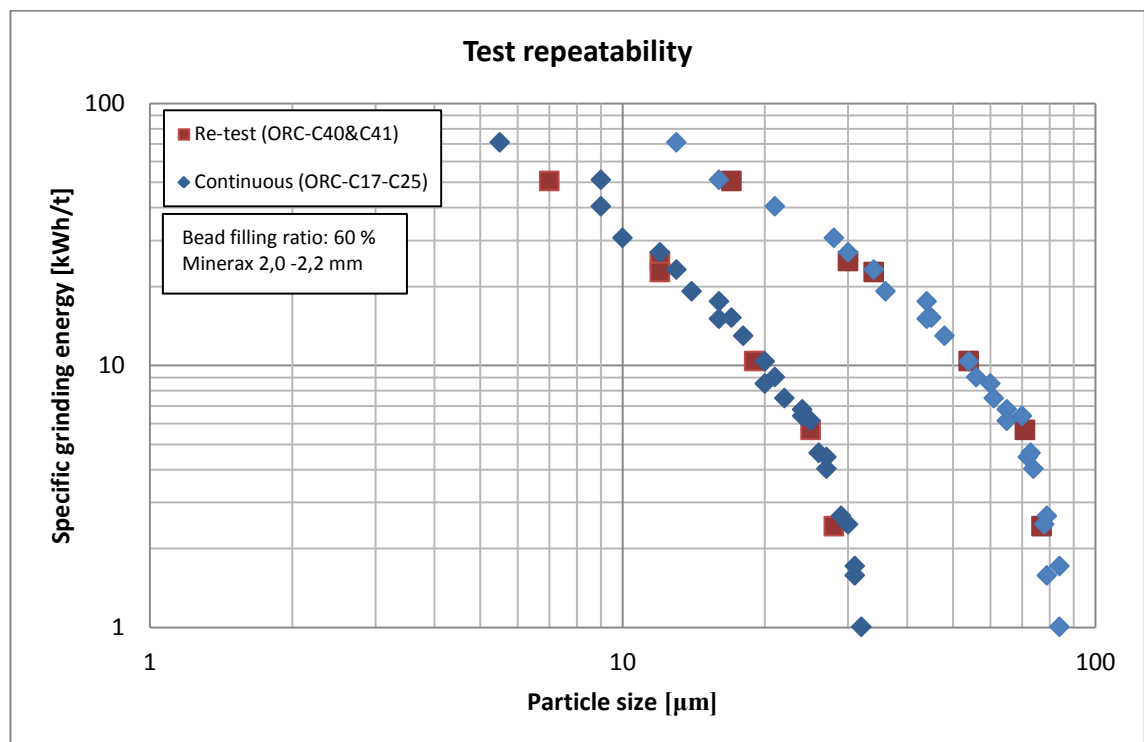
Figure 28.   Test repeatability

6.6 Effects of scalping on grinding efficiency

Scalping test was conducted in continuous mode. Energy levels were adjusted by changing the tip speed and retention time. In all tests grinding media filling ratio was 60 % and media type Minerax 2,0 – 2,2 mm. Besides the normal feed, three scalped feeds were tested. The F80 values for the scalped feeds are the following: 129 μm (sample 2), 121 μm (sample 3.) and 97 μm (sample 1.). The results of how scalping affects the grinding efficiency are depicted in Figure 29. The bigger the F80 value, the more energy was consumed in grinding.
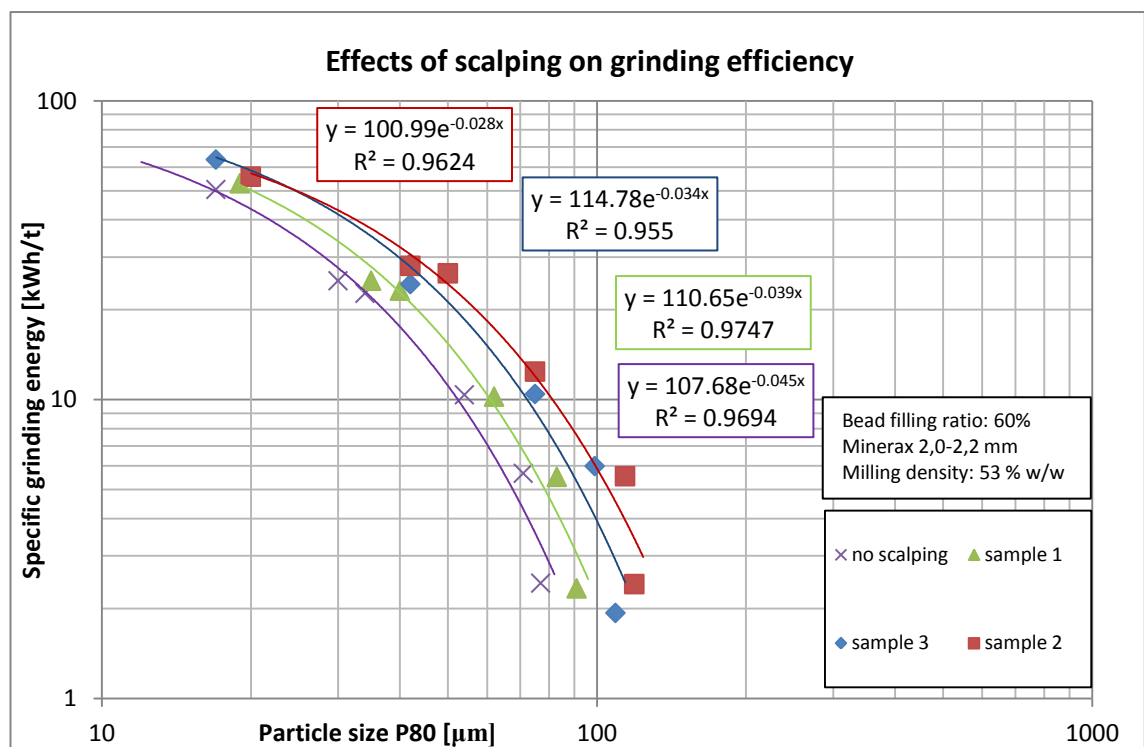
Figure 29.   Effects of scalping on grinding efficiency

6.7 Experimental results vs. energy theories

In this section, experimental results are plotted against energy consumption theories. The theories used are those of Kick, Von Rittinger, Bond, and the model obtained in the studies made by Schwedes, Stehr and Weit. Table 7 shows the equations of these models. Term "C" was chosen so that the equation would depict the experimental data as well as possible. Figure 30 shows the results of this comparison. It shows that Kick

and Bond predict the experimental data results well at the coarse end of the curve. At the fine end the correlation starts to deteriorate. In the Kick theory this occurs after the particle size is finer than 30 μm and in the Bond theory after 15 μm. The Schwedes, Stehr and Weit equations seems to fit the data well in the fine particle size range, but gives inaccurate results at the coarse end. For the four tested theories Von Rittenger gives the most accurate result and predicts energy consumption well over the whole size range tested.

Table 7.   Energy theories

	Kick	Bond	Von Rittinger	Schwedes, Stehr & Weit
Equation	$dE = -C\,\dfrac{dx}{x^n}$	$E = C\left(\dfrac{1}{\sqrt{x_{P80}}} - \dfrac{1}{\sqrt{x_{F80}}}\right)$	$E = C\left(\dfrac{1}{x_P} - \dfrac{1}{x_F}\right)$	$x_p = C * E_m^b$
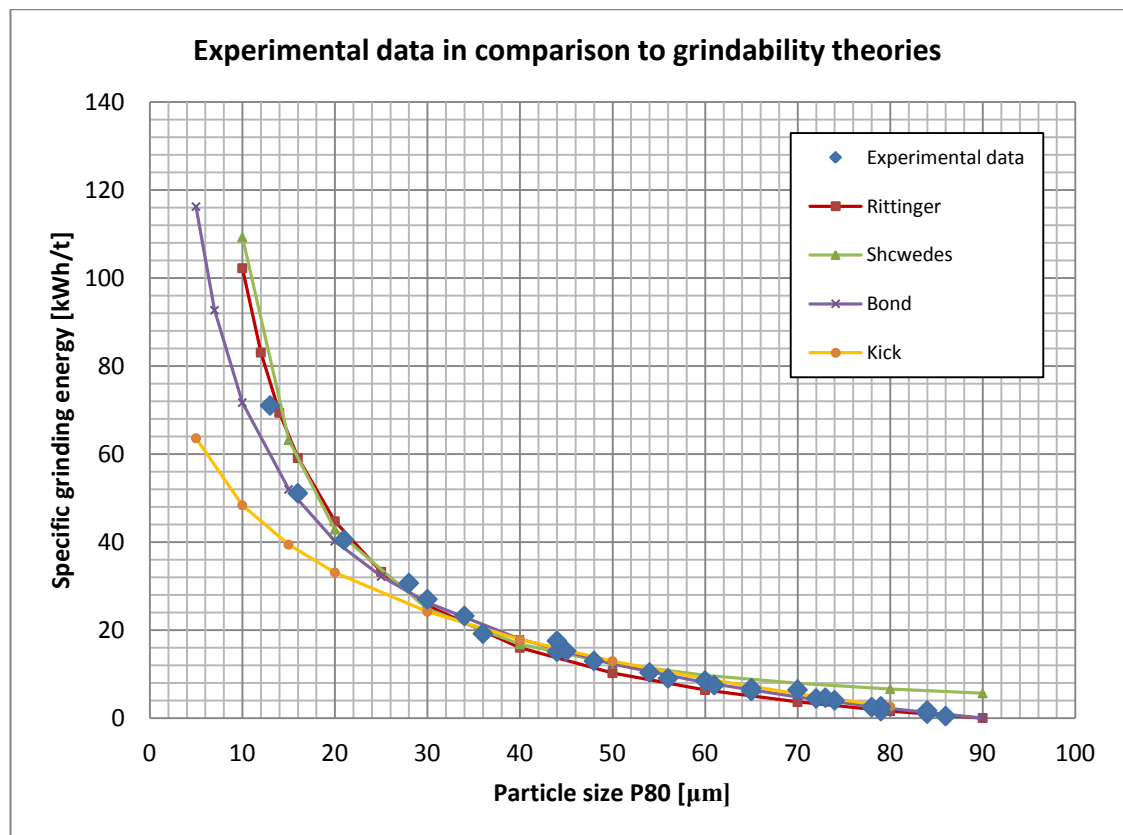
Figure 30.   Experimental data in comparison to energy grindability theories

7 DISCUSSION

The HIGmill^{TM} turns out to be very flexible to a change of operating parameters as far as grinding efficiency is concerned. Tip speed and retention time seem to have no effect on the grinding result within the tested range as long as the SGE stays the same. It means that the fluctuation in the slurry flow rate can be overcome by adjusting the tip speed. This can be regarded as a major benefit when operating a full-size mill in industrial applications.

Results from the milling density comparisons differed from what was expected. In the literature review, a higher milling density was suggested to give a better grinding result. However, this was not the case in the testwork conducted and milling density proved to have no notable effect on grinding efficiency within the size range tested. This is also beneficial in industrial applications because fluctuations in the feed solids can also be overcome by changing the tip speed.

Comparisons between bead types were made with nearly identical bead sizes and with same bead filling ratio. Due to the differences in bead densities the bead load varied significantly. However, when comparing different bead types with respect of grinding efficiency, bead type had no significant effect to the result.

The only parameter that was found to have affected the grinding efficiency of the parameters tested was the size of the grinding beads. This was also pointed out in the literature review. The trend seen in the bead size comparison showed that bigger bead size gave a better result with the feed size tested. Nor were any significant differences observed between the three biggest beads (2,0 - 2,2, 2,4 - 2,6 and 3,5 mm). The grinding efficiency with the lowest bead size (1,0 - 1,2 mm) was notably lower than with the other bead sizes tested. This suggests that the bead size should be at least 20 times greater than the feed F80 value to achieve effective size reduction. At the beginning of the grinding, results show that up to ~35 times greater beads give the best result. As the feed size decreases, the optimal bead size also decreases. When the gap between feed size and product size widens, the selection of optimal bead size becomes more difficult. At this point, a graded grinding media charge could be the best option.

Dumping between grinding stages in semi-continuous tests does not seem to have a major impact on grinding efficiency. Also continuous and semi-continuous tests seem to mirror each other when the same amount of energy is inputted. This means that basic testwork with the HIGmill^{TM} can be done in semi-continuous mode and with substantially lower amounts of feed sample. In addition there is no need to dump material between grinding stages, thus tests can be made with even less material.

In the test repeatability section the results from the re-tests were compared to the data obtained from the tip speed, retention time, and milling density tests. According to the comparison results, pilot HIGmill^{TM} tests can be said to be repeatable. In addition quartz, proved to be a very abrasive rock type and caused wear to the discs. Also, the re-tests were the last part of the testing program and multiple runs between the compared tests were carried out. The re-test gave the same result regardless of the disc wear and did not have effect on repeatability.

The effects of scalping were studied in comparison with a non-scalped feed. The result from the test was expected. The specific energy consumption grows, when the particle size of feed rises.

The comparison of experimental data with grindability theories gave surprising results. The literature suggests that the Bond theory and especially the Kick theory do not work in the fine grinding range. The results obtained in this study showed that both of the theories predict energy consumption well for comparatively small particle sizes. For example in this study the Bond theory works well to a limiting particle size of 15 μm. For the grindability tests compared, Von Rittenger theory gives the best SGE prediction over the size range tested.

7.1 Sources of error

The testwork conducted was large and multiphase, so some sources of error may also be discovered. In the grinding procedure flow rate measurements were taken manually, so some errors are possible. Also, density measurements were conducted manually. Variations in the measurements can be seen as a scatter in the figures. However, the results obtained are consistent and multiple test points were used to analyze the trend and behavior of a certain phenomenon. Thus, the possibility for error was reduced.

The Biggest challenge regarding the test was the reliability of the particle size analysis. As mentioned above, an absolute value for a certain distribution is very hard to obtain. Different devices, calculations, and sampling mechanisms create a different particle size distribution. This challenge was solved by the same person using the same device and the same procedure, and comparing the results between each other.

8 CONCLUSION

The HIGmill^{TM} proved to be very flexible to changes in parameters. If the specific grinding energy were kept constant, the grinding efficiency stayed the same regardless of changes in bead type, tip speed, retention time or milling density. Even the wear of the mill internals proved not to have any notable effect on the grinding result. This gives the HIGmill^{TM} a major advantage when used in industrial applications. Often constant feed quality is hard to maintain and usually some fluctuations in the slurry feed properties occur. In the HIGmill^{TM}, the fluctuation of the feed can be overcome by changing the tip speed so that the SGE value is always kept in the right range, thus keeping the product particle size in the desired size range.

Besides the variables mentioned, the effects of bead size were tested against grinding efficiency. Bead size had a notable effect on the grinding result and was also the only parameter tested where grinding efficiency could not be depicted by plotting specific energy and particle size distribution. For the particle size range tested, the results suggest that the bead size should be at least 20 times greater than the feed F80 value to achieve effective size reduction.

Semi-continuous tests were verified to be equivalent to the continuous test. In addition, dumping between grinding stages had no significant effect on grinding efficiency. This can be seen as a very positive outcome. It means that smaller sample amounts are needed to perform basic grinding tests. Large samples can turn out to be a limiting factor when making offers to customers. In greenfield projects in particular, large amounts of samples can be hard to obtain.

9 FURTHER INVESTIGATIONS

This study focused on the basic testwork conducted with the Outotec pilot HIGmill[TM]. The Testwork covered most of the basic issues related to the fine grinding. Studies pointed out that the effects of the grinding media size on grinding efficiency were notable. In addition, specific grinding energy was not able to predict the mill efficiency when different bead sizes were used. The literature suggests that the stress model approach can be used to account for the effects of the grinding media size. This approach should be investigated in the HIGmill[TM].

The literature suggests that the movement of beads varies with different mill chamber sizes. This will have an effect on the grinding efficiency. By studying the movement of the beads, more information for can be obtained for a scale-up procedure. The study could be conducted with pilot-scale HIG5 and HIG25 mills.

10 REFERENCES

ALTUN, O., BENZER, H. and ENDERLE, U., 2013. Effects of operating parameters on the efficiency of dry stirred milling. *Minerals Engineering,* **43-44**, pp. 58-66.

BARRY A. WILLS., 2006. *Wills' mineral processing technology.* 7th ed. edn. GB: Butterworth Heinemann.

BERNOTAT, S. and SCHÖNERT, K., 2000. Size Reduction. *Ullmann's Encyclopedia of Industrial Chemistry.* Wiley-VCH Verlag GmbH & Co. KGaA, .

BREITUNG-FAES, S. and KWADE, A., 2013. Prediction of energy effective grinding conditions. *Minerals Engineering,* **43-44**, pp. 36-43.

DAVEY, G., 2002. Ultrafine and fine grinding using the Metso Stirred Media Detritor,(SMD), *Proceedings of the 34th annual meeting of the Canadian Mineral Processors* 2002, pp. 153-169

ETZLER, F.M. and DEANNE, R., 1997. Particle size analysis: A comparison of various methods II. *Particle and Particle Systems Characterization,* **14**(6), pp. 278-282.

FLSMIDTH, 2013. Company website, referred to on 25.11.2013. Available at: http://www.flsmidth.com/

GAO, M. and WELLER, K., 1994. A comparison of tumbling mills and stirred ball mills for wet grinding, *Fifth Mill Operators Conference, Australian Institute of Mining and Metallurgy, Australia* 1994, pp. 61-67.

GAO, M., FORSSBERG, K.S.E. and WELLER, K.R., 1996. Power predictions for a pilot scale stirred ball mill. *International Journal of Mineral Processing,* **44-45**(SPEC. ISS.), pp. 641-652.

GAO, M., WELLER, K. and ALLUM, P., 1999. Scaling-up horizontal stirred mills from a 4-litre test mill to a 4000-litre "IsaMill", *Powder Technology Symposium, Pennsylvania State University, Pennsylvania, USA, September* 1999.

GAO, M., YOUNG, M. and ALLUM, P., 2002. IsaMill fine grinding technology and its industrial applications at Mount Isa Mines, *34th Annual Meeting Of The Canadian Mineral Processors* 2002.

GAO, M. and HOLMES, R., 2007. Grinding them down. *Materials World,* **15**(5), pp. 38-40.

GÜNTER, H., THEISEN, W. and WETZEL, D., 2000. MaxxMill - dry and wet grinding with stirred ball mills in comparison with conventional tumbling mills. *Aufbereitungs-Technik/Mineral Processing,* **41**(6), pp. 278-283.

HOLMES, H., 1995. Current and Future Trends in Grinding Mills, *M.E.S Annual meeting,* Camborne, Cornwall, UK.

HUKKI, R.T., 1964. *Mineraalien hienonnus ja rikastus.* Hki: Teknillisten tieteiden akatemia.

ISAMILL, 2013. Company website, referred to on 25.11.2013. Available at: http://www.isamill.com/EN/Pages/default.aspx

JANKOVIC, A., 2001. Media stress intensity analysis for vertical stirred mills. *Minerals Engineering,* **14**(10), pp. 1177-1186.

JANKOVIC, A., 2003. Variables affecting the fine grinding of minerals using stirred mills. *Minerals Engineering,* **16**(4), pp. 337-345.

JANKOVIC, A., 2008. *A Review of Regrinding and Fine Grinding Technology-The Facts and Myths,* .

KARIRANTA, P., 2012. Fluidi- ja partikkelitekniikka I. *Lecture series in University of Oulu in laboratory of fibre and particle engineering.*

KURKI, P., 2006. *Jauhautuvuuden määritys panos-jauhatuskokeilla*, Helsingin teknillinen korkeakoulu.

KWADE, A., 2006. Specific energy consumption, stress energy, and power draw of stirred media mills and their effect on the production rate, *2006 SME Annual Conference - Advances in Comminution* 2006, pp. 99-114.

KWADE, A., 1999a. Wet comminution in stirred media mills - Research and its practical application. *Powder Technology,* **105**(1-3), pp. 14-20.

KWADE, A., BLECHER, L. and SCHWEDES, J., 1996. Motion and stress intensity of grinding beads in a stirred media mill. Part 2: Stress intensity and its effect on comminution. *Powder Technology,* **86**(1), pp. 69-76.

KWADE, A. and STENDER, H.-., 1998. Constant grinding results at scale-up of stirred media mills. *Aufbereitungs-Technik,* **39**(8), pp. 373-382.

KWADE, A., 1999b. Determination of the most important grinding mechanism in stirred media mills by calculating stress intensity and stress number. *Powder Technology,* **105**(1–3), pp. 382-388.

KWADE, A. and SCHWEDES, J., 2007. Chapter 6 Wet Grinding in Stirred Media Mills. *Handbook of Powder Technology.* Elsevier Science B.V., pp. 251-382.

LEHTO, H., ROITTO, I., PAZ, A., and ÅSTHOLM, M., 2013. *Outotec HIGmills; Fine Grinding Technology, 2013 23rd International mining conference and exhibition of Turkey.*

LEVIN, J., 1989. Observations on the bond standard grindability test, and a proposal for a standard grindability test for fine materials. *Journal of The South African Institute of Mining and Metallurgy,* **89**(1), pp. 13-21.

LICHTER, J.K.H. and DAVEY, G., 2006. Selection and sizing of ultrafine and stirred grinding mills, *2006 SME Annual Conference - Advances in Comminution* 2006, pp. 69-85.

LOFTHOUSE, C.H. and JOHNS, F.E., 1999. The svedala (ECC International) detritor and the metals industry. *Minerals Engineering,* **12**(2), pp. 205-217.

LUKKARINEN, T., 1984. *Mineraalitekniikka. Osa 1, Mineraalien hienonnus.* [Hki]: Insinööritieto.

MALVERN GUIDE 1999. Operators guide, issue 2,0 (MAN 0247).

METSO 2013. Company website, referred to on 25.11.2013. Avalaible at: http://www.metso.com/

MINERALOGY DATABASE, 2013. referred to on 16.10.2013. Available at: http://webmineral.com/

MOLLS, H. and HORNLE, R., 1972. Wirkungsmechanismus der Nasszerkleinerung in der ruhwerkskugelmuhle. *DECHEMA-Monography,* **69**, pp. 631-661.

MORRELL, S., 2004. An alternative energy-size relationship to that proposed by Bond for the design and optimisation of grinding circuits. *International Journal of Mineral Processing,* **74**(1-4), pp. 133-141.

NDT, 2013. Introduction to Materials and Processes. *Lecture series in NDT Resource Center.* Referred 11.11.2013. Available at: http://www.ndt-ed.org/EducationResources/CommunityCollege/Materials/cc_mat_index.htm

NESSET, J., RADZISZEWSKI, P., HARDIE, C. and LEROUX, D., 2006. Assessing the performance and efficiency of fine grinding technologies, *Proceedings of 38th Annual Canadian Mineral Processor Operators Conference, January* 2006, pp. 17-19.

NIITTI, T., 1970. Rapid evaluation of grindability by a simple batch test, *IX th International Mineral Processing Congress, Czech Republic* 1970, pp. 41-45.

OUTOTEC, 2013. Company website, referred to on 25.11.2013. Available at: http://www.outotec.com/

PITCHUMANI, R., ZHUPANSKA, O., MEESTERS, G.M.H. and SCARLETT, B., 2004. Measurement and characterization of particle strength using a new robotic compression tester. *Powder Technology,* **143–144**(0), pp. 56-64.

PERES, A., DONDA, J. and GUIMARÃES, R., 2004. Water savings: a key to sustainability in mineral processing, *Proceedings of the 1st International Conference on Advances in Mineral Resources Management and Environmental Geotechnology (AMIREG 2004)* 2004, HELIOTOPOS CONFERENCES, p. 343.

PEUKERT, W., 2004. Material properties in fine grinding. *International Journal of Mineral Processing,* **74**(SUPPL.), pp. S3-S17.

PÖLLÄNEN, E. and KUOPANPORTTI, H., 1994. *Mekaaninen prosessitekniikka. 1, Luentomoniste.* University of Oulu.

RADZISZEWSKI, P., 2012. Assessing the stirred mill design space. *Minerals Engineering,* **41**, pp. 9-16.

RAHAL, D., ERASMUS, D. and MAJOR, K., 2011a. Knelson-Deswik Milling Technology: Bridging the Gap between Low and High Speed Stirred Mills.

RAHAL, D., ROBERTS, K. and RIVETT, T., 2011b. Knelson-Deswik mill: Evaluation of operating variables, *SME Annual Meeting and Exhibit and CMA 113th National Western Mining Conference 2011* 2011, pp. 302-307.

RAJAMANI, R.K., MISHRA, B.K., VENUGOPAL, R. and DATTA, A., 2000. Discrete element analysis of tumbling mills. *Powder Technology,* **109**(1–3), pp. 105-112.

ROUFAIL, R. and KLEIN, B., 2010. Mineral liberation and particle breakage in stirred mills. *Canadian Metallurgical Quarterly,* **49**(4), pp. 419-428.

SACHWEH, J., 2000. MaxxMill-Dry and Wet Grinding with Stirred Ball Mills in Comparison with Conventional Tumbling Mills. *AUFBEREITUNGSTECHNIK,* **41**(6), pp. 278-283.

SHI, F., MORRISON, R., CERVELLIN, A., BURNS, F. and MUSA, F., 2009. Comparison of energy efficiency between ball mills and stirred mills in coarse grinding. *Minerals Engineering,* **22**(7–8), pp. 673-680.

STADLER, R., POLKE, R., SCHWEDES, J. and VOCK, F., 1990. Wet grinding in agitated ball mills. *Chemie-Ingenieur-Technik,* **62**(11), pp. 907-915.

STENDER, H.-., KWADE, A. and SCHWEDES, J., 2004. Stress energy distribution in different stirred media mill geometries. *International Journal of Mineral Processing,* **74**(SUPPL.), pp. S103-S117.

STM, 2013. Company website, referred to on 25.11.2013. Available at: http://www.stmminerals.com/?pid=home

TUUNILA, R., 1997. Ultrafine grinding of FGD and phosphogypsum with an attrition bead mill and a jet mill: optimisation and modelling of grinding and mill comparison. Lappeenranta University of Technology.

VAN SCHOOR, J. and SANDENBERGH, R., 2012. Evaluation of the batch press as a laboratory tool to simulate medium-pressure roller crushers. *Journal of the Southern African Institute of Mining and Metallurgy,* **112**(3), pp. 185-196.

WANG, Y. and FORSSBERG, E., 2007. Enhancement of energy efficiency for mechanical production of fine and ultra-fine particles in comminution. *China Particuology,* **5**(3), pp. 193-201

WELLER, K., GAO, M., 1999a. Ultra-fine grinding, *1999 AJM Crushing and Grinding Conference,* Kalgoolie, Australia.

YUE, J. and KLEIN, B., 2006. Effects of bead size on ultrafine grinding in a stirred bead mill, *2006 SME Annual Conference - Advances in Comminution* 2006, pp. 87-98.

APPENDIX 1 TEST PLAN

number	Test 2 numb.	Test 3 numb	tip speed [m/s]	milling density [%]	bead size [mm]	bead type	bead density [t/m3]	retention time [min]	filling rate [%]	
HIG5-ORC-C7-B1	HIG5-ORC-C17-B1		2	63	2,0 - 2,2	minerax	3,91	2	60	
HIG5-ORC-C7-B2	HIG5-ORC-C17-B2		4	63	2,0 - 2,2	minerax	3,91	2	60	
HIG5-ORC-C7-B3	HIG5-ORC-C17-B3		6	63	2,0 - 2,2	minerax	3,91	2	60	
HIG5-ORC-C4-B1	HIG5-ORC-C18-B1	HIG5-ORC-C40-B1	2	53	2,0 - 2,2	minerax	3,91	2	60	effects of the slurry density, retention time 2
HIG5-ORC-C4-B2	HIG5-ORC-C18-B2	HIG5-ORC-C40-B2	4	53	2,0 - 2,2	minerax	3,91	2	60	
HIG5-ORC-C4-B3	HIG5-ORC-C18-B3	HIG5-ORC-C40-B3	6	53	2,0 - 2,2	minerax	3,91	2	60	
HIG5-ORC-C8-B1	HIG5-ORC-C19-B1		2	43	2,0 - 2,2	minerax	3,91	2	60	
HIG5-ORC-C8-B2	HIG5-ORC-C19-B2		4	43	2,0 - 2,2	minerax	3,91	2	60	
HIG5-ORC-C8-B3	HIG5-ORC-C19-B3		6	43	2,0 - 2,2	minerax	3,91	2	60	
HIG5-ORC-C9-A1	HIG5-ORC-C20-A1		2	63	2,0 - 2,2	minerax	3,91	1	60	
HIG5-ORC-C9-A2	HIG5-ORC-C20-A2		4	63	2,0 - 2,2	minerax	3,91	1	60	
HIG5-ORC-C9-A3	HIG5-ORC-C20-A3		6	63	2,0 - 2,2	minerax	3,91	1	60	
HIG5-ORC-C6-A1	HIG5-ORC-C21-A1		2	53	2,0 - 2,2	minerax	3,91	1	60	effects of the slurry density, retention time 1
HIG5-ORC-C6-A2	HIG5-ORC-C21-A2		4	53	2,0 - 2,2	minerax	3,91	1	60	
HIG5-ORC-C6-A3	HIG5-ORC-C21-A3		6	53	2,0 - 2,2	minerax	3,91	1	60	
HIG5-ORC-C10-A1	HIG5-ORC-C22-A1		2	43	2,0 - 2,2	minerax	3,91	1	60	
HIG5-ORC-C10-A1	HIG5-ORC-C22-A2		4	43	2,0 - 2,2	minerax	3,91	1	60	
HIG5-ORC-C10-A1	HIG5-ORC-C22-A3		6	43	2,0 - 2,2	minerax	3,91	1	60	
HIG5-ORC-C11-C1	HIG5-ORC-C23-C1		2	63	2,0 - 2,2	minerax	3,91	4	60	
HIG5-ORC-C11-C2	HIG5-ORC-C23-C2		4	63	2,0 - 2,2	minerax	3,91	4	60	
HIG5-ORC-C11-C3	HIG5-ORC-C23-C3		6	63	2,0 - 2,2	minerax	3,91	4	60	
HIG5-ORC-C5-C1	HIG5-ORC-C24-C2	HIG5-ORC-C41-C1	2	53	2,0 - 2,2	minerax	3,91	4	60	effects of the slurry density, retention time 4
HIG5-ORC-C5-C2	HIG5-ORC-C24-C2	HIG5-ORC-C41-C2	4	53	2,0 - 2,2	minerax	3,91	4	60	
HIG5-ORC-C5-C3	HIG5-ORC-C24-C2	HIG5-ORC-C41-C3	6	53	2,0 - 2,2	minerax	3,91	4	60	
HIG5-ORC-C14-C1	HIG5-ORC-C25-C2		2	43	2,0 - 2,2	minerax	3,91	4	60	
HIG5-ORC-C14-C2	HIG5-ORC-C25-C2		4	43	2,0 - 2,2	minerax	3,91	4	60	
HIG5-ORC-C14-C3	HIG5-ORC-C25-C2		6	43	2,0 - 2,2	minerax	3,91	4	60	
HIG5-ORC-C6-A2			4	53	2,0 - 2,2	minerax	3,91	1	60	
HIG5-ORC-C15-B1			4	53	2,0 - 2,2	minerax	3,91	2	60	effects of the retention time
HIG5-ORC-C15-C1			4	53	2,0 - 2,2	minerax	3,91	4	60	
HIG5-ORC-C15-D1			4	53	2,0 - 2,2	minerax	3,91	6	60	
HIG5-ORC-C4-B1			2	53	2,0 - 2,2	minerax	3,91	2	60	
HIG5-ORC-C12-B1			3	53	2,0 - 2,2	minerax	3,91	2	60	
HIG5-ORC-C12-B2			4	53	2,0 - 2,2	minerax	3,91	2	60	
HIG5-ORC-C12-B3			5	53	2,0 - 2,2	minerax	3,91	2	60	effects of the tip speed
HIG5-ORC-C13-B1			6	53	2,0 - 2,2	minerax	3,91	2	60	
HIG5-ORC-C13-B2			7	53	2,0 - 2,2	minerax	3,91	2	60	
HIG5-ORC-C13-B3			8	53	2,0 - 2,2	minerax	3,91	2	60	

HIG5-ORC-C26-B1	HIG5-ORC-C28-B1		2	53	1,0 - 1,2	minerax	3,957	2	60	effects of the bead size 1,0 - 1,2 mm
HIG5-ORC-C26-B2	HIG5-ORC-C28-B2		4	53	1,0 - 1,2	minerax	3,957	2	60	
HIG5-ORC-C26-B3	HIG5-ORC-C28-B3		6	53	1,0 - 1,2	minerax	3,957	2	60	
HIG5-ORC-C27-C1			2	53	1,0 - 1,2	minerax	3,957	4	60	
HIG5-ORC-C27-C2			4	53	1,0 - 1,2	minerax	3,957	4	60	
HIG5-ORC-C27-C3			6	53	1,0 - 1,2	minerax	3,957	4	60	
HIG5-ORC-C29-B1			2	53	3,5	minerax	3,982	2	60	Effects of the bead size 3,5 mm
HIG5-ORC-C29-B2			4	53	3,5	minerax	3,982	2	60	
HIG5-ORC-C29-B3			6	53	3,5	minerax	3,982	2	60	
HIG5-ORC-C30-B1			2	53	2,4-2,6	milmax	4,1	4	60	Effects of the bead size 2,4-2,6 mm
HIG5-ORC-C30-B2			4	53	2,4-2,6	milmax	4,1	4	60	
HIG5-ORC-C30-B3			6	53	2,4-2,6	milmax	4,1	4	60	
HIG5-ORC-C33-B1			1,5	53	n.2	steel	7,8	2	60	effects of bead type steel (additional)
HIG5-ORC-C33-B2			3	53	n.2	steel	7,8	2	60	
HIG5-ORC-C33-B3			4,5	53	n.2	steel	7,8	2	60	
esided not to perform			1,5	53	n.2	steel	7,8	4	60	
esided not to perform			3	53	n.2	steel	7,8	4	60	
esided not to perform			4,5	53	n.2	steel	7,8	4	60	
HIG5-ORC-C31-B1			2	53	n.2	keramos	3,6	2	60	effects of bead type Keramos (additional)
HIG5-ORC-C31-B2			4	53	n.2	keramos	3,6	2	60	
HIG5-ORC-C31-B3			6	53	n.2	keramos	3,6	2	60	
HIG5-ORC-C32-C1			2	53	n.2	keramos	3,6	4	60	
HIG5-ORC-C32-C2			4	53	n.2	keramos	3,6	4	60	
HIG5-ORC-C32-C3			6	53	n.2	keramos	3,6	4	60	
HIG5-ORC-C38-B1			2	53	2,0 - 2,2	minerax	3,91	2	60	scalped feed, cut size 20µm (additional)
HIG5-ORC-C38-B2			4	53	2,0 - 2,2	minerax	3,91	2	60	
HIG5-ORC-C38-B3			6	53	2,0 - 2,2	minerax	3,91	2	60	
HIG5-ORC-C39-C1			2	53	2,0 - 2,2	minerax	3,91	4	60	
HIG5-ORC-C39-C2			4	53	2,0 - 2,2	minerax	3,91	4	60	
HIG5-ORC-C39-C3			6	53	2,0 -2,2	minerax	3,91	4	60	
HIG5-ORC-C36-B1			2	53	2,0 - 2,2	minerax	3,91	2	60	scalped feed, cut size 35µm (additional)
HIG5-ORC-C36-B2			4	53	2,0 - 2,2	minerax	3,91	2	60	
HIG5-ORC-C36-B3			6	53	2,0 - 2,2	minerax	3,91	2	60	
HIG5-ORC-C37-C1			2	53	2,0 - 2,2	minerax	3,91	4	60	
HIG5-ORC-C37-C2			4	53	2,0 - 2,2	minerax	3,91	4	60	
HIG5-ORC-C37-C3			6	53	2,0 -2,2	minerax	3,91	4	60	
HIG5-ORC-C34-B1			2	53	2,0 - 2,2	minerax	3,91	2	60	scalped feed, cut size 50µm (additional)
HIG5-ORC-C34-B2			4	53	2,0 - 2,2	minerax	3,91	2	60	
HIG5-ORC-C34-B3			6	53	2,0 - 2,2	minerax	3,91	2	60	
HIG5-ORC-C35-C1			2	53	2,0 - 2,2	minerax	3,91	4	60	
HIG5-ORC-C35-C2			4	53	2,0 - 2,2	minerax	3,91	4	60	
HIG5-ORC-C35-C3			6	53	2,0 -2,2	minerax	3,91	4	60	

APPENDIX 2 HIGMILL^{TM} MODEL FIVE EMPTY MILL POWER CALIBRATION

Shaft speed	Tip speed	Power	Power
	EMPTY MILL		
	HIG 5/disc diameter 115 mm		
rpm	**m/s**	**W (Torque)**	**W (VSD)**
200	1,2	6	75
300	1,8	11	90
400	2,4	17	105
500	3,0	21	116
600	3,6	26	136
700	4,2	32	150
800	4,8	37	165

HIG 5 Power calibration
Empty mill

Power draw from torque dial

Power draw from frequency converter

$y = 8{,}541x - 4{,}2857$
$R^2 = 0{,}9985$
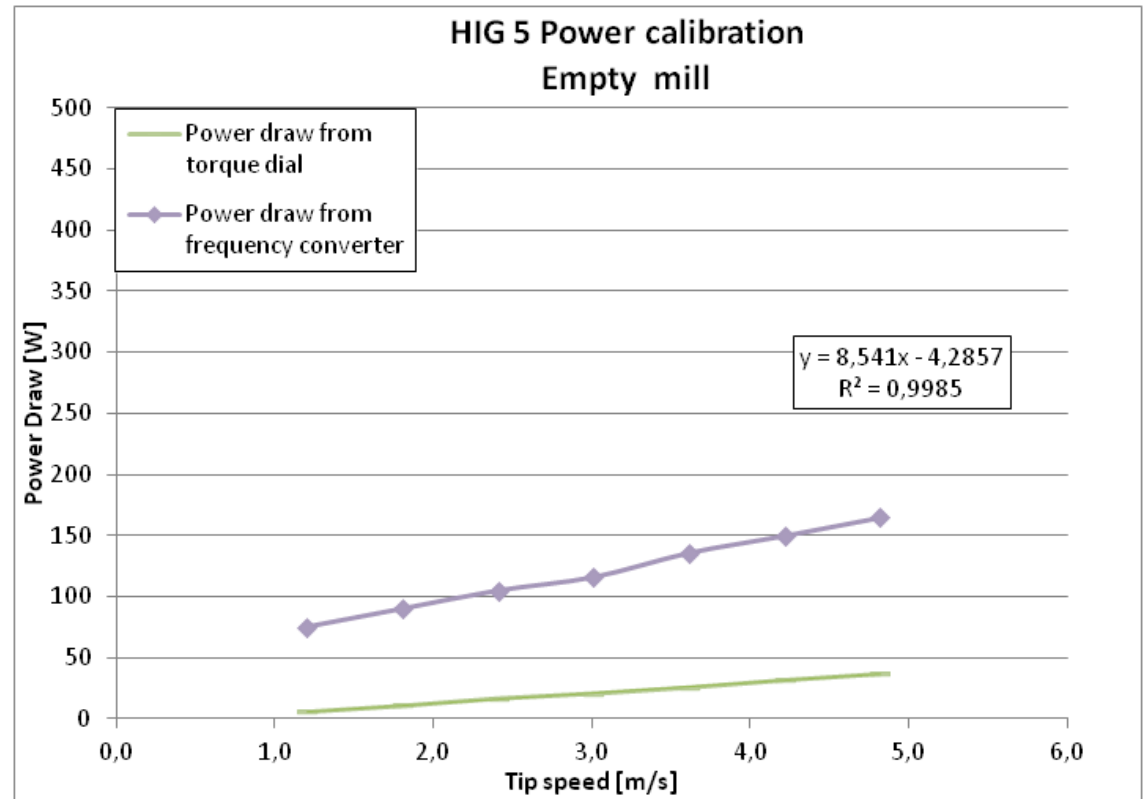
APPENDIX 3 FEED PARTICLE SIZE DISTRIBUTION

MASTERSIZER 2000

Result Analysis Report

Sample Name: HIG5-ORC-C18-Feed (Averaged	**SOP Name:**	**Measured:** 21. lokakuuta 2013 8:55:48	**Record number :** 466
Sample Source & type: HIG 5	**Measured by:** G_Oper	**Analysed:** 21. lokakuuta 2013 8:55:49	
Sample bulk lot ref:	**Result Source:** Averaged		

Particle Name: Fraunhofer	**Accessory Name:** Hydro 2000G (A)	**Analysis model:** General purpose	**Sensitivity:** Normal
Particle RI: 0.000	**Absorption:** 0	**Size range:** 0.020 to 2000.000 um	**Obscuration:** 14.37 %
Dispersant Name: Water	**Dispersant RI:** 1.330	**Weighted Residual:** 0.540 %	**Result Emulation:** Off

Concentration: 0.0171 %Vol	**Span :** 3.682	**Uniformity:** 1.25	**Result units:** Volume
Specific Surface Area: 0.774 m²/g	**Surface Weighted Mean D[3,2]:** 7.755 um	**Vol. Weighted Mean D[4,3]:** 55.490 um	

d(0.1): 2.751 um   **d(0.5): 34.221 um**   **d(0.9): 128.736 um**

Ultrasonic level : 100   Pump speed : 2500   Stirrer speed : 1000

—HIG-ORC-C7-Feed (Averaged Result), 17. lokakuuta 2013 9
—HIG5-ORC-C13-Feed (Averaged Result), 19. lokakuuta 2013
—HIG5-ORC-C8-Feed (Averaged Result), 18. lokakuuta 2013
—HIG5-ORC-C40-Feed (Averaged Result), 29. lokakuuta 2013
—HIG5-ORC-C21-Feed (Averaged Result), 21. lokakuuta 2013
—HIG5-ORC-C24-Feed (Averaged Result), 22. lokakuuta 2013
—HIG5-ORC-C18-Feed (Averaged Result), 21. lokakuuta 2013

HIG-ORC-C7-Feed (Averaged Result), 17. lokakuuta 2013
HIG5-ORC-C13-Feed (Averaged Result), 19. lokakuuta 20
HIG5-ORC-C8-Feed (Averaged Result), 18. lokakuuta 2013
HIG5-ORC-C40-Feed (Averaged Result), 29. lokakuuta 20
HIG5-ORC-C21-Feed (Averaged Result), 21. lokakuuta 20
HIG5-ORC-C24-Feed (Averaged Result), 22. lokakuuta 20
HIG5-ORC-C18-Feed (Averaged Result), 21. lokakuuta 20

Size (µm)	Vol Under %	Size (µm)	Vol Under %	Size (µm)	Vol Under %	Size (µm)	Vol Under %	Size (µm)	Vol Under %
0.100	0.00	4.000	13.47	44.000	57.49	149.000	92.73	1190.000	100.00
0.300	0.00	5.000	15.71	53.000	63.44	210.000	96.72	1680.000	100.00
0.500	0.18	10.000	24.14	63.000	69.17	297.000	98.45	2000.000	100.00
1.000	2.49	20.000	36.56	74.000	74.50	420.000	99.38		
2.000	7.29	32.000	48.13	80.000	77.03	595.000	100.00		
3.000	10.78	37.000	52.25	105.000	85.12	841.000	100.00		

APPENDIX 4 DATA FOR POWER DRAW COMPARISONS

Figure 18 data

WATER + BEADS		9,3 [kg]
HIG 5/115 mm/Minerax 2.0-2.		
shaft speed	Tip speed	Power
RPM	m/s	W (Torque)
200	1,2	133
300	1,8	229
400	2,4	349
500	3,0	494
600	3,6	677
700	4,2	871
800	4,8	1108
900	5,4	1373
1000	6,0	1672
1100	6,6	1904
1200	7,2	2176
1300	7,8	2459
1400	8,4	2753
1500	9,0	3118

Figure 19 data

Quartz		9,3 [kg]	
HIG 5/115 mm/Minerax (2,0-2,2mm)			
shaft speed	Tip speed	Power	Flow rate
RPM	m/s	W (Torque)	l/h
300	2	305	69
482	3	690	69
648	4	1220	69
830	5	1980	69
996	6	2600	69
1179	7	2900	69
1345	8	3070	69
300	2	295	112
482	3	667	112
648	4	1170	112
830	5	1921	112
996	6	2547	112
1179	7	3015	112

Figure 20 data

WATER + BEADS		9,3 [kg]	Minerax	WATER + BEADS		9,3 [kg]	Minerax	WATER + BEADS		9,3 [kg]	Minerax
HIG 5/115 mm/Minerax 3,5				HIG 5/115 mm/Minerax (2,0-2,2mm)				HIG 5/115 mm/Minerax 1.0-1.2			
shaft speed	Tip speed	Power	Power	shaft speed	Tip speed	Power	Power	shaft speed	Tip speed	Power	Power
RPM	m/s	W (Torque)	W (VSD)	RPM	m/s	W (Torque)	W (VSD)	RPM	m/s	W (Torque)	W (VSD)
200	1,2	184	232	200	1,2	138	198	200	1,2	86	146
300	1,8	297	302	300	1,8	236	300	300	1,8	165	232
400	2,4	479	556	400	2,4	369	449	400	2,4	274	357
500	3,0	738	827	500	3,0	524	614	500	3,0	402	480
600	3,6	1009	1098	600	3,6	737	840	600	3,6	571	655
700	4,2	1099	1222	700	4,2	991	1106	700	4,2	755	847
800	4,8	1314	1428	800	4,8	1263	1380	800	4,8	979	1076
900	5,4	1629	1762	900	5,4	1594	1725	900	5,4	1221	1334
1000	6,0	1999	2137	1000	6,0	1909	2039	1000	6,0	1403	1545
1100	6,6	2477	2623	1100	6,6	2190	2349	1100	6,6	1805	1922
1200	7,2	2907	3055	1200	7,2	2516	2684	1200	7,2	2263	2402
1300	7,8	2262	2422	1300	7,8	2890	3036	1300	7,8	2679	2834
1400	8,4	2759	2960	1400	8,4	3295	3472	1400	8,4	2978	3135
				1500	9,0	3647	3825	1500	9,0	3422	2571

Figure 21 data

WATER + BEADS		9,3 [kg]	Minerax	WATER + BEADS		18,6 [kg]		WATER + BEADS		8,59 [kg]	Keramos
HIG 5/115 mm/Minerax (2,0-2,2mm)				HIG 5/115 mm/steel (n. 2,0mm)				HIG 5/115 mm/keramos (n. 2,0mm)			
shaft speed	Tip speed	Power	Power	shaft speed	Tip speed	Power	Power	shaft speed	Tip speed	Power	Power
RPM	m/s	W (Torque)	W (VSD)	RPM	m/s	W (Torque)	W (VSD)	RPM	m/s	W (Torque)	W (VSD)
200	1,2	138	198	200	1,2	408	453	200	1,2	124	176
300	1,8	236	300	300	1,8	632	698	300	1,8	205	270
400	2,4	369	449	400	2,4	921	1004	400	2,4	318	393
500	3,0	524	614	500	3,0	1303	1410	500	3,0	465	555
600	3,6	737	840	600	3,6	1716	1826	600	3,6	665	765
700	4,2	991	1106	700	4,2	1991	2116	700	4,2	895	1004
800	4,8	1263	1380	800	4,8	2497	2647	800	4,8	1181	1282
900	5,4	1594	1725	900	5,4	3031	3153	900	5,4	1482	1597
1000	6,0	1909	2039	1000	6,0	3576	3728	1000	6,0	1781	1916
1100	6,6	2190	2349	1100	6,6	4271	4409	1100	6,6	2120	2266
1200	7,2	2516	2684					1200	7,2	2484	2637
1300	7,8	2890	3036					1300	7,8	2898	3071
1400	8,4	3295	3472					1400	8,4	3376	3528
1500	9,0	3647	3825					1500	9,0	3911	4080

APPENDIX 5 TESTWORK DATA

PARAMETERS	Unit	HIG5 ORC-C4-B1	HIG5 ORC-C4-B2	HIG5 ORC-C4-B3	HIG5 ORC-C4-B4	HIG5 ORC-C5-C1	HIG5 ORC-C5-C2	HIG5 ORC-C5-C3	HIG5 ORC-C6-A1	HIG5 ORC-C6-A2	HIG5 ORC-C6-A3	HIG5 ORC-C7-B1	HIG5 ORC-C7-B2	HIG5 ORC-C7-B3	HIG5 ORC-C8-B1	HIG5 ORC-C8-B2	HIG5 ORC-C8-B3
Date	dd-mm-yyyy	7.8.2013	7.8.2013	7.8.2013	7.8.2013	12.8.2013	12.8.2013	12.8.2013	12.8.2013	12.8.2013	12.8.2013	12.8.2013	12.8.2013	12.8.2013	12.8.2013	12.8.2013	12.8.2013
Sampling time	nn:mm							12.00									
End Time	nn:mm																
Sampling Interval (min) (4 x Ret.time)	min	0,0	0,0	0,0	0,0	0,0	0,0	0,0	0,0	0,0	0,0	0,0	0,0	0,0	0,0	0,0	0,0
Sample amount (solids)/test point	kg	0,0	0,0	0,0	0,0	0,0	0,0	0,0	0,0	0,0	0,0	0,0	0,0	0,0	0,0	0,0	0,0
Sample amount (slurry)/test point	l	0,0	0,0	0,0	0,0	0,0	0,0	0,0	0,0	0,0	0,0	0,0	0,0	0,0	0,0	0,0	0,0
Feed Material	No.																
Feed Type		Fine	Fine	Fine	Fine	Fine	Fine	Fine	Fine	Fine	Fine	Fine	Fine	Fine	Fine	Fine	Fine
F80 of Feed	[µm]	90	90	90	90	90	90	90	90	90	90	96	96	96	90	90	90
P80 (Target)	[µm]											90	90	90			
Feed material density	kg/l	2,65	2,65	2,65	2,65	2,65	2,65	2,65	2,65	2,65	2,65	2,65	2,65	2,65	2,65	2,65	2,65
Feed solids by Volume	%	30,0	30,0	30,0	30,0	30,0	30,0	30,0	30,0	30,0	30,0	39,1	39,1	39,1	22,2	22,2	22,2
Feed solids (by mass) target	w%	53,2	53,2	53,2	53,2	53,2	53,2	53,2	53,2	53,2	53,2	63,0	63,0	63,0	43,0	43,0	43,0
Feed solids %(measured)	w%	52,1	52,1	51,4	51,4	52,8	53,5	53,5	52,8	52,8	52,8	63,3	62,7	62,1	38,9	38,9	38,9
Feed flow rate target (Slurry feed)	l/h	**112**	**112**	**112**	**112**	**60**	**60**	**60**	**240**	**240**	**240**	**120**	**120**	**120**	**120**	**120**	**120**
Measured Feed flow rate (Slurry feed)	l/h	114,7	115,4	114,8	114,1	58,8	58,1	59,0	251,2	248,6	250,7	122,2	122,4	122,0	119,4	123,3	123,1
Time per 1 liter Meas. Feed	(sec/L)	31,38	31,2	31,37	31,55	61,22	61,98	60,99	14,33	14,48	14,36	29,45	29,41	29,51	30,16	29,2	29,24
Pump speed	Hz	SPX10-45Hz	SPX10-45Hz	SPX10-45Hz	SPX10-45Hz	SPX10-23Hz	SPX10-23Hz	SPX10-23Hz	SPX15-20Hz	SPX15-20Hz	SPX15-20Hz	SPX10-48Hz	SPX10-48Hz	SPX10-48Hz	SPX10-48Hz	SPX10-48Hz	SPX10-48Hz
Slurry density (target)	kg/l	1,495	1,495	1,495	1,495	1,495	1,495	1,495	1,495	1,495	1,495	1,645	1,645	1,645	1,366	1,366	1,366
Slurry density (measured)	kg/l	1,480	1,480	1,470	1,470	1,490	1,500	1,500	1,490	1,490	1,490	1,650	1,640	1,630	1,320	1,320	1,320
Slurry kg/l (solids target)	solid kg/l	0,795	0,795	0,795	0,795	0,795	0,795	0,795	0,795	0,795	0,795	1,036	1,036	1,036	0,588	0,588	0,588
Slurry kg/l (solids measured)	solid kg/l	0,771	0,771	0,755	0,755	0,787	0,803	0,803	0,787	0,787	0,787	1,044	1,028	1,012	0,514	0,514	0,514
Solids feed	kg/h	88	89	87	86	46	47	47	198	196	197	128	126	123	61	63	63
Grinding Media (bead type)	No.																
Grinding Media Type		Ceramic / Miner	ramic / Miner	ramic / Miner	ramic / Miner	ramic / Miner	ramic / Miner	ramic / Miner	ramic / Miner	ramic / Miner	ramic / Miner	ramic / Miner	ramic / Miner	ramic / Miner	ramic / Miner	ramic / Miner	ramic / Miner
Grinding Media densiiy	t/m3	3,9	3,9	3,9	3,9	3,9	3,9	3,9	3,9	3,9	3,9	3,9	3,9	3,9	3,9	3,9	3,9
Grinding Media Size	mm	2.0-2.2	2.0-2.2	2.0-2.2	2.0-2.2	2.0-2.2	2.0-2.2	2.0-2.2	2.0-2.2	2.0-2.2	2.0-2.2	2.0-2.2	2.0-2.2	2.0-2.2	2.0-2.2	2.0-2.2	2.0-2.2
Grinding Media Filling level	l %	60	60	60	60	60	60	60	60	60	60	60	60	60	60	60	60
Mass of grinding media charge	kg	9,3	9,3	9,3	9,3	9,3	9,3	9,3	9,3	9,3	9,3	9,3	9,3	9,3	9,3	9,3	9,3
Disc Diameter	mm	115	115	115	115	115	115	115	115	115	115	115	115	115	115	115	115
Mill Speed	rpm	**332**	**665**	**997**	**1329**	**332**	**665**	**997**	**332**	**665**	**997**	**332**	**665**	**997**	**332**	**665**	**997**
Tip speed	m/s	2,0	4,0	6,0	8,0	2,0	4,0	6,0	2,0	4,0	6,0	2,0	4,0	6,0	2,0	4,0	6,0
Mill Power predicted	W	360	1080	1940	3020	215	680	1510	215	680	1510	215	680	1510	215	680	1510
Mill Power calculated from Torque 1	W	259	1004	2152	3120	283	1085	2214	189	779	1854	179	854	2077	281	1004	2196
Mill Power from VSD 2	W	337	1120	2312	3317	360	1186	2381	266	903	1984	258	975	2216	384	1109	2349
Torque Measurement in V 4	Nm	7	14	20	22	8	15	21	5	11	17	5	12	19	8	14	20
Torque Measurement in V	V																
Speed pump 1 (SPX10)	rpm	1317	1317	1317	1317	690	690	690				1411	1411	1411	1411	1410	1411
Speed pump 2 (SPX15)	rpm								597	597	597						
SGE predicted (related to dry tons)	[kWh/t]	4,04	12,13	21,79	33,92	4,51	14,26	31,66	1,13	3,56	7,91	1,73	5,47	12,14	3,05	9,64	21,41
SGE (related to dry tons) mesured flow	**[kWh/t]**	**2,93**	**11,29**	**24,84**	**36,22**	**6,12**	**23,26**	**46,71**	**0,96**	**3,98**	**9,40**	**1,40**	**6,79**	**16,83**	**4,58**	**15,85**	**34,71**
kW/t (grinding media)	kW/t_media	28	108	231	335	30	117	238	20	84	199	19	92	223	30	108	236
P10 of product ORC	[µm]	2,9	2,2	1,8	1,7	2,4	1,8	1,5	2,9	2,6	2,3	2,9	2,5	2,1	2,5	2,1	1,7
P50 of product ORC	[µm]	36	22	13	11	26	12	8	37,0	30,0	23,0	37	29	19	29	18	11
P80 of product ORC	[µm]	95	61	35	26	73	36	21	92,0	78,0	59,0	94	77	49	76	51	30
P90 of product ORC	[µm]	140	96	54	38	109	57	32	133,0	115,0	89,0	136	116	74	110	81	47

HIG5 ORC-C9-A1	HIG5 ORC-C9-A2	HIG5 ORC-C9-A3	HIG5 ORC-C10-A1	HIG5 ORC-C10-A2	HIG5 ORC-C10-A3	HIG5 ORC-C11-C1	HIG5 ORC-C11-C2	HIG5 ORC-C11-C3	HIG5 ORC-C12-B1	HIG5 ORC-C12-B2	HIG5 ORC-C12-B3	HIG5 ORC-C13-B1	HIG5 ORC-C13-B2	HIG5 ORC-C13-B3	HIG5 ORC-C14-C1	HIG5 ORC-C14-C2	HIG5 ORC-C14-C3	HIG5 ORC-C15-B1	HIG5 ORC-C15-C1	HIG5 ORC-C15-D1
12.8.2013	12.8.2013	12.8.2013	13.8.2013	13.8.2013	13.8.2013	13.8.2013	13.8.2013	13.8.2013	13.8.2013	13.8.2013	13.8.2013	13.8.2013	13.8.2013	13.8.2013	14.8.2013	14.8.2013	14.8.2013	14.8.2013	14.8.2013	14.8.2013
0,0	0,0	0,0	0,0	0,0	0,0	0,0	0,0	0,0	0,0	0,0	0,0	0,0	0,0	0,0	0,0	0,0	0,0	0,0	0,0	0,0
0,0	0,0	0,0	0,0	0,0	0,0	0,0	0,0	0,0	0,0	0,0	0,0	0,0	0,0	0,0	0,0	0,0	0,0	0,0	0,0	0,0
0,0	0,0	0,0	0,0	0,0	0,0	0,0	0,0	0,0	0,0	0,0	0,0	0,0	0,0	0,0	0,0	0,0	0,0	0,0	0,0	0,0
Fine	Fine	Fine	Fine	Fine	Fine	Fine	Fine	Fine	Fine	Fine	Fine	Fine	Fine	Fine	Fine	Fine	Fine	Fine	Fine	Fine
90	90	90	90	90	90	90	90	90	90	90	90	90	90	90	90	90	90	90	90	90
2,65	2,65	2,65	2,65	2,65	2,65	2,65	2,65	2,65	2,65	2,65	2,65	2,65	2,65	2,65	2,65	2,65	2,65	2,65	2,65	2,65
39,1	39,1	39,1	22,2	22,2	22,2	39,1	39,1	39,1	30,0	30,0	30,0	30,0	30,0	30,0	22,2	22,2	22,2	30,0	30,0	30,0
63,0	63,0	63,0	43,0	43,0	43,0	63,0	63,0	63,0	53,2	53,2	53,2	53,2	53,2	53,2	43,0	43,0	43,0	53,2	53,2	53,2
62,7	62,7	62,1	40,8	41,6	40,8	62,1	62,7	62,1	52,8	53,5	53,5	52,8	52,8	52,1	41,6	43,4	41,6	52,1	52,1	51,4
240	240	240	240	240	240	60	60	60	120	120	120	120	120	120	60	60	60	120	60	40
234,7	238,3	239,0	242,6	235,4	239,7	58,2	57,6	59,6	126,5	126,1	126,2	124,8	127,8	126,9	60,4	60,0	59,3	129,4	58,3	40,6
15,34	15,11	15,06	14,84	15,29	15,02	61,84	62,54	60,36	28,46	28,55	28,52	28,84	28,17	28,36	59,65	60,05	60,74	27,81	61,75	88,66
SPX15-20Hz	SPX15-20Hz	SPX15-20Hz	SPX15-20Hz	SPX15-20Hz	SPX15-20Hz	SPX10-23Hz	SPX10-23Hz	SPX10-23Hz	SPX10-48Hz	SPX10-48Hz	SPX10-48Hz	SPX10-48Hz	SPX10-48Hz	SPX10-48Hz	SPX10-23Hz	SPX10-23Hz	SPX10-23Hz	SPX10-48Hz	SPX10-23Hz	SPX10-16Hz
1,645	1,645	1,645	1,365	1,365	1,365	1,645	1,645	1,645	1,495	1,495	1,495	1,495	1,495	1,495	1,365	1,365	1,365	1,495	1,495	1,495
1,640	1,640	1,630	1,340	1,350	1,340	1,630	1,640	1,630	1,490	1,500	1,500	1,490	1,490	1,480	1,350	1,370	1,350	1,480	1,480	1,470
1,036	1,036	1,036	0,587	0,587	0,587	1,036	1,036	1,036	0,795	0,795	0,795	0,795	0,795	0,795	0,587	0,587	0,587	0,795	0,795	0,795
1,028	1,028	1,012	0,546	0,562	0,546	1,012	1,028	1,012	0,787	0,803	0,803	0,787	0,787	0,771	0,562	0,594	0,562	0,771	0,771	0,755
241	245	242	132	132	131	59	59	60	100	101	101	98	101	98	34	36	33	100	45	31
ramic / Mine	ramic / Mine	ramic / Mine	ramic / Mine	ramic / Mine	ramic / Mine	ramic / Mine	ramic / Mine	ramic / Mine	ramic / Mine	ramic / Mine	ramic / Mine	ramic / Mine	ramic / Mine	ramic / Mine	ramic / Mine	ramic / Mine	ramic / Mine	ramic / Mine	ramic / Mine	ramic / Mine
3,9	3,9	3,9	3,9	3,9	3,9	3,9	3,9	3,9	3,9	3,9	3,9	3,9	3,9	3,9	3,9	3,9	3,9	3,9	3,9	3,9
2.0-2.2	2.0-2.2	2.0-2.2	2.0-2.2	2.0-2.2	2.0-2.2	2.0-2.2	2.0-2.2	2.0-2.2	2.0-2.2	2.0-2.2	2.0-2.2	2.0-2.2	2.0-2.2	2.0-2.2	2.0-2.2	2.0-2.2	2.0-2.2	2.0-2.2	2.0-2.2	2.0-2.2
60	60	60	60	60	60	60	60	60	60	60	60	60	60	60	60	60	60	60	60	60
9,3	9,3	9,3	9,3	9,3	9,3	9,3	9,3	9,3	9,3	9,3	9,3	9,3	9,3	9,3	9,3	9,3	9,3	9,3	9,3	9,3
115	115	115	115	115	115	115	115	115	115	115	115	115	115	115	115	115	115	115	115	115
332	665	997	332	665	997	332	665	997	498	665	831	997	1163	1329	332	665	997	665	665	665
2,0	4,0	6,0	2,0	4,0	6,0	2,0	4,0	6,0	3,0	4,0	5,0	6,0	7,0	8,0	2,0	4,0	6,0	4,0	4,0	4,0
215	680	1510	215	680	1510	215	680	1510	215	680	1510	215	680	1510	215	680	1510	215	680	1510
96	590	1527	227	849	1899	255	998	2190	530	942	1477	2143	2619	2980	300	1062	2115	907	1020	1053
172	694	1661	304	964	2066	326	1113	2316	618	1037	1616	2274	2800	3182	375	1169	2303	1012	1124	1143
2	8	14	6	12	18	7	14	20	9	13	16	20	21	21	8	14	19	12	14	14,5
						690	690	690	1410	1411	1410	1411	1411	1411	690	690	690	1410	690	486
597	597	597	597	597	597															
0,86	2,73	6,07	1,53	4,83	10,72	3,46	10,94	24,29	2,25	7,13	15,83	2,25	7,13	15,83	6,10	19,31	42,88	2,25	14,26	47,48
0,40	2,41	6,31	1,71	6,41	14,51	4,33	16,87	36,29	5,32	9,30	14,57	21,82	26,04	30,45	8,84	29,81	63,48	9,09	22,70	34,36
10	63	164	24	91	204	27	107	235	57	101	159	230	282	320	32	114	227	98	110	113
3	2,9	2,5	2,9	2,4	2,1	2,6	2	1,6	2,5	2,3	2,1	1,9	1,8	1,8	2,3	1,7	1,4	2,3	1,9	1,7
39	35	29	35	25	18	32	18	11	29	23	18	15	14	12	25	12	6	24	15	11
96	88	73	88	65	46	84	48	26	77	63	48	39	33	30	71	33	15	66	41	29
139	128	107	127	97	67	124	76	38	115	98	76	60	50	43	107	53	22	102	66	46

HIG5 ORC-C17-B1	HIG5 ORC-C17-B2	HIG5 ORC-C17-B3	HIG5 ORC-C18-B1	HIG5 ORC-C18-B2	HIG5 ORC-C18-B3	HIG5 ORC-C19-B1	HIG5 ORC-C19-B2	HIG5 ORC-C19-B3	HIG5 ORC-C20-A1	HIG5 ORC-C20-A2	HIG5 ORC-C20-A3	HIG5 ORC-C21-A1	HIG5 ORC-C21-A2	HIG5 ORC-C21-A3	HIG5 ORC-C22-A1	HIG5 ORC-C22-A2	HIG5 ORC-C22-A3	HIG5 ORC-C23-C1	HIG5 ORC-C23-C2	HIG5 ORC-C23-C3
30.9.2013	30.9.2013	30.9.2013	30.9.2013	30.9.2013	30.9.2013	30.9.2013	30.9.2013	30.9.2013	30.9.2013	30.9.2013	30.9.2013	1.10.2013	1.10.2013	1.10.2013	1.10.2013	1.10.2013	1.10.2013	1.10.2013	1.10.2013	1.10.2013
																				16 min
0,0	0,0	0,0	0,0	0,0	0,0	0,0	0,0	0,0	0,0	0,0	0,0	0,0	0,0	0,0	0,0	0,0	0,0	0,0	0,0	0,0
0,0	0,0	0,0	0,0	0,0	0,0	0,0	0,0	0,0	0,0	0,0	0,0	0,0	0,0	0,0	0,0	0,0	0,0	0,0	0,0	0,0
0,0	0,0	0,0	0,0	0,0	0,0	0,0	0,0	0,0	0,0	0,0	0,0	0,0	0,0	0,0	0,0	0,0	0,0	0,0	0,0	0,0
Fine	Fine	Fine	Fine	Fine	Fine	Fine	Fine	Fine	Fine	Fine	Fine	Fine	Fine	Fine	Fine	Fine	Fine	Fine	Fine	Fine
90	90	90	90	90	90	90	90	90	90	90	90	90	90	90	90	90	90	90	90	90
2,65	2,65	2,65	2,65	2,65	2,65	2,65	2,65	2,65	2,65	2,65	2,65	2,65	2,65	2,65	2,65	2,65	2,65	2,65	2,65	2,65
39,1	39,1	39,1	30,0	30,0	30,0	22,2	22,2	22,2	39,1	39,1	39,1	30,0	30,0	30,0	22,2	22,2	22,2	39,1	39,1	39,1
63,0	63,0	63,0	53,2	53,2	53,2	43,0	43,0	43,0	63,0	63,0	63,0	53,2	53,2	53,2	43,0	43,0	43,0	63,0	63,0	63,0
62,1	61,5	61,5	52,8	53,5	52,8	42,5	42,5	42,5	62,7	63,3	63,3	53,5	54,2	53,5	43,4	42,5	42,5	62,1	62,7	62,1
120	120	120	120	120	120	120	120	120	240	240	240	240	240	240	240	240	240	60	60	60
129,1	129,1	126,8	129,2	129,1	127,9	128,2	127,2	125,9	235,1	240,3	239,8	246,6	236,8	242,4	251,6	244,4	238,3	59,9	60,0	59,3
27,88	27,88	28,38	27,86	27,89	28,14	28,08	28,3	28,59	15,31	14,98	15,01	14,6	15,2	14,85	14,31	14,73	15,11	60,14	59,97	60,74
SPX10-48Hz	SPX10-48Hz	SPX10-48Hz	SPX10-48Hz	SPX10-48Hz	SPX10-48Hz	SPX10-48Hz	SPX10-48Hz	SPX10-48Hz	SPX15-20Hz	SPX15-20Hz	SPX15-20Hz	SPX15-20Hz	SPX15-20Hz	SPX15-20Hz	SPX15-20Hz	SPX15-20Hz	SPX15-20Hz	SPX10-23Hz	SPX10-23Hz	SPX10-23Hz
1,645	1,645	1,645	1,495	1,495	1,495	1,365	1,365	1,365	1,645	1,645	1,645	1,495	1,495	1,495	1,365	1,365	1,365	1,645	1,645	1,645
1,630	1,620	1,620	1,490	1,500	1,490	1,360	1,360	1,360	1,640	1,650	1,650	1,500	1,510	1,500	1,370	1,360	1,360	1,630	1,640	1,630
1,036	1,036	1,036	0,795	0,795	0,795	0,587	0,587	0,587	1,036	1,036	1,036	0,795	0,795	0,795	0,587	0,587	0,587	1,036	1,036	1,036
1,012	0,996	0,996	0,787	0,803	0,787	0,578	0,578	0,578	1,028	1,044	1,044	0,803	0,819	0,803	0,594	0,578	0,578	1,012	1,028	1,012
131	129	126	102	104	101	74	74	73	242	251	250	198	194	195	149	141	138	61	62	60
ramic/Mine	ramic/Mine	ramic/Mine	ramic/Mine	ramic/Mine	ramic/Mine	ramic/Mine	ramic/Mine	ramic/Mine	ramic/Mine	ramic/Mine	ramic/Mine	ramic/Mine	ramic/Mine	ramic/Mine	ramic/Mine	ramic/Mine	ramic/Mine	ramic/Mine	ramic/Mine	ramic/Mine
3,9	3,9	3,9	3,9	3,9	3,9	3,9	3,9	3,9	3,9	3,9	3,9	3,9	3,9	3,9	3,9	3,9	3,9	3,9	3,9	3,9
2.0-2.2	2.0-2.2	2.0-2.2	2.0-2.2	2.0-2.2	2.0-2.2	2.0-2.2	2.0-2.2	2.0-2.2	2.0-2.2	2.0-2.2	2.0-2.2	2.0-2.2	2.0-2.2	2.0-2.2	2.0-2.2	2.0-2.2	2.0-2.2	2.0-2.2	2.0-2.2	2.0-2.2
60	60	60	60	60	60	60	60	60	60	60	60	60	60	60	60	60	60	60	60	60
9,3	9,3	9,3	9,3	9,3	9,3	9,3	9,3	9,3	9,3	9,3	9,3	9,3	9,3	9,3	9,3	9,3	9,3	9,3	9,3	9,3
115	115	115	115	115	115	115	115	115	115	115	115	115	115	115	115	115	115	115	115	115
332	665	997	332	665	997	332	665	997	332	665	997	332	665	997	332	665	997	332	665	997
2,0	4,0	6,0	2,0	4,0	6,0	2,0	4,0	6,0	2,0	4,0	6,0	2,0	4,0	6,0	2,0	4,0	6,0	2,0	4,0	6,0
215	680	1510	215	680	1510	215	680	1510	215	680	1510	215	680	1510	215	680	1510	215	680	1510
224	964	1922	271	1074	1931	299	1108	1966	109	621	1539	199	867	1757	236	960	1787	281	1066	2427
296	1072	2054	337	1171	2062	368	1210	2082	176	716	1661	269	982	1893	311	1069	1904	348	1171	2549
6	13	18	7	15	18	8	15	19	3	8	14	5	12	16	6	13	16	8	15	22
1411	1411	1411	1411	1411	1411	1411	1411	1411										690	690	690
									597	597	597	597	597	597	596	596	596			
1,73	5,47	12,14	2,25	7,13	15,83	3,05	9,65	21,44	0,86	2,73	6,07	1,13	3,56	7,91	1,53	4,83	10,72	3,46	10,94	24,29
1,71	7,50	15,22	2,66	10,36	19,18	4,03	15,06	27,00	0,45	2,48	6,15	1,01	4,47	9,03	1,58	6,79	12,97	4,64	17,28	40,47
24	104	207	29	115	208	32	119	211	12	67	165	21	93	189	25	103	192	30	115	261
2,6	2,2	2	2,5	2,1	1,8	2,4	2	1,7	2,7	2,5	2,3	2,7	2,5	2,2	2,6	2,3	2,1	2,3	1,9	1,5
31	22	17	29	20	14	27	16	12	35	30	25	32	27	21	31	24	18	26	16	9
84	61	45	79	54	36	74	44	30	86	78	65	84	72	56	79	65	48	73	44	21
124	93	68	117	84	53	110	70	44	126	114	96	122	108	85	115	99	73	109	69	30

HIG5 ORC-C24-C1	HIG5 ORC-C24-C2	HIG5 ORC-C24-C3	HIG5 ORC-C25-C1	HIG5 ORC-C25-C2	HIG5 ORC-C25-C3	HIG5 ORC-C26-B1	HIG5 ORC-C26-B2	HIG5 ORC-C26-B3	HIG5 ORC-C27-C1	HIG5 ORC-C27-C2	HIG5 ORC-C27-C3	HIG5 ORC-C28-B1	HIG5 ORC-C28-B2	HIG5 ORC-C28-B3	HIG5 ORC-C29-B1	HIG5 ORC-C29-B2	HIG5 ORC-C29-B3	HIG5 ORC-C30-B1	HIG5 ORC-C30-B2	HIG5 ORC-C30-B3
1.10.2013	1.10.2013	1.10.2013	1.10.2013	1.10.2013	1.10.2013	2.10.2013	2.10.2013	2.10.2013	2.10.2013	2.10.2013	2.10.2013	2.10.2013	2.10.2013	2.10.2013	3.10.2013	3.10.2013	3.10.2013	7.10.2013	7.10.2013	7.10.2013
0,0	0,0	0,0	0,0	0,0	0,0	0,0	0,0	0,0	0,0	0,0	0,0	0,0	0,0	0,0	0,0	0,0	0,0	0,0	0,0	0,0
0,0	0,0	0,0	0,0	0,0	0,0	0,0	0,0	0,0	0,0	0,0	0,0	0,0	0,0	0,0	0,0	0,0	0,0	0,0	0,0	0,0
0,0	0,0	0,0	0,0	0,0	0,0	0,0	0,0	0,0	0,0	0,0	0,0	0,0	0,0	0,0	0,0	0,0	0,0	0,0	0,0	0,0
Fine	Fine	Fine	Fine	Fine	Fine	Fine	Fine	Fine	Fine	Fine	Fine	Fine	Fine	Fine	Fine	Fine	Fine	Fine	Fine	Fine
90	90	90	90	90	90	90	90	90	90	90	90	90	90	90	90	90	90	90	90	90
2,65	2,65	2,65	2,65	2,65	2,65	2,65	2,65	2,65	2,65	2,65	2,65	2,65	2,65	2,65	2,65	2,65	2,65	2,65	2,65	2,65
30,0	30,0	30,0	22,2	22,2	22,2	30,0	30,0	30,0	30,0	30,0	30,0	30,0	30,0	30,0	30,0	30,0	30,0	30,0	30,0	30,0
53,2	53,2	53,2	43,0	43,0	43,0	53,2	53,2	53,2	53,2	53,2	53,2	53,2	53,2	53,2	53,2	53,2	53,2	53,2	53,2	53,2
52,8	52,8	52,8	43,4	43,4	41,6	53,5	53,5	53,5	52,8	52,1	51,4	52,8	52,8	52,8	53,5	53,5	53,5	53,5	53,5	53,5
60	60	60	60	60	60	120	120	120	60	60	60	120	120	120	120	120	120	120	120	120
59,6	60,6	61,3	60,4	60,9	61,2	126,5	126,4	127,9	61,8	61,6	61,9	128,2	130,8	127,7	127,6	128,6	133,3	132,3	132,6	133,3
60,39	59,4	58,72	59,58	59,12	58,83	28,45	28,49	28,14	58,27	58,48	58,2	28,09	27,53	28,2	28,22	28	27	27,21	27,15	27,01
SPX10-23Hz	SPX10-23Hz	SPX10-23Hz	SPX10-23Hz	SPX10-23Hz	SPX10-23Hz	SPX10-48Hz	SPX10-48Hz	SPX10-48Hz	SPX10-23Hz	SPX10-23Hz	SPX10-23Hz	SPX10-48Hz	SPX10-48Hz	SPX10-48Hz	SPX10-48Hz	SPX10-48Hz	SPX10-48Hz	SPX10-48Hz	SPX10-48Hz	SPX10-48Hz
1,495	1,495	1,495	1,365	1,365	1,365	1,495	1,495	1,495	1,495	1,495	1,495	1,495	1,495	1,495	1,495	1,495	1,495	1,495	1,495	1,495
1,490	1,490	1,490	1,370	1,370	1,350	1,500	1,500	1,500	1,490	1,480	1,470	1,490	1,490	1,490	1,490	1,500	1,490	1,500	1,500	1,500
0,795	0,795	0,795	0,587	0,587	0,587	0,795	0,795	0,795	0,795	0,795	0,795	0,795	0,795	0,795	0,795	0,795	0,795	0,795	0,795	0,795
0,787	0,787	0,787	0,594	0,594	0,562	0,803	0,803	0,803	0,787	0,771	0,755	0,787	0,787	0,787	0,787	0,803	0,787	0,803	0,803	0,803
47	48	48	36	36	34	102	101	103	49	47	47	101	103	100	100	103	105	106	106	107
ramic / Mine	ramic / Mine	ramic / Mine	ramic / Mine	ramic / Mine	ramic / Mine	ramic / Mine	ramic / Mine	ramic / Mine	ramic / Mine	ramic / Mine	ramic / Mine	ramic / Mine	ramic / Mine	ramic / Mine	ramic / Mine	ramic / Mine	ramic / Mine	ramic / Milm	ramic / Milm	ramic / Milm
3,9	3,9	3,9	3,9	3,9	3,9	3,9	3,9	3,9	3,9	3,9	3,9	3,9	3,9	3,9	3,9	3,9	3,9	4,1	4,1	4,1
2.0-2.2	2.0-2.2	2.0-2.2	2.0-2.2	2.0-2.2	2.0-2.2	1.0-1.2	1.0-1.2	1.0-1.2	1.0-1.2	1.0-1.2	1.0-1.2	1.0-1.2	1.0-1.2	1.0-1.2	4	4	4	2,4-2,6	2,4-2,6	2,4-2,6
60	60	60	60	60	60	60	60	60	60	60	60	60	60	60	60	60	60	60	60	60
9,3	9,3	9,3	9,3	9,3	9,3	9,3	9,3	9,3	9,3	9,3	9,3	9,3	9,3	9,3	9,3	9,3	9,3	9,3	9,3	9,3
115	115	115	115	115	115	115	115	115	115	115	115	115	115	115	115	115	115	115	115	115
332	665	997	332	665	997	332	665	997	332	665	997	332	665	997	332	665	997	332	665	997
2,0	4,0	6,0	2,0	4,0	6,0	2,0	4,0	6,0	2,0	4,0	6,0	2,0	4,0	6,0	2,0	4,0	6,0	2,0	4,0	6,0
215	680	1510	215	680	1510	215	680	1510	215	680	1510	215	680	1510	215	680	1510	215	680	1510
301	1107	2465	306	1110	2443	98	407	1068	199	760	2060	105	424	1082	425	1519	3132	298	1148	2487
367	1212	2601	375	1210	2584	168	510	1200	266	866	2193	180	525	1215	489	1642	3252	367	1264	2626
8	15	23	8	15	23	2	5	10	5	10	19	3	6	10	12	22	29	8	16	23
690	690	690	690	690	690	1411	1411	1411	690	690	690	1411	1411	1411	1411	1411	1411	1411	1411	1411
4,51	14,26	31,66	6,10	19,31	42,88	2,25	7,13	15,83	4,51	14,26	31,66	2,25	7,13	15,83	2,25	7,13	15,83	2,25	7,13	15,83
6,42	23,21	51,09	8,52	30,68	71,02	0,96	4,01	10,40	4,09	16,01	44,12	1,04	4,12	10,77	4,23	14,71	29,85	2,80	10,78	23,24
32	119	265	33	119	263	11	44	115	21	82	222	11	46	116	46	163	337	32	123	267
2,3	1,7	1,4	2,1	1,6	1,3	2,7	2,5	2,1	2,5	2	1,5	2,6	2,4	2,1	2,4	1,9	1,6	2,5	2,1	1,7
24	13	9	20	10	5,5	34	29	23	31	21	9	33	29	22	26	16	11	28	19	12
70	34	16	60	28	13	89	80	68	83	68	34	87	80	67	66	37	27	76	50	30
105	56	24	92	43	20	130	118	102	121	106	67	127	119	102	97	53	40	114	78	45

HIG5 ORC-C31-B1	HIG5 ORC-C31-B2	HIG5 ORC-C31-B3	HIG5 ORC-C32-C1	HIG5 ORC-C32-C2	HIG5 ORC-C32-C3	HIG5 ORC-C33-B1	HIG5 ORC-C33-B2	HIG5 ORC-C33-B3	HIG5 ORC-C34-B1	HIG5 ORC-C34-B2	HIG5 ORC-C34-B3	HIG5 ORC-C35-C1	HIG5 ORC-C35-C2	HIG5 ORC-C35-C3	HIG5 ORC-C36-B1	HIG5 ORC-C36-B2	HIG5 ORC-C36-B3	HIG5 ORC-C37-C1	HIG5 ORC-C37-C2	HIG5 ORC-C37-C3
8.10.2013	8.10.2013	8.10.2013	8.10.2013	8.10.2013	8.10.2013	9.10.2013	9.10.2013	9.10.2013	11.10.2013	11.10.2013	11.10.2013	11.10.2013	11.10.2013	11.10.2013	14.10.2013	14.10.2013	14.10.2013	14.10.2013	14.10.2013	14.10.2013
0,0	0,0	0,0	0,0	0,0	0,0	0,0	0,0	0,0	0,0	0,0	0,0	0,0	0,0	0,0	0,0	0,0	0,0	0,0	0,0	0,0
0,0	0,0	0,0	0,0	0,0	0,0	0,0	0,0	0,0	0,0	0,0	0,0	0,0	0,0	0,0	0,0	0,0	0,0	0,0	0,0	0,0
0,0	0,0	0,0	0,0	0,0	0,0	0,0	0,0	0,0	0,0	0,0	0,0	0,0	0,0	0,0	0,0	0,0	0,0	0,0	0,0	0,0
Fine	Fine	Fine	Fine	Fine	Fine	Fine	Fine	Fine	Fine	Fine	Fine	Fine	Fine	Fine	Fine	Fine	Fine	Fine	Fine	Fine
90	90	90	90	90	90	90	90	90	122	122	122	120	120	120	128	128	128	110	110	110
									scalped	scalped	scalped	scalped	scalped	scalped						
2,65	2,65	2,65	2,65	2,65	2,65	2,65	2,65	2,65	2,65	2,65	2,65	2,65	2,65	2,65	2,65	2,65	2,65	2,65	2,65	2,65
30,0	30,0	30,0	30,0	30,0	30,0	30,0	30,0	30,0	30,0	30,0	30,0	30,0	30,0	30,0	30,0	30,0	30,0	30,0	30,0	30,0
53,2	53,2	53,2	53,2	53,2	53,2	53,2	53,2	53,2	53,2	53,2	53,2	53,2	53,2	53,2	53,2	53,2	53,2	53,2	53,2	53,2
51,4	51,4	51,4	53,5	53,5	53,5	53,5	53,5	52,8	54,9	54,9	54,2	54,2	52,8	51,4	50,6	49,8	49,8	52,1	52,1	52,8
120	**120**	**120**	**60**	**60**	**60**	**120**	**120**	**120**	**120**	**120**	**120**	**60**	**60**	**60**	**120**	**120**	**120**	**60**	**60**	**60**
133,2	132,7	132,8	58,8	59,0	56,6	130,6	134,6	130,1	135,5	134,9	131,8	58,8	57,9	58,3	131,1	132,1	128,5	61,2	61,7	61,2
27,02	27,12	27,1	61,24	61,02	63,63	27,57	26,74	27,67	26,56	26,68	27,31	61,19	62,15	61,71	27,46	27,25	28,02	58,78	58,36	58,83
SPX10-48Hz	SPX10-48Hz	SPX10-48Hz	SPX10-21Hz	SPX10-21Hz	SPX10-21Hz	SPX10-48Hz	SPX10-48Hz	SPX10-48Hz	SPX10-47Hz	SPX10-47Hz	SPX10-47Hz	SPX10-21Hz	SPX10-21Hz	SPX10-21Hz	SPX10-46Hz	SPX10-46Hz	SPX10-46Hz	SPX10-22Hz	SPX10-22Hz	SPX10-22Hz
1,495	1,495	1,495	1,495	1,495	1,495	1,495	1,495	1,495	1,495	1,495	1,495	1,495	1,495	1,495	1,495	1,495	1,495	1,495	1,495	1,495
1,470	1,470	1,470	1,500	1,500	1,500	1,500	1,500	1,490	1,520	1,520	1,510	1,510	1,490	1,470	1,460	1,450	1,450	1,480	1,480	1,490
0,795	0,795	0,795	0,795	0,795	0,795	0,795	0,795	0,795	0,795	0,795	0,795	0,795	0,795	0,795	0,795	0,795	0,795	0,795	0,795	0,795
0,755	0,755	0,755	0,803	0,803	0,803	0,803	0,803	0,787	0,835	0,835	0,819	0,819	0,787	0,755	0,739	0,723	0,723	0,771	0,771	0,787
101	100	100	47	47	45	105	108	102	113	113	108	48	46	44	97	95	93	47	48	48
keramos	keramos	keramos	keramos	keramos	keramos	steel	steel	steel	ceramic/Miner	ceramic/Miner	ceramic/Miner	ceramic/Miner	ceramic/Miner	ceramic/Miner	ceramic/Miner	ceramic/Miner	ceramic/Miner	ceramic/Miner	ceramic/Miner	ceramic/Miner
3,6	3,6	3,6	3,6	3,6	3,6	7,8	7,8	7,8	3,9	3,9	3,9	3,9	3,9	3,9	3,9	3,9	3,9	3,9	3,9	3,9
2	2	2	2	2	2	2	2	2	2,0-2,2	2,0-2,2	2,0-2,2	2,0-2,2	2,0-2,2	2,0-2,2	2,0-2,2	2,0-2,2	2,0-2,2	2,0-2,2	2,0-2,2	2,0-2,2
60	60	60	60	60	60	60	60	60	60	60	60	60	60	60	60	60	60	60	60	60
8,59	8,59	8,59	8,59	8,59	8,59	18,6	18,6	18,6	9,3	9,3	9,3	9,3	9,3	9,3	9,3	9,3	9,3	9,3	9,3	9,3
115	115	115	115	115	115	115	115	115	115	115	115	115	115	115	115	115	115	115	115	115
332	**665**	**997**	**332**	**665**	**997**	**249**	**498**	**748**	**332**	**665**	**997**	**332**	**665**	**997**	**332**	**665**	**997**	**332**	**665**	**997**
2,0	4,0	6,0	2,0	4,0	6,0	1,5	3,0	4,5	2,0	4,0	6,0	2,0	4,0	6,0	2,0	4,0	6,0	2,0	4,0	6,0
215	680	1510	215	680	1510	215	680	1510	215	680	1510	215	680	1510	215	680	1510	215	680	1510
245	1012	2200	290	1118	2286	488	1570	3343	219	1178	2632	289	1302	2803	234	1186	2606	262	1260	2687
219	1117	2342	360	1226	2419	555	1674	3467	292	1282	2771	364	1718	2937	296	1290	2762	330	1369	2829
7	14	20	8	16	21	18	30	43	6	16	24	8	18	26	6	16	24	7	18	25
1411	1411	1411	632	632	632	1411	1411	1411	1384	1384	1384	632	632	632	1350	1350	1350	661	661	661
2,25	7,13	15,83	4,51	14,26	31,66	2,25	7,13	15,83	2,25	7,13	15,83	4,51	14,26	31,66	2,25	7,13	15,83	4,51	14,26	31,66
2,44	**10,10**	**21,94**	**6,14**	**23,60**	**50,32**	**4,65**	**14,52**	**32,65**	**1,93**	**10,45**	**24,38**	**6,00**	**28,56**	**63,65**	**2,42**	**12,42**	**28,07**	**5,55**	**26,50**	**55,80**
29	118	256	34	130	266	26	84	180	24	127	283	31	140	301	25	128	280	28	135	289
2,4	2	1,7	2,2	1,6	1,4	2,4	1,9	1,6	13	4,4	2,3	7,8	2,2	1,3	15	4	2,3	10	2,4	1,6
27	19	12	23	11	7	25	16	10	58	35	19	50	17	7,3	65	35	18	59	20	8,6
77	55	32	69	33	16	71	44	25	109	75	42	99	42	17	119	75	42	114	50	20
115	87	50	106	57	24	107	70	36	149	106	61	137	65	25	160	105	62	157	76	30

HIG5 ORC-C38-B1	HIG5 ORC-C38-B2	HIG5 ORC-C38-B3	HIG5 ORC-C39-C1	HIG5 ORC-C39-C2	HIG5 ORC-C39-C3	HIG5 ORC-C40-B1	HIG5 ORC-C40-B2	HIG5 ORC-C40-B3	HIG5 ORC-C41-C1	HIG5 ORC-C41-C2	HIG5 ORC-C41-C3
14.10.2013	14.10.2013	14.10.2013	14.10.2013	14.10.2013	14.10.2013	15.10.2013	15.10.2013	15.10.2013	15.10.2013	15.10.2013	15.10.2013
0,0	0,0	0,0	0,0	0,0	0,0	0,0	0,0	0,0	0,0	0,0	0,0
0,0	0,0	0,0	0,0	0,0	0,0	0,0	0,0	0,0	0,0	0,0	0,0
0,0	0,0	0,0	0,0	0,0	0,0	0,0	0,0	0,0	0,0	0,0	0,0
Fine	Fine	Fine	Fine	Fine	Fine	Fine	Fine	Fine	Fine	Fine	Fine
95	95	95	98	98	98	90	90	90	90	90	90
2,65	2,65	2,65	2,65	2,65	2,65	2,65	2,65	2,65	2,65	2,65	2,65
30,0	30,0	30,0	30,0	30,0	30,0	30,0	30,0	30,0	30,0	30,0	30,0
53,2	53,2	53,2	53,2	53,2	53,2	53,2	53,2	53,2	53,2	53,2	53,2
53,5	53,5	52,8	55,6	54,9	53,5	54,2	53,5	53,5	53,5	54,2	53,5
120	120	120	60	60	60	120	120	120	60	60	60
130,5	132,3	126,7	61,1	61,2	60,4	128,4	124,9	126,6	61,0	60,8	61,7
27,58	27,22	28,41	58,94	58,87	59,56	28,03	28,82	28,43	58,99	59,2	58,3
SPX10-46Hz	SPX10-46Hz	SPX10-46Hz	SPX10-22Hz	SPX10-22Hz	SPX10-22Hz	SPX10-45Hz	SPX10-45Hz	SPX10-45Hz	SPX10-22Hz	SPX10-22Hz	SPX10-22Hz
1,495	1,495	1,495	1,495	1,495	1,495	1,495	1,495	1,495	1,495	1,495	1,495
1,500	1,500	1,490	1,530	1,520	1,500	1,500	1,510	1,500	1,500	1,510	1,500
0,795	0,795	0,795	0,795	0,795	0,795	0,795	0,795	0,795	0,795	0,795	0,795
0,803	0,803	0,787	0,851	0,835	0,803	0,803	0,819	0,803	0,803	0,819	0,803
105	106	100	52	51	49	103	102	102	49	50	50
ramic/Mine	ramic/Mine	ramic/Mine	ramic/Mine	ramic/Mine	ramic/Mine	ramic/Mine	ramic/Mine	ramic/Mine	ramic/Mine	ramic/Mine	ramic/Mine
3,9	3,9	3,9	3,9	3,9	3,9	3,9	3,9	3,9	3,9	3,9	3,9
2,0-2,2	2,0-2,2	2,0-2,2	2,0-2,2	2,0-2,2	2,0-2,2	2.0-2.2	2.0-2.2	2.0-2.2	2.0-2.2	2.0-2.2	2.0-2.2
60	60	60	60	60	60	60	60	60	60	60	60
9,3	9,3	9,3	9,3	9,3	9,3	9,3	9,3	9,3	9,3	9,3	9,3
115	115	115	115	115	115	115	115	115	115	115	115
332	665	997	332	665	997	332	665	997	332	665	997
2,0	4,0	6,0	2,0	4,0	6,0	2,0	4,0	6,0	2,0	4,0	6,0
215	680	1510	215	680	1510	215	680	1510	215	680	1510
245	1088	2495	287	1184	2573	251	1063	2544	278	1131	2507
311	1189	2618	352	1282	2702	322	1173	2402	348	1248	2633
7	15	23	8	16	24	7	15	22	8	16	23
1349	1349	1349	661	661	661	1317	1317	1317	661	661	661
2,25	7,13	15,83	4,51	14,26	31,66	2,25	7,13	15,83	4,51	14,26	31,66
2,34	10,24	25,02	5,52	23,18	53,01	2,43	10,39	25,02	5,67	22,71	50,56
26	117	268	31	127	277	27	114	274	30	122	270

PARAMETERS	Unit	HIG5 ORC-SC3-B1	HIG5 ORC-SC3-B2	HIG5 ORC-SC3-B3	HIG5 ORC-SC3-B4	HIG5 ORC-SC3-B5	HIG5 ORC-SC4-B1	HIG5 ORC-SC4-B2	HIG5 ORC-SC4-B3	HIG5 ORC-SC4-B4	HIG5 ORC-SC4-B5	HIG5 ORC-SC7-B1	HIG5 ORC-SC7-B2	HIG5 ORC-SC7-B3	HIG5 ORC-SC7-B4	HIG5 ORC-SC7-B5	HIG5 ORC-SC8-B1	HIG5 ORC-SC8-B2	HIG5 ORC-SC8-B3	HIG5 ORC-SC8-B4	HIG5 ORC-SC8-B5
Date	dd-mm-yyyy											######	######	######	######	######	######	######	######	######	######
Sampling time	hh:mm					7:12															
End Time	hh:mm																				
Sampling Interval (min) (4 x Ret.time)	min	8.4	8.4	8.4	8.4	8.4	8.4	8.4	8.4	8.4	8.4	8.0	8.0	8.0	8.0	8.0	8.0	8.0	8.0	8.0	8.0
Sample amount (solids) / test point	kg	12.4	12.4	12.4	12.4	12.4	12.4	12.4	12.4	12.4	12.4	12.7	12.7	12.7	12.7	12.7	12.7	12.7	12.7	12.7	12.7
Sample amount (slurry) / test point	l	15.6	15.6	15.6	15.6	15.6	15.6	15.6	15.6	15.6	15.6	16.0	16.0	16.0	16.0	16.0	16.0	16.0	16.0	16.0	16.0
Feed Material	No.																				
Feed Type		Fine	Fine	Fine	Fine	Fine	Fine	Fine	Fine	Fine	Fine	Fine	Fine	Fine	Fine	Fine	Fine	Fine	Fine	Fine	Fine
F80 of Feed	[μm]	90	90	90	90	90	90	90	90	90	90	90	90	90	90	90	94	94	94	94	94
P80 (Target)	[μm]																90	90	90	90	90
Feed material density	kg/l	2.65	2.65	2.65	2.65	2.65	2.65	2.65	2.65	2.65	2.65	2.65	2.65	2.65	2.65	2.65	2.65	2.65	2.65	2.65	2.65
Feed solids by Volume	%	30.0	30.0	30.0	30.0	30.0	30.0	30.0	30.0	30.0	30.0	30.0	30.0	30.0	30.0	30.0	30.0	30.0	30.0	30.0	30.0
Feed solids (by mass) target	w%	53.2	53.2	53.2	53.2	53.2	53.2	53.2	53.2	53.2	53.2	53.2	53.2	53.2	53.2	53.2	53.2	53.2	53.2	53.2	53.2
Feed solids % (measured)	w%	53.5	52.8	53.5	52.1	50.6	52.8	52.1	52.1	51.4	49.8	52.8	52.8	53.5	52.8	52.8	53.5	53.5	53.5	52.8	52.1
Feed flow rate target (Slurry feed)	l/h	112	112	112	112	112	112	112	112	112	112	120	120	120	120	120	120	120	120	120	120
Measured Feed flow rate (Slurry feed)	l/h	114.5	114.3	116.1	112.7	113.2	114.2	114.7	114.4	115.0	112.5	132.4	129.7	134.1	132.4	130.5	130.4	133.2	134.5	133.2	134.4
Time per 1 liter Meas. Feed	(sec/L)	31.43	31.5	31	31.93	31.81	31.52	31.39	31.46	31.31	31.99	27.19	27.76	26.84	27.2	27.59	27.6133	27.02	26.76	27.02	26.79
Pump speed	Hz	PX10-45H	PX10-45H	PX10-45H	PX10-45H	PX10-45H	PX10-45H	PX10-45H	PX10-45H	PX10-45H	PX10-45H	PX10-48H	PX10-48H	PX10-48H	PX10-48H	PX10-48H	PX10-48H	PX10-48H	PX10-48H	PX10-48H	PX10-48Hz
Slurry density (target)	kg/l	1.495	1.495	1.495	1.495	1.495	1.495	1.495	1.495	1.495	1.495	1.495	1.495	1.495	1.495	1.495	1.495	1.495	1.495	1.495	1.495
Slurry density (measured)	kg/l	1.500	1.490	1.500	1.480	1.460	1.490	1.480	1.480	1.470	1.450	1.490	1.490	1.500	1.490	1.490	1.500	1.500	1.500	1.490	1.480
Slurry kg/l (solids target)	solid kg/l	0.795	0.795	0.795	0.795	0.795	0.795	0.795	0.795	0.795	0.795	0.795	0.795	0.795	0.795	0.795	0.795	0.795	0.795	0.795	0.795
Slurry kg/l (solids measured)	solid kg/l	0.803	0.787	0.803	0.771	0.739	0.787	0.771	0.771	0.755	0.723	0.787	0.787	0.803	0.787	0.787	0.803	0.803	0.803	0.787	0.771
Solids feed	kg/h	92	90	93	87	84	90	88	88	87	81	104	102	108	104	103	105	107	108	105	104
Grinding Media (bead type)	No.																				
Grinding Media Type		Ceramic/Min	amic/Min	amic/Min	amic/Min	amic/Min	amic/Min	amic/Min	amic/Min	amic/Min	amic/Min	amic/Min	amic/Min	amic/Min	amic/Min	amic/Min	amic/Min	amic/Min	amic/Min	amic/Min	amic/Mine
Grinding Media densitiy	t/m3	3.9	3.9	3.9	3.9	3.9	3.9	3.9	3.9	3.9	3.9	3.9	3.9	3.9	3.9	3.9	3.9	3.9	3.9	3.9	3.9
Grinding Media Size	mm	2.0-2.2	2.0-2.2	2.0-2.2	2.0-2.2	2.0-2.2	2.0-2.2	2.0-2.2	2.0-2.2	2.0-2.2	2.0-2.2	2.0-2.2	2.0-2.2	2.0-2.2	2.0-2.2	2.0-2.2	2.0-2.2	2.0-2.2	2.0-2.2	2.0-2.2	2.0-2.2
Grinding Media Filling level	[%]	60	60	60	60	60	60	60	60	60	60	60	60	60	60	60	60	60	60	60	60
Mass of grinding media charge	kg	9.3	9.3	9.3	9.3	9.3	9.3	9.3	9.3	9.3	9.3	9.3	9.3	9.3	9.3	9.3	9.3	9.3	9.3	9.3	9.3
Disc Diameter	mm	115	115	115	115	115	115	115	115	115	115	115	115	115	115	115	115	115	115	115	115
Mill Speed	rpm	415	415	415	415	415	415	415	415	415	415	415	415	415	415	415	415	415	415	415	415
Tip speed	m/s	2.5	2.5	2.5	2.5	2.5	2.5	2.5	2.5	2.5	2.5	2.5	2.5	2.5	2.5	2.5	2.5	2.5	2.5	2.5	2.5
Mill Power predicted	W	360	360	360	360	360	360	360	360	360	360	360	360	360	360	360	360	360	360	360	360
Mill Power calculated from Torque 1	W	400	402	404	403	405	392	395	396	393	390	425	434	417	420	419	417	416	418	417	420
Mill Power from VSD 2	W	482	483	487	487	485	474	480	481	472	470	510	515	505	502	505	491	495	489	495	490
Torque Measurement in V 4	Nm	9	9	9	9	9	8	8	8	8	8	9	9	9	9	9	9	9	9	9	9
Torque Measurement in V	V																				
Speed pump 1 (SPX10)	rpm	1316	1316	1316	1316	1316	1316	1316	1316	1316	1316	1411	1411	1411	1411	1411	1411	1411	1411	1411	1411
Speed pump 2 (SPX15)	rpm																				
SGE predicted (related to dry tons)	[kWh/t]	4.04	4.04	4.04	4.04	4.04	4.04	4.04	4.04	4.04	4.04	3.77	3.77	3.77	3.77	3.77	3.77	3.77	3.77	3.77	3.77
SGE (related to dry tons) mesured flow	[kWh/t]	4.35	4.47	4.33	4.64	4.84	4.36	4.47	4.49	4.53	4.80	4.08	4.25	3.87	4.03	4.08	3.98	3.89	3.87	3.98	4.05
kW/t (grinding media)	kW/t_media	43	43	43	43	44	42	42	43	42	42	46	47	45	45	45	45	45	45	45	45
Product temperature (Mill)	DegC																				
Product temperature (Flow)	DegC																				
P50 of product	[μm]	35	26	19	17	13	31	24	20	17	14	28	22	19	16	14	27	22	19	16	13
P80 of product	[μm]	87	77	59	56	40	82	71	63	55	42	75	63	57	48	43	74	61	53	48	36
RET Time	(sec)	125	125	125	125	125	125	125	125	125	125	120	120	120	120	120	120	120	120	120	120
Cumulative SGE	[kWh/t]	4.35	8.82	13.15	17.79	22.63	4.36	8.83	13.32	17.85	22.64	4.08	8.33	12.20	16.24	20.32	3.98	7.87	11.74	15.72	19.77